

Cosenza, E. and Zandonini, R. "Composite Construction"
Structural Engineering Handbook
Ed. Chen Wai-Fah
Boca Raton: CRC Press LLC, 1999

Composite Construction

6.1 Introduction

Historical Overview • Scope • Design Codes

6.2 Materials

Concrete • Reinforcing Steel • Structural Steel • Steel Decking
• Shear Connectors

6.3 Simply-Supported Composite Beams

Beam Response and Failure Modes • The Effective Width of Concrete Flange • Elastic Analysis • Plastic Analysis • Vertical Shear • Serviceability Limit States • Worked Examples¹

6.4 Continuous Beams

Introduction • Effective Width • Local Buckling and Classification of Cross-Sections • Elastic Analysis of the Cross-Section • Plastic Resistance of the Cross-Section • Serviceability Limit States • Ultimate Limit State • The Lateral-Torsional Buckling • Worked Examples

6.5 The Shear Connection

The Shear Transfer Mechanisms • The Shear Strength of Mechanical Shear Connectors • Steel-Concrete Interface Separation • Shear Connectors Spacing • Shear Connection Detailing • Transverse Reinforcement • The Shear Connection in Fully and Partially Composite Beams • Worked Examples

6.6 Composite Columns

Types of Sections and Advantages • Failure Mechanisms • The Elastic Behavior of the Section • The Plastic Behavior of the Section • The Behavior of the Members • Influence of Local Buckling • Shear Effects • Load Introduction Region • Restrictions for the Application of the Design Methods • Worked Examples

6.7 Composite Slabs

The Steel Deck • The Composite Slab • Worked Examples

[Notations](#) .

[References](#) .

[Codes and Standards](#) .

[Further Reading](#) .

Edoardo Cosenza
*University of Naples,
Napoli, Italy*

Riccardo Zandonini
*Department of Structural
Mechanics and Design,
University of Trento,
Povo, Italy*

6.1 Introduction

6.1.1 Historical Overview

The history of structural design may be explained in terms of a continuous progress toward optimal constructional systems with respect to aesthetic, engineering, and economic parameters. If the attention is focused on the structure, optimality is mainly sought through improvement of the form

and of the materials. Moreover, creative innovation of the form combined with advances of material properties and technologies enables pursuit of the human challenge to the “natural” limitations to the height (buildings) and span (roofs and bridges) of the structural systems.

Advances may be seen to occur as a step-by-step process of development. While the enhancement of the properties of already used materials contributes to the “in-step” continuous advancement, new materials as well as the synergic combination of known materials permit structural systems to make a step forward in the way to optimality.

Use of composite or hybrid material solutions is of particular interest, due to the significant potential in overall performance improvement obtained through rather modest changes in manufacturing and constructional technologies. Successful combinations of materials may even generate a new material, as in the case of reinforced concrete or, more recently, fiber-reinforced plastics. However, most often the synergy between structural components made of different materials has shown to be a fairly efficient choice. The most important example in this field is represented by the steel-concrete composite construction, the enormous potential of which is not yet fully exploited after more than one century since its first appearance.

“Composite bridges” and “composite buildings” appeared in the U.S. in the same year, 1894 [34, 46]:

1. The Rock Rapids Bridge in Rock Rapids, Iowa, made use of curved steel I-beams embedded in concrete.
2. The Methodist Building in Pittsburgh had concrete-encased floor beams.

The composite action in these cases relied on interfacial bond between concrete and steel. Efficiency and reliability of bond being rather limited, attempts to improve concrete-to-steel joining systems were made since the very beginning of the century, as shown by the shearing tabs system patented by Julius Kahn in 1903 (Figure 6.1a). Development of efficient mechanical shear connectors progressed

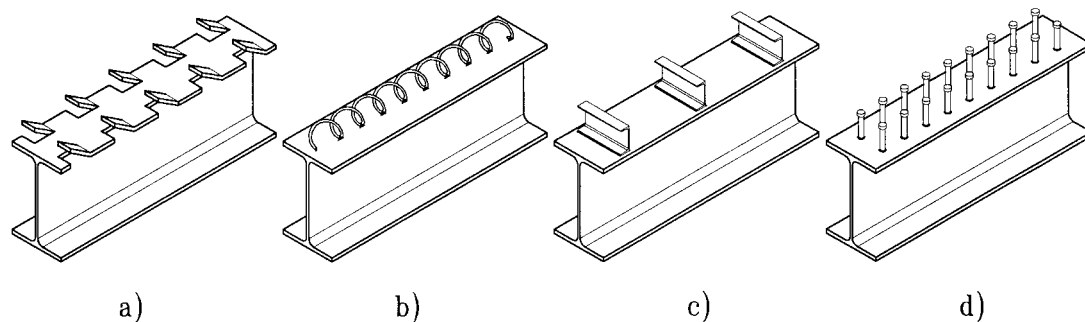


FIGURE 6.1: Historical development of shear connectors. (a) Shearing tabs system (Julius Kahn 1903). (b) Spiral connectors. (c) Channels. (d) Welded studs.

quite slowly, despite the remarkable efforts both in Europe (spiral connectors and rigid connectors) and North America (flexible channel connectors). The use of welded headed studs (in 1956) was hence a substantial breakthrough. By coincidence, welded studs were used the same year in a bridge (Bad River Bridge in Pierre, South Dakota) and a building (IBM’s Education Building in Poughkeepsie, New York). Since then, the metal studs have been by far the most popular shear transferring device in steel-concrete composite systems for both building and bridge structures.

The significant interest raised by this “new material” prompted a number of studies, both in Europe and North America, on composite members (columns and beams) and connecting devices. The increasing level of knowledge then enabled development of Code provisions, which first appeared for buildings (the New York City Building Code in 1930) and subsequently for bridges (the AASHTO specifications in 1944).

In the last 50 years extensive research projects made possible a better understanding of the fairly complex phenomena associated with composite action, codes evolved significantly towards acceptance of more refined and effective design methods, and constructional technology progressed at a brisk pace. However, these developments may be considered more a consequence of the increasing popularity of composite construction than a cause of it. In effect, a number of advantages with respect to structural steel and reinforced concrete were identified and proven, as:

- high stiffness and strength (beams, girders, columns, and moment connections)
- inherent ductility and toughness, and satisfactory damping properties (e.g., encased columns, beam-to-column connections)
- quite satisfactory performance under fire conditions (all members and the whole system)
- high constructability (e.g., floor decks, tubular infilled columns, moment connections)

Continuous development toward competitive exploitation of composite action was first concentrated on structural elements and members, and was based mainly on technological innovation as in the use of steel-concrete slabs with profiled steel sheeting and of headed studs welded through the metal decking, which successfully spread composite slab systems in the building market since the 1960s. Innovation of types of structural forms is a second important factor on which more recent advances (in the 1980s) were founded: composite trusses and stub girders are two important examples of novel systems permitting fulfillment of structural requirements and easy accommodation of air ducts and other services.

A very recent trend in the design philosophy of tall buildings considers the whole structural system as a body where different materials can cohabit in a fairly beneficial way. Reinforced concrete, steel, and composite steel-concrete members and subsystems are used in a synergic way, as in the cases illustrated in Figure 6.2. These mixed systems often incorporate composite superframes, whose columns, conveniently built up by taking advantage of the steel erection columns (Figure 6.3), tend to become more and more similar to highly reinforced concrete columns. The development of such systems stresses again the vitality of composite construction, which seems to increase rather than decline.

6.1.2 Scope

The variety of structural forms and the continuous evolution of composite systems precludes the possibility of comprehensive coverage. This chapter has the more limited goal of providing practicing structural engineers with a reference text dealing with the key features of the analysis and design of composite steel-concrete members used in building systems. The attention is focused on the response and design criteria under static loading of individual components (members and elements) of traditional forms of composite construction. Recent developments in floor systems and composite connections are dealt with in Chapters 18 and 23, respectively.

Emphasis is given to the behavioral aspects and to the suitable criteria to account for them in the design process. Introduction to the practical usage of these criteria requires that reference is made to design codes. This is restricted to the main North American and European Specifications and Standards, and has the principal purpose of providing general information on the different application rules. A few examples permit demonstration of the general design criteria.

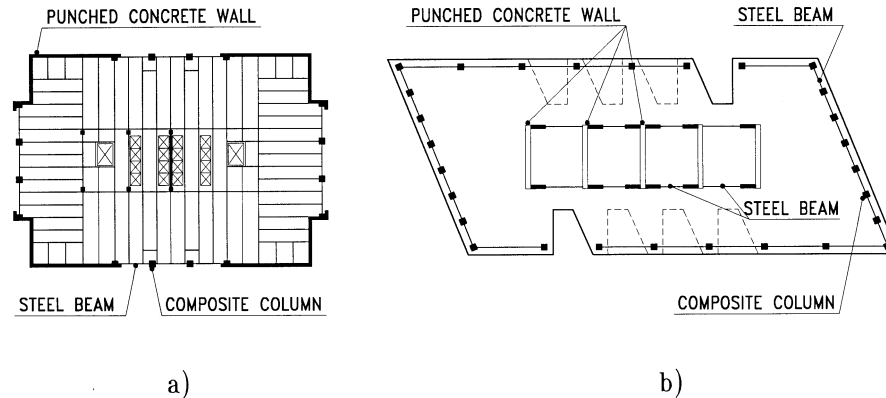


FIGURE 6.2: Composite systems in buildings. (a) Momentum Place, Dallas, Texas. (b) First City Tower, Houston, Texas. (After Griffis, L.G. 1992. Composite Frame Construction, *Constructional Steel Design. An International Guide*, P.J. Dowling, et al., Eds., Elsevier Applied Science, London.)

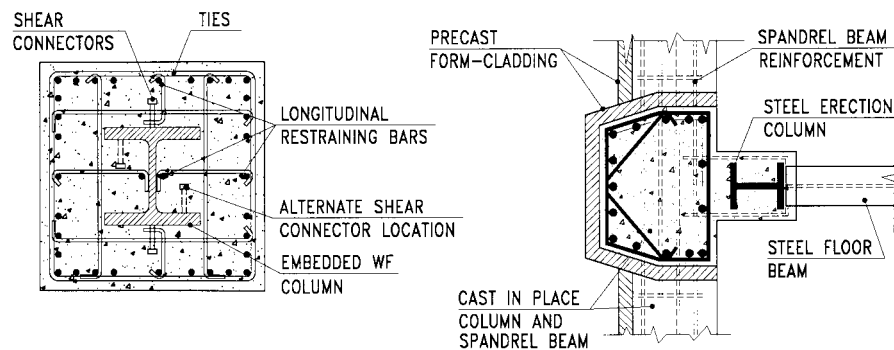


FIGURE 6.3: Columns in composite superframes. (After Griffis, L.G. 1992. Composite Frame Construction, *Constructional Steel Design. An International Guide*, P.J. Dowling, et al., Eds., Elsevier Applied Science, London.)

Problems related to members in special composite systems as composite superframes are not included, due to the limited space. Besides, their use is restricted to fairly tall buildings, and their construction and design requires rather sophisticated analysis methods, often combined with “creative” engineering understanding [21].

6.1.3 Design Codes

The complexity of the local and global response of composite steel-concrete systems, and the number of possible different situations in practice led to the use of design methods developed by empirical processes. They are based on, and calibrated against, a set of test data. Therefore, their applicability is limited to the range of parameters covered by the specific experimental background.

This feature makes the reference to codes, and in particular to their application rules, of substantial importance for any text dealing with design of composite structures. In this chapter reference is made to two codes:

1. AISC-LRFD Specifications [1993]
2. Eurocode 4 [1994]

Besides, the ASCE Standards [1991] for the design of composite slabs are referred to, as this subject is not covered by the AISC-LRFD Specifications. These codes may be considered representative of the design approaches of North America and Europe, respectively. Moreover, they were issued or revised very recently, and hence reflect the present state of knowledge. Both codes are based on the limit states methodology and were developed within the framework of first order approaches to probabilistic design. However, the format adopted is quite different. This operational difference, together with the general scope of the chapter, required a “simplified” reference to the codes. The key features of the formats of the two codes are highlighted here, and the way reference is made to the code recommendations is then presented.

The Load and Resistance Factor Design (LRFD) specifications adopted a design criterion, which expresses reliability requirements in terms of the general formula

$$\phi R_n \geq E_m \left(\sum \gamma_{Fi} F_{i,m} \right) \quad (6.1)$$

where on the resistance side R_n represents the nominal resistance and ϕ is the “resistance factor”, while on the loading side E_m is the “mean load effect” associated to a given load combination $\sum \gamma_{Fi} F_{i,m}$ and γ_{Fi} is the “load factor” corresponding to mean load $F_{i,m}$. The nominal resistance is defined as the resistance computed according to the relevant formula in the Code, and relates to a specific limit state. This “first-order” simplified probabilistic design procedure was calibrated with reference to the “safety index” β expressed in terms of the mean values and the coefficients of variation of the relevant variables only, and assumed as a measure of the degree of reliability. Application of this procedure requires that (1) the nominal strength be computed using the nominal specified strengths of the materials, (2) the relevant resistance factor be applied to obtain the “design resistance”, and (3) this resistance be finally compared with the corresponding mean load effect (Equation 6.1).

In Eurocode 4, the fundamental reliability equation has the form

$$R_d (f_{i,k} / \gamma_{m,i}) \geq E_d \left(\sum \gamma_{Fi} F_{i,k} \right) \quad (6.2)$$

where on the resistance side the design value of the resistance, R_d , appears, determined as a function of the characteristic values of the strengths $f_{i,k}$ of the materials of which the member is made. The factors $\gamma_{m,i}$ are the “material partial safety factors”; Eurocode 4 adopts the following material partial safety factors:

$$\gamma_c = 1.5; \gamma_s = 1.10; \gamma_{sr} = 1.15$$

for concrete, structural steel, and reinforcing steel, respectively.

On the loading side the design load effect, E_d , depends on the relevant combination of the characteristic factored loads $\gamma_{Fi} F_{i,k}$. Application of this checking format requires the following steps: (1) the relevant resistance factor be applied to obtain the “design strength” of each material, (2) the design strength R_d be then computed using the factored materials’ strengths, and (3) the resistance R_d be finally compared with the corresponding design load effect E_d (Equation 6.2).

Therefore, the two formats are associated with two rather different resistance parameters (R_n and R_d), and design procedures. A comprehensive and specific reference to the two codes would lead to a uselessly complex text. It seemed consistent with the purpose of this chapter to refer in any case to the “unfactored” values of the resistances as explicitly (LRFD) or implicitly (Eurocode 4) given in code recommendations, i.e., to resistances based on the nominal and characteristic values of material strengths, respectively. Factors (ϕ or $\gamma_{m,i}$) to be applied to determine the design resistance are specified only when necessary. Finally, in both codes considered, an additional reduction factor equal to 0.85 is introduced in order to evaluate the design strength of concrete.

6.2 Materials

Figure 6.4 shows stress-strain curves typical of concrete, and structural and reinforcing steel. The

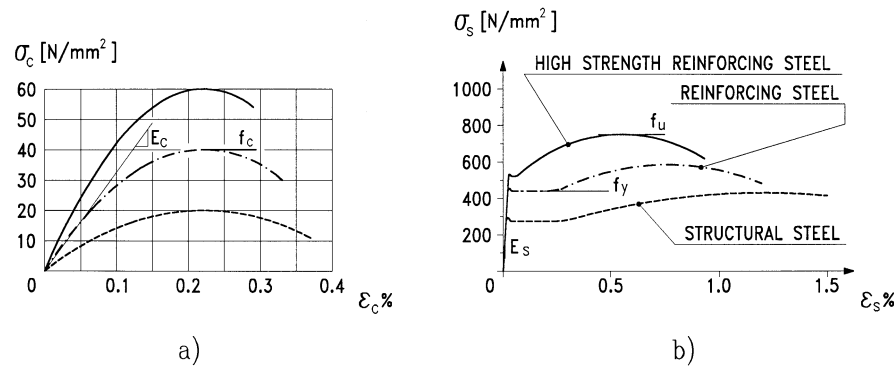


FIGURE 6.4: Stress-strain curves. (a) Typical compressive stress-strain curves for concrete. (b) Typical stress-strain curves for steel.

properties are covered in detail in Chapters 3 and 4 of this Handbook, which deal with steel and reinforced concrete structures, respectively. The reader will hence generally refer to these sections. However, some data are provided specific to the use of these materials in composite construction, which include limitations imposed by the present codes to the range of material grades that can be selected, in view of the limited experience presently available. Moreover, the main characteristics of the materials used for elements or components typical of composite construction, like stud connectors and metal steel decking, are given.

6.2.1 Concrete

Composite action implies that forces are transferred between steel and concrete components. The transfer mechanisms are fairly complex. Design methods are supported mainly by experience and test data, and their use should be restricted to the range of concrete grades and strength classes sufficiently investigated. It should be noted that concrete strength significantly affects the local and overall performance of the shear connection, due to the inverse relation between the resistance and the strain capacity of this material. Therefore, the capability of redistribution of forces within the shear connection is limited by the use of high strength concretes, and consequently the applicability of plastic analysis and of design methods based on full redistribution of the shear forces supported by the connectors (as the partial shear connection design method discussed in Section 6.7.2) is also limited.

The LRFD specifications [AISC, 1993] prescribe for composite flexural elements that concrete meet quality requirements of ACI [1989], made with ASTM C33 or rotary-kiln produced C330 aggregates with concrete unit weight not less than 14.4 kN/m³ (90 pcf)¹. This allows for the development of the

¹The Standard International (S.I.) system of units is used in this chapter. Quantities are also expressed (in parenthesis) in American Inch-Pound units, when reference is made to American Code specified values.

full flexural capacity according to test results by Olgaard et al. [38]. A restriction is also imposed on the concrete strength in composite compressed members to ensure consistency of the specifications with available experimental data: the strength upper limit is 55 N/mm² (8 ksi) and the lower limit is 20 N/mm² (3 ksi) for normal weight concrete, and 27 N/mm² (4 ksi) for lightweight concrete.

The recommendations of Eurocode 4 [CEN, 1994] are applicable for concrete strength classes up to the C50/60 (see Table 6.1), i.e., to concretes with cylinder characteristic strength up to 50 N/mm². The use of higher classes should be justified by test data. Lightweight concretes with unit weight not less than 16 kN/m³ can be used.

TABLE 6.1 Values of Characteristic Compressive strength (f_c), Characteristic tensile strength (f_{ct}), and Secant Modulus of Elasticity (E_c) proposed by Eurocode 4

		Class of concrete ^a						
		C 20/25	C 25/30	C 30/37	C 35/45	C 40/50	C 45/55	C 50/60
f_c	(N/mm ²)	20	25	30	35	40	45	50
f_{ct}	(N/mm ²)	2.2	2.6	2.9	3.2	3.5	3.8	4.1
E_c	(kN/mm ²)	29	30.5	32	33.5	35	36	37

^a Classification refer to the ratio of cylinder to cube strength.

Compression tests permit determination of the immediate concrete strength f_c . The strength under sustained loads is obtained by applying to f_c a reduction factor 0.85.

Time dependence of concrete properties, i.e., shrinkage and creep, should be considered when determining the response of composite structures under sustained loads, with particular reference to member stiffness. Simple design methods can be adopted to treat them.

Stiffness and stress calculations of composite beams may be based on the transformed cross-section approach first developed for reinforced concrete sections, which uses the modular ratio $n = E_s/E_c$ to reduce the area of the concrete component to an equivalent steel area. A value of the modular ratio may be suitably defined to account for the *creep effect* in the analysis:

$$n_{ef} = \frac{E_s}{E_{c.ef}} = \frac{E_s}{[E_c/(1 + \phi)]} \quad (6.3)$$

where

$E_{c.ef}$ = an effective modulus of elasticity for the concrete

ϕ = a creep coefficient approximating the ratio of creep strain to elastic strain for sustained compressive stress

This coefficient may generally be assumed as 1 leading to a reduction by half of the modular ratio for short term loading; a value $\phi = 2$ (i.e., a reduction by a factor 3) is recommended by Eurocode 4 when a significant portion of the live loads is likely to be on the structure quasi-permanently. The effects of shrinkage are rarely critical in building design, except when slender beams are used with span to depth ratio greater than 20.

The total long-term drying *shrinkage* strains ε_{sh} varies quite significantly, depending on concrete, environmental characteristics, and the amount of restraint from steel reinforcement. The following design values are provided by the Eurocode 4 for ordinary cases:

1. Dry environments

- 325×10^{-6} for normal weight concrete
- 500×10^{-6} for lightweight concrete

2. Other environments and infilled members

- 200×10^{-6} for normal weight concrete
- 300×10^{-6} for lightweight concrete

Finally, the same value of the *coefficient of thermal expansion* may be conveniently assumed as for the steel components (i.e., 10×10^{-6} per °C), even for lightweight concrete.

6.2.2 Reinforcing Steel

Rebars with yield strength up to 500 N/mm^2 (72 ksi) are acceptable in most instances. The reinforcing steel should have adequate ductility when plastic analysis is adopted for continuous beams. This factor should hence be carefully considered in the selection of the steel grade, in particular when high strength steels are used.

A different requirement is implied by the limitation of 380 N/mm^2 (55 ksi) specified by AISC for the yield strength of the reinforcement in encased composite columns; this is aimed at ensuring that buckling of the reinforcement does not occur before complete yielding of the steel components.

6.2.3 Structural Steel

Structural steel alloys with yield strength up to 355 N/mm^2 (50 ksi for American grades) can be used in composite members, without any particular restriction. Studies of the performance of composite members and joints made of high strength steel are available covering a yield strength range up to 780 N/mm^2 (113 ksi) (see also [47]). However, significant further research is needed to extend the range of structural steels up to such levels of strength. Rules applicable to steel grades Fe420 and Fe460 (with $f_y = 420$ and 460 N/mm^2 , respectively) have been recently included in the Eurocode 4 as Annex H [1996]. Account is taken of the influence of the higher strain at yielding on the possibility to develop the full plastic sagging moment of the cross-section, and of the greater importance of buckling of the steel components.

The AISC specification applies the same limitation to the yield strength of structural steel as for the reinforcement (see the previous section).

6.2.4 Steel Decking

The increasing popularity of composite decking, associated with the trend towards higher flexural stiffnesses enabling possibility of greater unshored spans, is clearly demonstrated by the remarkable variety of products presently available. A wide range of shapes, depths (from 38 to 200 mm [1.5 to 7.9 in.]), thicknesses (from 0.76 to 1.52 mm [5/64 to 5/16 in.]), and steel grades (with yield strength from 235 to 460 N/mm^2 [34 to 67 ksi]) may be adopted. Mild steels are commonly used, which ensure satisfactory ductility.

The minimum thickness of the sheeting is dictated by protection requirements against corrosion. Zinc coating should be selected, the total mass of which should depend on the level of aggressiveness of the environment. A coating of total mass 275 g/m^2 may be considered adequate for internal floors in a non-aggressive environment.

6.2.5 Shear Connectors

The steel quality of the connectors should be selected according to the method of fixing (usually welding or screwing). The welding techniques also should be considered for welded connectors (studs, anchors, hoops, etc.).

Design methods implying redistribution of shear forces among connectors impose that the connectors do possess adequate deformation capacity. A problem arises concerning the mechanical properties to be required to the stud connectors. Standards for material testing of welded studs are not available. These connectors are obtained by cold working the bar material, which is then subject to localized plastic straining during the heading process. The Eurocode hence specifies requirements for the ultimate-to-yield strength ratio ($f_u/f_y \geq 1.2$) and to the elongation at failure (not less than 12% on a gauge length of $5.65 \sqrt{A_o}$, with A_o cross-sectional area of the tensile specimen) to be fulfilled by the finished (cold drawn) product. Such a difficulty in setting an appropriate definition of requirements in terms of material properties leads many codes to prescribe, for studs, cold bending tests after welding as a means to check “ductility”.

6.3 Simply-Supported Composite Beams

Composite action was first exploited in flexural members, for which it represents a “natural” way to enhance the response of structural steel. Many types of composite beams are currently used in building and bridge construction. Typical solutions are presented in Figures 6.5, 6.6, and 6.7. With reference to the steel member, either rolled or welded I sections are the preferred solution in building systems (Figure 6.5a); hollow sections are chosen when torsional stiffness is a critical design factor (Figure 6.5b). The trend towards longer spans (higher than 10 m) and the need of freedom in accommodating services made the composite truss become more popular (Figure 6.5c). In bridges, multi-girder (Figure 6.6a) and box girder can be adopted; box girders may have either a closed (Figure 6.6b) or an open (Figure 6.6c) cross-section. With reference to the concrete element, use of traditional solid slabs are now basically restricted to bridges. Composite decks with steel

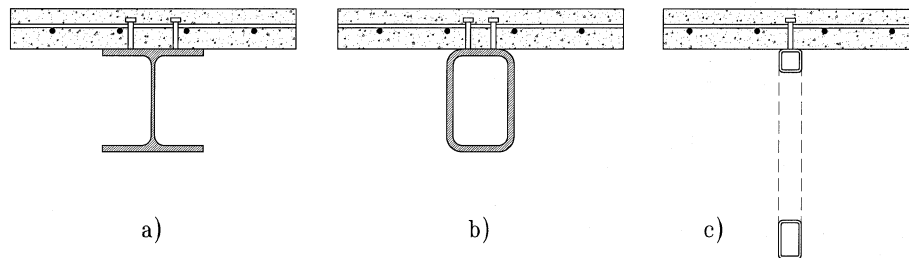


FIGURE 6.5: Typical composite beams. (a) I-shape steel section. (b) Hollow steel section. (c) Truss system.

profiled sheetings are the most popular solution (Figure 6.7a,b) in building structures because their use permits elimination of form-works for concrete casting and also reduction of the slab depth, as for example in the recently developed “slim floor” system shown in Figure 6.7c. Besides, full or partial encasement of the steel section significantly improves the performance in fire conditions (Figures 6.7d and 6.7e).

The main features of composite beam behavior are briefly presented, with reference to design. Due to the different level of complexity, and the different behavioral aspects involved in the analysis and design of simply supported and continuous composite beams, separate chapters are devoted to these two cases.

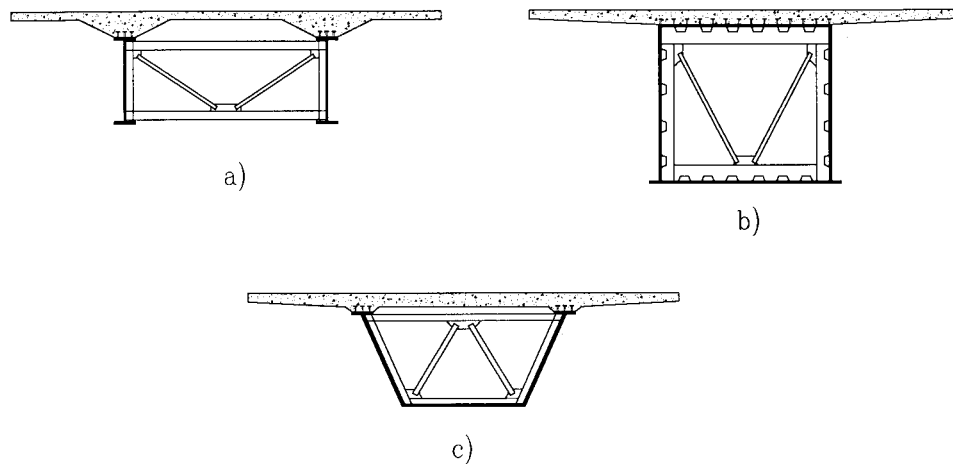


FIGURE 6.6: Typical system for composite bridges. (a) Multi-girder. (b) Box girder with closed cross-section. (c) Box girder with open cross-section.

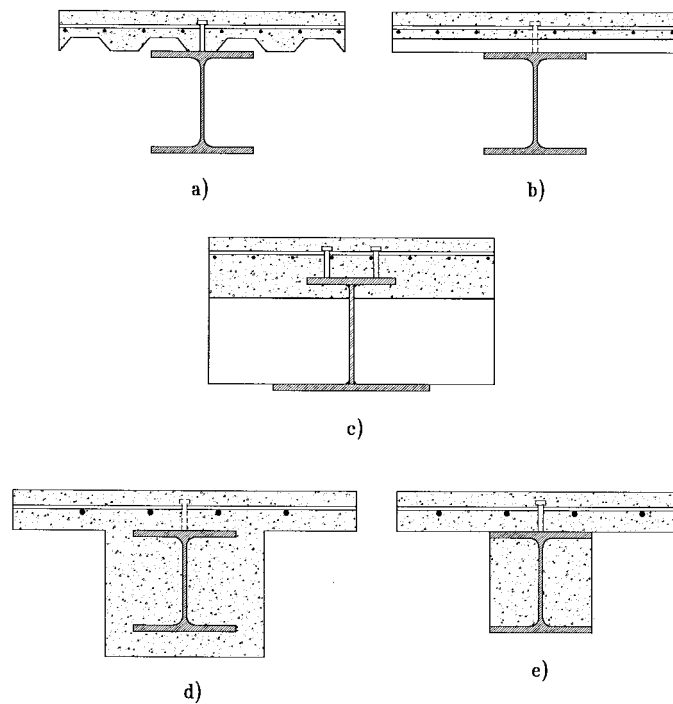


FIGURE 6.7: Typical system for composite floors. (a) Deck rib parallel to the steel beam. (b) Deck rib normal to the steel beam. (c) Slim-floor system. (d) Fully encased steel section. (e) Partially encased steel section.

6.3.1 Beam Response and Failure Modes

Simply supported beams are subjected to positive (sagging) moment and shear. Composite steel-concrete systems are advantageous in comparison with both reinforced concrete and structural steel members:

- With respect to reinforced concrete beams, concrete is utilized in a more efficient way, i.e., it is mostly in compression. Concrete in tension, which may be a significant portion of the member in reinforced concrete beams, does not contribute to the resistance, while it increases the dead load. Moreover, cracking of concrete in tension has to be controlled, to avoid durability problems as reinforcement corrosion. Finally, construction methods can be chosen so that form-work is not needed.
- With respect to structural steel beams, a large part of the steel section, or even the entire steel section, is stressed in tension. The importance of local and flexural-torsional buckling is substantially reduced, if not eliminated, and plastic resistance can be achieved in most instances. Furthermore, the sectional stiffness is substantially increased, due to the contribution of the concrete flange deformability problems are consequently reduced, and tend not to be critical.

In summary, it can be stated that simply supported composite beams are characterized by an efficient use of both materials, concrete and steel; low sensitivity to local and flexural-torsional buckling; and high stiffness.

The design analyses may focus on few critical phenomena and the associated limit states. For the usual uniform loading pattern, typical failure modes are schematically indicated in Figure 6.8: mode I is by attainment of the ultimate moment of resistance in the midspan cross-section, mode II

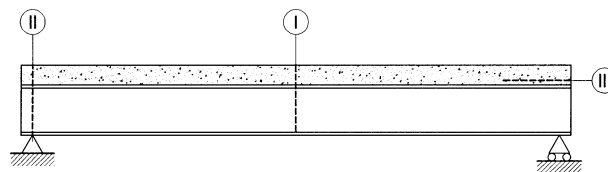


FIGURE 6.8: Typical failure modes for composite beam: critical sections.

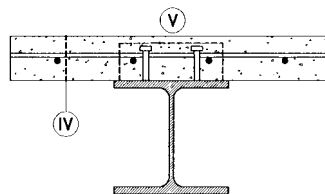


FIGURE 6.9: Potential shear failure planes.

is by shear failure at the supports, and mode III is by achievement of the maximum strength of the shear connection between steel and concrete in the vicinity of the supports. A careful design of the structural details is necessary in order to avoid local failures as the longitudinal shear failure of the slab along the planes shown in Figure 6.9, where the collapse under longitudinal shear does

not involve the connectors, or the concrete flange failure by splitting due to tensile transverse forces. The behavioral features and design criteria for the shear connection and the slabs are dealt with in Chapters 5 and 7, respectively. In the following the main concepts related to the design analysis of simply supported composite beams are presented, under the assumption that interface slip can be disregarded and the strength of the shear connection is not critical. In the following, the behavior of the elements is examined in detail, analyzing at first the evaluation of the concrete flange effective width.

During construction the member can be temporarily supported (i.e., shored construction) at intermediate points, in order to reduce stresses and deformation of the steel section during concrete casting. The construction procedures can affect the structural behavior of the composite beam. In the case of the unshored construction, the weight of fresh concrete and constructional loads are supported by the steel member alone until concrete has achieved at least 75% of its strength and the composite action can develop, and the steel section has to be checked for all the possible loading condition arising during construction. In particular, the verification against lateral-torsional buckling can become important because there is not the benefit of the restraint provided by concrete slab, and the steel section has to be suitably braced horizontally.

In the case of shored constructions, the overall load, including self weight, is resisted by the composite member. This method of construction is advantageous from a statical point of view, but it may lead to significant increase of cost. The props are usually placed at the half and the quarters of the span, so that full shoring is obtained. The effect of the construction method on the stress state and deformation of the members generally has to be accounted for in design calculations. It is interesting to observe that if the composite section does possess sufficient ductility, the method of construction does not influence the ultimate capacity of the structure. The different responses of shored and unshored “ductile” members are shown in Figure 6.10: the behavior under service loading is very

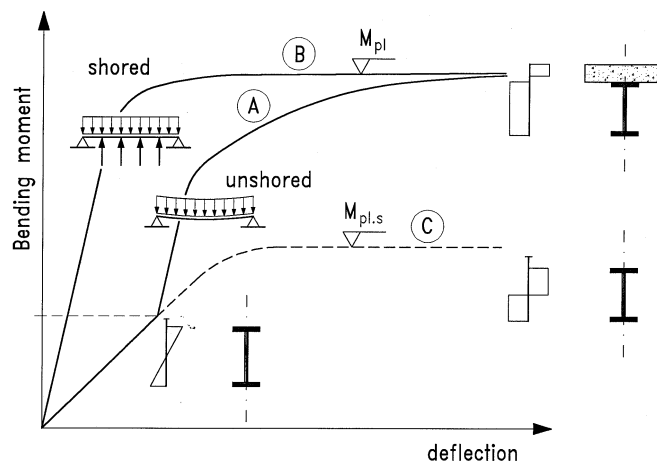


FIGURE 6.10: Bending moment relationship for unshored (curve A) and shored (curve B) composite beams and steel beam (curve C).

different but, if the elements are ductile enough, the two structures attain the same ultimate capacity. More generally, the composite member ductility permits a number of phenomena, such as shrinkage of concrete, residual stresses in the steel sections, and settlement of supports, to be neglected at ultimate. On the other hand, all these actions can substantially influence the performance in service

and the ultimate capacity of the member in the case of slender cross-sections susceptible to local buckling in the elastic range.

6.3.2 The Effective Width of Concrete Flange

The traditional form of composite beam (Figure 6.7) can be modeled as a T-beam, the flange of which is the concrete slab. Despite the inherent in plane stiffness, the geometry, characterized by a significant width for which the shear lag effect is non-negligible, and the particular loading condition (through concentrated loads at the steel-concrete interface), make the response of the concrete “flange” truly bi-dimensional in terms of distribution of strains and stresses. However, it is possible to define a suitable breadth of the concrete flange permitting analysis of a composite beam as a mono-dimensional member by means of the usual beam theory. The definition of such an “effective width” may be seen as the very first problem in the analysis of composite members in bending. This width can be determined by the equivalence between the responses of the beam computed via the beam theory, and via a more refined model accounting for the actual bi-dimensional behavior of the slab. In principle, the equivalence should be made with reference to the different parameters characterizing the member performance (i.e., the elastic limit moment, the ultimate moment of resistance, the maximum deflections), and to different loading patterns. A number of numerical studies of this problem are available in the literature based on equivalence of the elastic or inelastic response [1, 2, 9, 23], and rather refined approaches were developed to permit determination of elastic effective widths depending on the various design situations and related limit states. Some codes provide detailed, and quite complex, rules based on these studies. However, recent parametric numerical analyses, the findings of which were validated by experimental results, indicated that simple expressions for effective width calculations can be adopted, if the effect of the non-linear behavior of concrete and steel is taken into account. Moreover, the assumption, in design global analyses, of a constant value for the effective width b_{eff} leads to satisfactorily accurate results. These outcomes are reflected by recent design codes. In particular, both the Eurocode 4 and the AISC specifications assume, in the analysis of simply supported beams, a constant effective width b_{eff} obtained as the

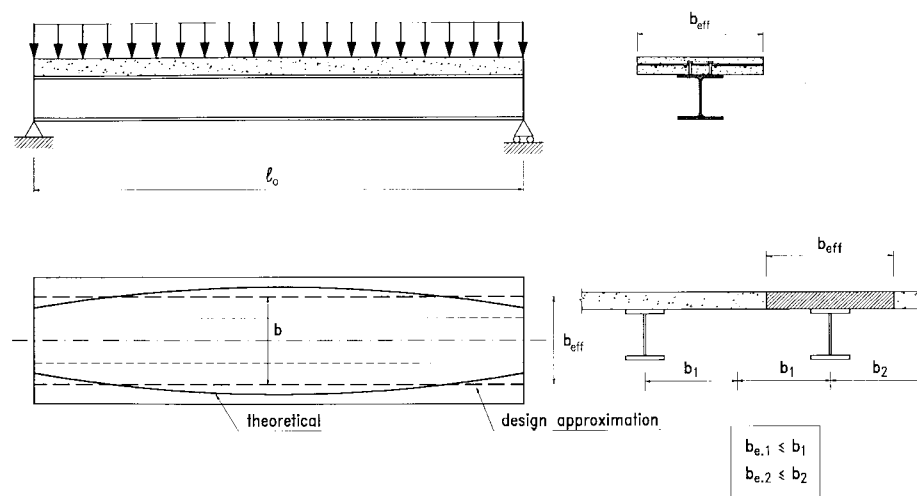


FIGURE 6.11: Effective width of slab.

sum of the effective widths $b_{e,i}$ at each side of the beam web, determined via the following expression (Figure 6.11):

$$b_{e,i} = \frac{l_o}{8} \quad (6.4)$$

where l_o is the beam span. The values of $b_{e,i}$ should be lower than one-half the distance between center-lines of adjacent beams or the distance to the slab free edge, as shown in Figure 6.11.

6.3.3 Elastic Analysis

When the interface slip can be neglected as assumed here, a similar procedure for the analysis of reinforced concrete sections can be adopted for composite members subject to bending. In fact, the cross-sections remain plane and then the strains vary linearly along the section depth. The stress diagram is also linear if the concrete stress is multiplied by the modular ratio $n = E_s/E_c$ between the elastic moduli E_s and E_c of steel and concrete, respectively. As further assumptions, the concrete tensile strength is neglected, as it is the presence of reinforcement placed in the concrete compressive area in view of its modest contribution. The theory of the transformed sections can be used, i.e., the composite section is replaced by an equivalent all-steel section², the flange of which has a breadth equal to b_{eff}/n . The translational equilibrium of the section requires the centroidal axis

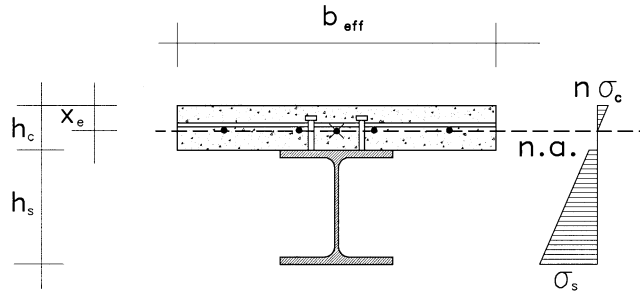


FIGURE 6.12: Elastic stress distribution with neutral axis in slab.

to be coincident with the neutral axis. Therefore, the position of the neutral axis can be determined by imposing that the first moment of the effective area of the cross-section is equal to zero. In the case of a solid concrete slab, and if the elastic neutral axis lies in the slab (Figure 6.12), this condition leads to the equation:

$$S = \frac{1}{n} \frac{b_{\text{eff}} \cdot x_e^2}{2} - A_s \cdot \left(\frac{h_s}{2} + h_c - x_e \right) = 0 \quad (6.5)$$

that is quadratic in the unknown x_e (which is the distance of elastic neutral axis to the top fiber of the concrete slab). Once the value of x_e is calculated, the second moment of area of the transformed cross-section can be evaluated by the following expression:

$$I = \frac{1}{n} \frac{b_{\text{eff}} \cdot x_e^3}{3} + I_s + A_s \cdot \left(\frac{h_s}{2} + h_c - x_e \right)^2 \quad (6.6)$$

²Transformation to an equivalent all-concrete section is a viable alternative.

The same procedure (Figure 6.13) is used if the whole cross-section is effective, i.e., if the elastic neutral axis lies in the steel profile. In this case it results:

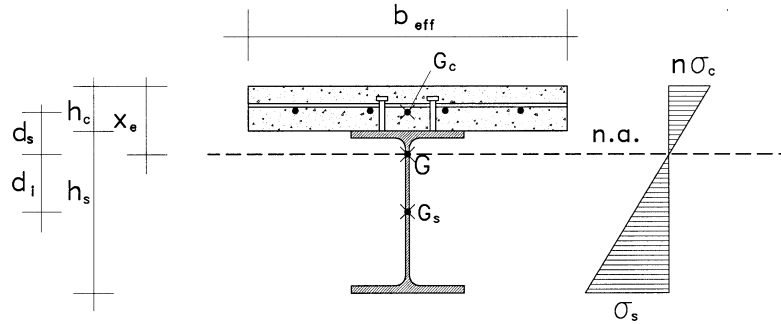


FIGURE 6.13: Elastic stress distribution with neutral axis in steel beam.

$$x_e = d_s + \frac{h_c}{2} \quad (6.7)$$

where

$$d_s = \frac{A_s}{A_s + b_{\text{eff}} \cdot h_c / n} \cdot \frac{h_c + h_s}{2}$$

where d_s is the distance between the centroid of the slab and the centroid of the transformed section;

$$I = I_s + \frac{1}{n} \frac{b_{\text{eff}} \cdot h_c^3}{12} + A^* \cdot \frac{(h_s + h_c)^2}{4} \quad (6.8)$$

where

$$A^* = \frac{A_s \cdot b_{\text{eff}} \cdot h_c / n}{A_s + b_{\text{eff}} \cdot h_c / n}$$

Extension of Equations 6.5 to 6.8 to beams with composite steel-concrete slabs is straightforward. The application to this case is provided by Example 6.2.

When the neutral axis depth and the second moment of area of the composite section are known, the maximum stress of concrete in compression and of structural steel in tension associated with a bending moment M are evaluated by the following expressions:

$$\sigma_c = \frac{1}{n} \frac{M}{I} \cdot x_e \quad (6.9)$$

$$\sigma_s = \frac{M}{I} \cdot (h_s + h_c - x_e) \quad (6.10)$$

These stresses must be lower than the relevant maximum design stresses allowed at the elastic limit condition. In the case of unshored construction, determination of the elastic stress distribution should take into account that the steel section alone resists all the permanent loads acting on the steelwork before composite action can develop.

In many instances, it is convenient to refer, in cross-sectional verifications, to the applied moment rather than to the stress distribution. Therefore, it is useful to define an “elastic moment of resistance” as the moment at which the strength of either structural steel or concrete is achieved. This elastic

limit moment can be determined as the lowest of the moments associated with the attainment of the elastic limit condition, and obtained from Equations 6.9 and 6.10 by imposing the maximum stress equal to the design limit stress values of the relevant material (i.e., that $\sigma_c = f_{c.d}$ and $\sigma_s = f_{y.s.d}$). As the nominal resistances are assumed as in the AISC specifications

$$M_{el} = \min \left\{ f_{c.d} \cdot \frac{n \cdot I}{x_e}, f_{y.s.d} \cdot \frac{I}{h_s + h_c - x_e} \right\} \quad (6.11)$$

The stress check is then indirectly satisfied if (and only if) it results:

$$M \leq M_{el} \quad (6.12)$$

where M is the maximum value of the bending moment for the load combination considered.

The elastic analysis approach, based on the transformed section concept, requires the evaluation of the modular coefficient n . Through an appropriate definition of this coefficient it is possible to compute the stress distribution under sustained loads as influenced by creep of concrete. In particular, the reduction of the effective stiffness of the concrete due to creep is reflected by a decrease of the modular ratio, and consequently the stress in the concrete slab decreases, while the stress in the steel section increases. Values can be obtained for the reduced effective modulus of elasticity $E_{c.ef}$ of concrete, accounting for the relative proportion of long- to short-term loads. Codes may suggest values of $E_{c.ef}$ defined accordingly to common load proportions in practice (see Section 6.2.1 for Eurocode 4 specifications). Selection of the appropriate modular ratio n would permit, in principle, the variation of the stress distribution in the cross-section to be checked at different times during the life of the structure.

6.3.4 Plastic Analysis

Refined non-linear analysis of the composite beam can be carried out accounting for yielding of the steel section and inelasticity of the concrete slab. However, the stress state typical of composite beams under sagging moments usually permits the plastic moment of the composite section to be achieved. In most instances the plastic neutral axis lies in the slab and the whole of the steel section is in tension, which results in:

- local buckling not being a critical phenomenon
- concrete strains being limited, even when the full yielding condition of the steel beam is achieved

Therefore, the plastic method of analysis is applicable to most simply supported composite beams. Such a tool is so practically advantageous that it is the non-linear design method for these members. In particular, this approach is based on equilibrium equations at ultimate, and does not depend on the constitutive relations of the materials and on the construction method. The plastic moment can be computed by application of the rectangular stress block theory. Moreover, the concrete may be assumed, in composite beams, to be stressed uniformly over the full depth x_{pl} of the compression side of the plastic neutral axis, while for the reinforced concrete sections usually the stress block depth is limited to $0.8 x_{pl}$. The evaluation of the plastic moment requires calculation of the following quantities:

$$F_{c,max} = 0.85b_{eff} \cdot h_c \cdot f_c \quad (6.13)$$

$$F_{s,max} = A_s \cdot f_{y.s} \quad (6.14)$$

These are, respectively, the maximum compression force that the slab can resist and the maximum tensile force that the steel profile can resist. If $F_{c,max}$ is greater than $F_{s,max}$, the plastic neutral axis lies

in the slab; in this case (Figure 6.14) the interaction force between slab and steel profile is $F_{s,max}$ and the plastic neutral axis depth is defined by a simple first order equation:

$$F_{c,max} > F_{s,max} \Rightarrow F_c = F_s = A_s \cdot f_{y,s} \quad (6.15)$$

$$0.85b_{eff} \cdot x_{pl} \cdot f_c = A_s \cdot f_{y,s} \quad (6.16)$$

$$x_{pl} = \frac{A_s \cdot f_{y,s}}{0.85b_{eff} \cdot f_c} \quad (6.17)$$

It can be observed that using stress block, the plastic analysis allows evaluation of the neutral axis

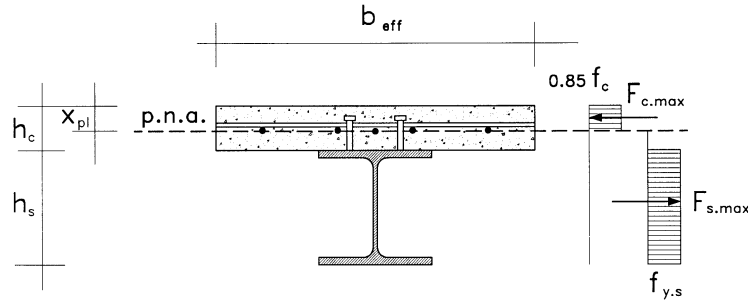


FIGURE 6.14: Plastic stress distribution with neutral axis in slab.

depth by means of an equation of lower degree than in the elastic analysis: in this last case Equation 6.5 the stresses have a linear distribution and the equation is of the second order. The internal bending moment lever arm (distance between line of action of the compression and tension resultants) is then evaluated by the following expression:

$$h^* = \frac{h_s}{2} + h_c - \frac{x_{pl}}{2} \quad (6.18)$$

The plastic moment can then be determined as:

$$M_{pl} = A_s \cdot f_{y,s} \cdot h^* \quad (6.19)$$

If $F_{s,max}$ is greater than $F_{c,max}$, the neutral axis lies in the steel profile (Figure 6.15); in this case it results:

$$F_{c,max} < F_{s,max} \Rightarrow F_c = F_s = 0.85b_{eff} \cdot h_c \cdot f_c \quad (6.20)$$

Two different cases can take place; in the first case:

$$F_c > F_w = d \cdot t_w \cdot f_{y,s} \quad (6.21)$$

where

t_w = the web thickness

d = the clear distance between the flanges

and:

$$M_{pl} \simeq F_{s,max} \cdot \frac{h_s}{2} + F_c \cdot \frac{h_c}{2} \quad (6.22)$$

In the second case:

$$F_c < F_w = d \cdot t_w \cdot f_{y,s} \quad (6.23)$$

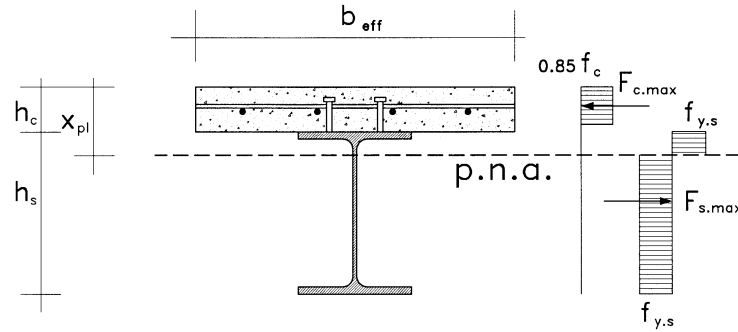


FIGURE 6.15: Plastic stress distribution with neutral axis in steel beam.

and:

$$M_{pl} = M_{pl.s} + F_c \cdot \frac{h_s + h_c}{2} - \frac{F_c^2}{4 \cdot t_w \cdot f_{y.s}} \quad (6.24)$$

where

$M_{pl.s}$ = the plastic moment of the steel profile

The design value of the plastic moment of resistance has to be computed in accordance to the format assumed in the reference code. If the Eurocode 4 provisions are used, in Equations 6.13 and 6.14, the “design values” of strength $f_{c.d}$ and $f_{y.s.d}$ shall be used (see Section 6.1.3) instead of the “unfactored” strength f_c and $f_{y.s}$; i.e., the design plastic moment given by Equation 6.19 is evaluated in the following way:

$$M_{pl.d} = A_s \cdot f_{y.s.d} \cdot h^* \quad (6.25a)$$

where h^* has to be computed with reference to the plastic neutral axis x_{pl} associated with design values of the material strengths.

If the AISC specification are considered, the nominal values of the material strengths shall be used and the safety factor $\phi_b = 0.9$ affects the nominal value of the plastic moment:

$$M_{pl.d} = \phi_b (A_s \cdot f_{y.s} \cdot h^*) \quad (6.25b)$$

6.3.5 Vertical Shear

In composite elements shear is carried mostly by the web of the steel profile; the contributions of concrete slab and steel flanges can be neglected in the design due to their width. The design shear strength can be determined by the same expression as for steel profiles:

$$V_{pl} = A_v \cdot f_{y.s.V} \quad (6.26)$$

where

A_v = the shear area of the steel section

$f_{y.s.V}$ = the shear strength of the structural steel

With reference to the usual case of I steel sections, and considering the different values assumed for $f_{y.s.V}$, the AISC and Eurocode specifications provide the same shear resistance; in fact:

$$\text{AISC} \quad V_{pl} = h_s \cdot t_w \cdot (0.6 \cdot f_{y.s}) \quad (6.27a)$$

$$\text{Eurocode} \quad V_{pl} = 1.04 \cdot h_s \cdot t_w \cdot \frac{f_{y.s}}{\sqrt{3}} \quad (6.27b)$$

and $(1.04 / \sqrt{3}) = 0.60$.

The design value of the plastic shear capacity is obtained either by multiplying the value of V_{pl} from Equation 6.27a by a Φ_v factor equal to 0.90 (AISC), or by using in Equation 6.27b the design value of $f_{y.s.d}$ (Eurocode).

For slender beam webs (i.e., when their depth-to-thickness ratio is lower than $69 / \sqrt{235/f_{y.s}}$ with $f_{y.s}$ in N/mm²) the shear resistance should be suitably determined by taking into account web buckling in shear.

The shear-moment interaction is not important in simply supported beams (in fact for usual loading conditions where the moment is maximum the shear is zero; where the shear is maximum the moment is zero). The situation in continuous beams is different (see Chapter 4).

6.3.6 Serviceability Limit States

The adequacy of the performance under service loads requires that the use, efficiency, or appearance of the structure are not impaired. Besides, the stress state in concrete also needs to be limited due to the possible associated durability problems. Micro-cracking of concrete (when stressed over $0.5 f_c$) may allow development of rebars corrosion in aggressive environments. This aspect has to be addressed with reference to the specific design conditions.

As to the member deformability, the stiffness of a composite beams in sagging bending is far higher than in the case of steel members of equal depth, due to the significant contribution of the concrete flange (see Equations 6.6 and 6.8). Therefore, deflection limitation is less critical than in steel systems. However, the effect of concrete creep and shrinkage has to be evaluated, which may significantly increase the beam deformation as computed for short-term loads. In service the beam should behave elastically. Under the assumption of full interaction the usual formulae for beam deflection calculation can be used. As an example, the deflection under a uniformly distributed load, p , is obtained as:

$$\delta = \frac{5}{384} \frac{p \cdot l^4}{E_s \cdot I} \quad (6.28)$$

For unshored beams, the construction sequence and the deflection of the steel section under the permanent loads has to be taken into account before development of composite action is added to the deflections of the composite beam under the relevant applied loads.

The value of the moment of inertia I of the transformed section, and hence the value of δ , depends on the modular ratio, n . Therefore, the effective modulus (EM) theory enables the effect of concrete creep to be incorporated in design calculations without any additional complexity. Determination of the deflection under sustained loads simply requires that an effective modular ratio $n_{ef} = E_s / E_{c.ef}$ is used when computing I via Equation 6.6 or 6.8.

The effect of the shrinkage strain ε_{sh} could be evaluated considering that the compatibility of the composite beam requires a tension force N_{sh} to develop in the slab equal to:

$$N_{sh} = \varepsilon_{sh} \cdot E_{c.ef} \cdot b \cdot h_c \quad (6.29)$$

This force is applied in the centroid of the slab and, due to equilibrium, produces a positive moment M_{sh} equal to:

$$M_{sh} = N_{sh} \cdot d_s \quad (6.30)$$

where d_s is given by Equation 6.7. This moment is constant along the beam. The additional deflection can be determined as:

$$\delta_{sh} = \frac{M_{sh} \cdot l^2}{8 \cdot E_s \cdot I} = 0.125 \cdot \varepsilon_{sh} \cdot \frac{b \cdot h_c \cdot d_s}{n_{ef} \cdot I} \cdot l^2 \quad (6.31)$$

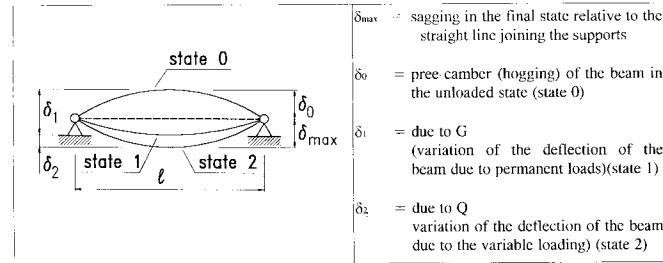
Typical values of ε_{sh} are given in Section 6.2.1. The influence of shrinkage on the deflection is usually important in a dry environment and for span-to-beam depth ratios greater than 20.

In partially composite beams, the deflection associated with the interface slip has also to be accounted for. A simplified treatment is presented in the Section on page 6-66.

The total deflection should be lower than limit values compatible with the serviceability requirements specific to the building system considered. Reference values given by the Eurocode 4 are presented in Table 6.2.

TABLE 6.2 Eurocode 4 Limiting Values for Vertical Deflections

Conditions	Limits	
	δ_{max}	δ_2
roofs generally	L/200	L/250
roofs frequently carrying personnel other than for maintenance	L/250	L/300
floors generally	L/250	L/300
floors and roofs supporting brittle finish on non-flexible partitions	L/250	L/350
floors supporting columns (unless the deflection has been included in the global analysis for the ultimate limit state)	L/400	L/500
* where δ_{max} can impair the appearance of the buildings	L/250	-
For cantilever: L = twice cantilever span		



The vibration control is strongly correlated to the deflection control. In fact it can be shown that the fundamental frequency of a simply supported floor beam is given by:

$$f = \frac{18}{\sqrt{\delta}} \quad (6.32)$$

where

δ = the immediate deflection (mm) due to the self weight. A value of f equal to 4 Hertz (cycles for second) may be considered acceptable for the comfort of people in buildings

6.3.7 Worked Examples³

EXAMPLE 6.1: Composite beam with solid concrete slab

In Figure 6.16 it is reported that the cross-section of a simply supported beam with a span length l equals 10 m; the steel profile (IPE 500) is characterized by $A_s = 11600 \text{ mm}^2$ and $I_s = 4.82 \cdot 10^8 \text{ mm}^4$. The solid slab has a thickness of 120 mm; the spacing with adjacent beams is 5000 mm. The beam is subjected to a uniform load $p = 40 \text{ kN/m}$ (16 kN/m of dead load, 24 kN/m of live load) at the serviceability condition. A shored construction is considered.

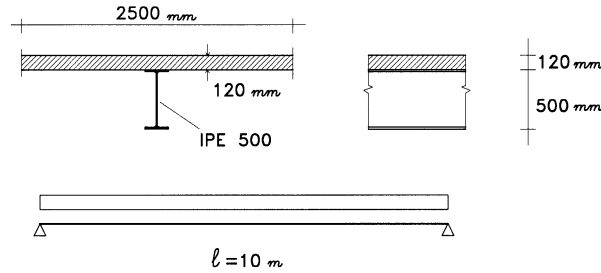


FIGURE 6.16: Cross-section of a simply supported beam with a span length l equals 10 m.

1. Determination of design moment:

The design moment for service conditions is

$$M = \frac{40 \cdot 10^2}{8} = 500 \text{ kNm}$$

For the ultimate limit state, considering a factor of 1.35 for the dead load and 1.5 for the live load, it is

$$M = \frac{(1.35 \cdot 16 + 1.5 \cdot 24) \cdot 10^2}{8} = 720 \text{ kNm}$$

2. Evaluation of the effective width (Section 6.3.2):

Applying Equation 6.4 it results:

$$b_{\text{eff}} = 2 \cdot \frac{l}{8} = 2 \cdot \frac{10000}{8} = 2500 \text{ mm}$$

Thus, only 2500 mm of 5000 mm are considered as effective.

3. Elastic analysis of the cross-section (Section 6.3.3):

The following assumptions are made:

³All examples refer to Eurocode rules, with which the authors are more familiar.

$$\begin{aligned} E_c &= 30500 \text{ N / mm}^2 \\ E_s &= 210000 \text{ N / mm}^2 \end{aligned}$$

Therefore, at the short time the modular ratio results:

$$n = \frac{210000}{30500} = 6.89$$

Equation 6.5 becomes:

$$\frac{1}{6.89} \frac{2500}{2} \cdot x_e^2 - 11600 \cdot \left(\frac{500}{2} + 120 - x_e \right) = 0$$

then:

$$\begin{aligned} 181.4x_e^2 + 11600 \cdot x_e - 4292000 &= 0 \\ x_e &= 125.1 \text{ mm} > 120 \text{ mm} \end{aligned}$$

i.e., the entire slab is under compression and Equation 6.7 shall be considered:

$$x_e = \frac{120}{2} + \frac{11600}{11600 + 120 \cdot 2500/6.89} \frac{120 + 500}{2} = 125.2 \text{ mm}$$

From Equation 6.8 it results:

$$\begin{aligned} A^* &= \frac{11600 \cdot 2500 \cdot 120/6.89}{11600 + 2500 \cdot 120/6.89} = 9160 \text{ mm}^2 \\ I &= \frac{1}{6.89} \frac{2500 \cdot 120^3}{12} + 4.82 \cdot 10^8 + 9160 \frac{(500 + 120)^2}{4} = 1.41 \cdot 10^9 \text{ mm}^4 \end{aligned}$$

The maximum stress in concrete and steel are the following (see Equations 6.9 and 6.10):

$$\begin{aligned} \sigma_c &= \frac{500 \cdot 10^6}{6.89 \cdot 1.41 \cdot 10^9} \cdot 125.2 = 6.4 \text{ N / mm}^2 \\ \sigma_s &= \frac{500 \cdot 10^6}{1.41 \cdot 10^9} \cdot (500 + 120 - 125.2) = 175.5 \text{ N / mm}^2 \end{aligned}$$

For the long term calculation, a creep coefficient $\phi = 2$ is assumed obtaining the following modular ratio:

$$n_{ef} = 6.89 \cdot 3 = 20.67$$

Equation 6.6 gives:

$$\begin{aligned} \frac{2500}{20.67 \cdot 2} \cdot x_e^2 - 11600 \cdot \left(\frac{500}{2} + 120 - x_e \right) &= 0 \\ 60.47 \cdot x_e^2 + 11600 \cdot x_e - 4292000 &= 0 \\ x_e &= 187.2 \text{ mm} > 120 \text{ mm} \end{aligned}$$

The elastic neutral axis lies in the steel profile web and the slab is entirely compressed. Therefore, it is (Equations 6.7, and 6.8):

$$\begin{aligned}x_e &= \frac{120}{2} + \frac{11600}{11600 + 120 \cdot 2500/20.67} \cdot \frac{120 + 500}{2} = 197.7 \text{ mm} \\A^* &= \frac{11600 \cdot 2500 \cdot 120/20.67}{11600 + 2500 \cdot 120/20.67} = 6447 \text{ mm}^2 \\I &= \frac{2500 \cdot 120^3}{20.67 \cdot 12} + 4.82 \cdot 10^8 + 6447 \cdot \frac{(500 + 120)^2}{4} = 1.12 \cdot 10^9 \text{ mm}^4\end{aligned}$$

The stresses result:

$$\begin{aligned}\sigma_c &= \frac{500 \cdot 10^6}{20.67 \cdot 1.12 \cdot 10^9} \cdot 197.7 = 4.3 \text{ N / mm}^2 \\ \sigma_s &= \frac{500 \cdot 10^6}{1.12 \cdot 10^9} \cdot (620 - 197.7) = 188.5 \text{ N / mm}^2\end{aligned}$$

The concrete stress decreases 33% while the steel stress increases 7%.

4. Plastic analysis of the cross-section (Section 6.3.4):

The design strength of materials are assumed as $f_{c,d} = 14.2 \text{ N/mm}^2$ (including the coefficient 0.85) for concrete and $f_{y,s,d} = 213.6 \text{ N/mm}^2$ for steel. By means Equations 6.13, and 6.14 it is:

$$\begin{aligned}F_{c,\max} &= 2500 \cdot 120 \cdot 14.2 = 4260000 \text{ N} = 4260 \text{ kN} \\ F_{s,\max} &= 11600 \cdot 213.6 = 2477760 \text{ N} = 2478 \text{ kN}\end{aligned}$$

Consequently, it is assumed:

$$F_c = F_s = 2478 \text{ kN}$$

and, considering the design strength in Equation 6.17:

$$x_{pl} = \frac{11600 \cdot 213.6}{2500 \cdot 14.2} = 69.8 \text{ mm}$$

The internal arm is (Equation 6.18):

$$h^* = \frac{500}{2} + 120 - \frac{69.8}{2} = 335 \text{ mm}$$

and the plastic moment results (Equation 6.19):

$$M_{pl} = 2478 \cdot 0.335 = 830 \text{ kNm}$$

Thus, the value of the plastic resistance is greater than the design moment at the ultimate conditions ($M = 720 \text{ kNm}$).

5. Ultimate shear of the section (Section 6.3.5):

$$\begin{aligned}A_v &= 1.04 \cdot 500 \cdot 10.2 = 5304 \text{ mm}^2 \\ V_{pl} &= 5304 \frac{213.6}{\sqrt{3}} = 654100 \text{ N} = 654 \text{ kN}\end{aligned}$$

6. Control of deflection (Section 6.3.6):

The deflection at short term is

$$\delta(t = 0) = \frac{5}{384} \cdot \frac{40 \cdot 10000^4}{210000 \cdot 1.41 \cdot 10^9} = 17.6 \text{ mm} = \frac{1}{568} \cdot l$$

The deflection at long term is increased by the creep and shrinkage effects. The 50% of the live load is considered as long term load; thus, in this verification the load is $16 + 0.5 \cdot 24 = 28 \text{ kN/m}$. If only the creep effect is taken into account, the following result is obtained:

$$\delta(t = \infty) = \frac{5}{384} \cdot \frac{28 \cdot 10000^4}{210000 \cdot 1.12 \cdot 10^9} = 15.5 \text{ mm}$$

As regards the shrinkage effect, a final value of the strain is assumed equal to

$$\varepsilon_{sh} = 200 \cdot 10^{-6}$$

and the increment of deflection due to shrinkage results (Equation 6.32):

$$\delta_{sh} = 0.125 \cdot 200 \cdot 10^{-6} \cdot \frac{120 \cdot 5000 \cdot (197.7 - 60)}{20.67 \cdot 1.12 \cdot 10^9} \cdot 10000^2 = 8.9 \text{ mm}$$

The final value of the deflection is

$$\delta(t = \infty) = 15.5 + 8.9 = 24.4 \text{ mm} = \frac{l}{410}$$

EXAMPLE 6.2: Composite beam with concrete slab with metal decking.

In Figure 6.17 it is reported that the cross-section of a simple supported beam with a span length l equals 10 m; the difference with the previous example consists in the use of a profiled steel sheeting. The structural steel (IPE 500) is characterized by $A_s = 11600 \text{ mm}^2$ and $I_s = 4.82 \cdot 10^8 \text{ mm}^4$. The slab thickness is $55 + 65 \text{ mm}$. The spacing of beams is 5000 mm. The beam is subjected to a uniform load $p = 40 \text{ kN/m}$ (16 kN/m of dead load, 24 kN/m of live load) at serviceability condition.

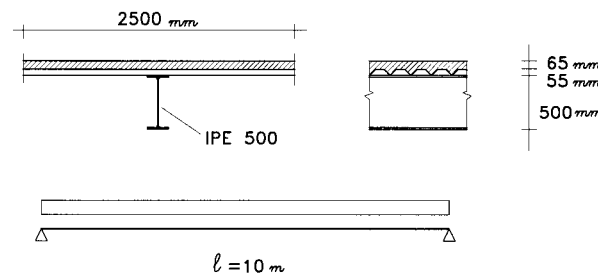


FIGURE 6.17: Cross-section of a simple supported beam with a span length l equals 10 m.

1. Determination of design moment:

The design moment for service conditions is

$$M = \frac{40 \cdot 10^2}{8} = 500 \text{ kNm}$$

For the ultimate limit state, considering a factor of 1.35 for the dead load and of 1.5 for the live load, it is

$$M = \frac{(1.35 \cdot 16 + 1.5 \cdot 24) \cdot 10^2}{8} = 720 \text{ kNm}$$

2. Evaluation of the effective width (Section 6.3.2):

$$b_{\text{eff}} = 2 \cdot \frac{10000}{8} = 2500 \text{ mm}$$

only 2500 of 5000 mm are considered as effective.

3. Elastic analysis of the cross-section (Section 6.3.3):

At a short time, the results are the following:

$$181.4x_e^2 + 11600 \cdot x_e - 4292000 = 0$$

$$x_e = 125.1 \text{ mm} > 65 \text{ mm}$$

i.e., the entire slab is under compression and Equation 6.7 shall be considered:

$$x_e = \frac{65}{2} + \frac{11600}{11600 + 65 \cdot 2500/6.89} \cdot \left(120 + \frac{500}{2} - \frac{65}{2}\right) = 143.8 \text{ mm}$$

$$I = \frac{2500 \cdot 65}{6.89} \cdot \left(143.8 - \frac{65}{2}\right) + \frac{2500 \cdot 65^3}{12 \cdot 6.89} + 4.82 \cdot 10^8$$

$$+ 11600 \cdot \left(\frac{500}{2} + 120 - 143.8\right) = 1.38 \cdot 10^9 \text{ mm}^4$$

$$\sigma_c = 7.6 \text{ N / mm}^2$$

$$\sigma_s = 172.5 \text{ N / mm}^2$$

For long term calculation it is

$$x_e = \frac{65}{2} + \frac{11600}{11600 + 65 \cdot 2500/20.67} \cdot \left(120 + \frac{500}{2} - \frac{65}{2}\right) = 233.7 \text{ mm}$$

The elastic neutral axis lies in the steel profile web and the slab is entirely compressed.

$$I = 1.02 \cdot 10^9 \text{ mm}^4$$

The stresses result:

$$\sigma_c = 5.5 \text{ N / mm}^2$$

$$\sigma_s = 189.4 \text{ N / mm}^2$$

The concrete stress decreases 28% while the steel stress increases 10%.

4. Plastic analysis of the section (Section 6.3.4):

$$F_{c,\text{max}} = 2500 \cdot 65 \cdot 14.2 = 2308000 \text{ N} = 2308 \text{ kN}$$

$$F_{s,\text{max}} = 11600 \cdot 213.6 = 2477760 \text{ N} = 2478 \text{ kN}$$

Consequently, it is

$$F_c = F_s = 2308 \text{ kN}$$

In this case

$$\begin{aligned} t_w &= 10.2 \text{ mm} & t_f &= 16 \text{ mm} \\ F_w &= (500 - 32) \cdot 10.2 \cdot 213.6 = 1019641/\text{N} = 1020 \text{ kN} \\ F_c &> F_w \end{aligned}$$

Therefore, the plastic neutral axis lies in the web of the steel profile:

$$M_{pl} \simeq 2308 \cdot \left(120 - \frac{65}{2}\right) + 2478 \cdot \frac{500}{2} = 821 \text{ kNm}$$

5. Ultimate shear of the section (Section 6.3.5):

$$\begin{aligned} A_v &= 1.04 \cdot 500 \cdot 10.2 = 5304 \text{ mm}^2 \\ V_{pl} &= 654 \text{ kN} \end{aligned}$$

6. Control of deflection (Section 6.3.6):

The control at short term provides:

$$\delta(t = 0) = 18 \text{ mm} = \frac{1}{556} \cdot l$$

The deflection at long term is increased by the creep and shrinkage effects. The 50% of the live load is considered as long term load; thus, in this verification the load is $16 + 0.5 \cdot 24 = 28 \text{ kN/m}$. If only the creep effect is taken into account, the following result is obtained:

$$\delta(t = \infty) = \frac{5}{384} \cdot \frac{28 \cdot 10000^4}{210000 \cdot 1.02 \cdot 10^9} = 17.0 \text{ mm}$$

As regards the shrinkage effect, a final value of the strain is assumed equal to:

$$\begin{aligned} \varepsilon_{sh} &= 200 \cdot 10^{-6} \\ \delta_{sh} &= 0.125 \cdot 200 \cdot 10^{-6} \cdot \frac{65 \cdot 5000 \cdot (233.7 - 32.5)}{20.67 \cdot 1.02 \cdot 10^9} \cdot 10000^2 = 7.8 \text{ mm} \end{aligned}$$

The final value of the deflection is

$$\delta(t = \infty) = 17.0 + 7.8 = 24.8 \text{ mm} = \frac{1}{403} \cdot l$$

6.4 Continuous Beams

6.4.1 Introduction

Beam continuity may represent an efficient structural solution with reference to both load capacity and stiffness. In composite buildings, different kinds of continuity may, in principle, be achieved, as indicated by Puhali et al. [40], between the beams and the columns and, possibly, between adjacent beams. Furthermore, the degree of continuity can vary significantly in relation to the performance of joints as to both strength and stiffness: joints can be designed to be full or partial strength (strength) and rigid, semi-rigid, or pinned (stiffness). Despite the growing popularity of semi-rigid partial strength joints (see Chapter 23), rigid joints may still be considered the solution most used in building frames. Structural solutions for the flooring system were also proposed (see for example Brett et al., [7]), which allow an efficient use of beam continuity without the burden of costly joints.

In bridge structures, the use of continuous beams is very advantageous for it enables joints along the beams to be substantially reduced, or even eliminated. This results in a remarkable reduction in design work load, fabrication and construction problems, and structural cost.

From the structural point of view, the main benefits of continuous beams are the following:

- at the serviceability limit state: deformability is lower than that of simply supported beams, providing a reduction of deflections and vibrations problems
- at the ultimate limit state: moment redistribution may allow an efficient use of resistance capacity of the sections under positive and negative moment.

However, the continuous beam is subjected to hogging (negative) bending moments at intermediate supports, and its response in these regions is not efficient as under sagging moments, for the slab is in tension and the lower part of the steel section is in compression. The first practical consequence is the necessity of an adequate reinforcement in the slab. Besides, the following problems arise:

- at the serviceability limit state: concrete in tension cracks and the related problems such as control of the cracks width, the need of a minimum reinforcement, etc., have to be accounted for in the design. Moreover, deformability increases reducing the beneficial effect of the beam continuity
- at the ultimate limit state: compression in steel could cause buckling problems either locally (in the bottom flange in compression and/or in the web) or globally (distortional lateral-torsional buckling)

Other problems can arise as well; i.e., in simply supported beams, the shear-moment interaction is usually negligible, while at the intermediate supports of continuous beams both shear and bending can simultaneously attain high values, and shear-moment interaction becomes critical.

In the following, the various aspects described above are discussed. In this Section the assumption of full shear-concrete interaction is still maintained, i.e., the shear connection is assumed to be a “full” shear connection (see Section 6.5). Problems related to use of the partial shear connection are discussed in detail in Section 6.5.7.

6.4.2 Effective Width

The general definition of the effective width, b_{eff} , is the same for the simply supported beam (Section 6.3.2). The determination of the effective width along a continuous beam is certainly a more complex problem. Besides the type of loading and geometrical characteristics, several other parameters are involved, which govern the strain (stress) state in the slab in the hogging moment regions. This complexity results in different provisions in the various national codes. However, it should be

noted that the variability of b_{eff} along the beam would imply, if accounted for, a substantial burden for design analysis. For a continuous composite beam, it was shown that the selection in the global analysis of a suitable effective width constant within each span allows us to obtain internal forces with satisfactory accuracy. On the other hand, sectional verification should be performed with reference to the “local” value of b_{eff} . The effective width in the moment negative zone allows evaluation of the reinforcement area that is effective in the section.

The AISC provisions suggest use of Equation 6.4, considering the full span length and center-to-center support for the analysis of continuous beams. No recommendations are provided for sectional verification.

Eurocode 4 also recommends that in the global analysis b_{eff} is assumed to be constant over the whole length of each span, and equal to the value at midspan. The resistance of the critical cross-sections is determined using the values of b_{eff} computed via Equation 6.4, where the length l is replaced by the length l_0 defined as in Figure 6.18. The effective width depends on the type of applied moment (hogging or sagging) and span (external, internal, cantilever). The value of b_{eff} in the hogging moment enables determination of the effective area of steel reinforcement to be considered in design calculations.

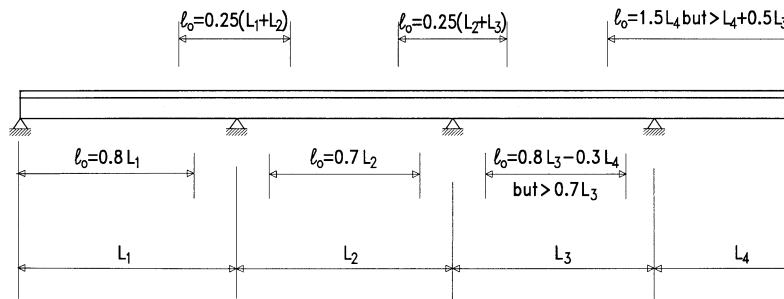


FIGURE 6.18: Equivalent span for effective width of concrete flange.

6.4.3 Local Buckling and Classification of Cross-Sections

Local buckling has to be accounted for in the very preliminary phase of design; due to the occurrence of local buckling, sections subjected to negative moment may not attain their plastic moment of resistance or develop the plastic rotation required for the full moment redistribution, associated with the formation of a beam plastic mechanism. In order to enable a preliminary assessment of strength and rotation capacity, steel sections can be classified according to the slendernesses of the flanges and of the web [10]. Four different member behaviors could be identified, according to the importance of local buckling effects:

1. members that develop the full plastic moment capacity and also possess a rotation capacity sufficient to make, in most practical cases, a beam plastic mechanism
2. members that can develop their plastic moment of resistance, but then have limited rotation capacity
3. members that achieve the elastic moment of resistance associated with yielding of steel in the more stressed fiber, but not the plastic moment of resistance

4. members for which local buckling occurs still in the elastic range, so that even the elastic limit moment cannot be developed and elastic local buckling govern resistance

In Figure 6.19, the four behaviors described above are schematically presented.

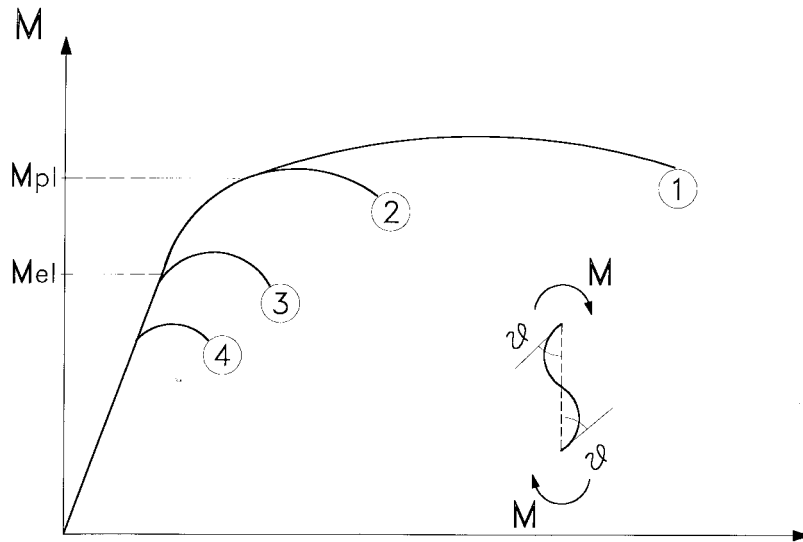


FIGURE 6.19: Different behaviors of composite members expressed in terms of moment-rotation ($M-\theta$) relationships.

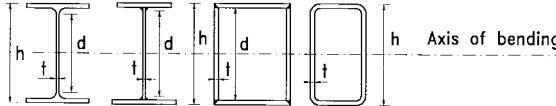
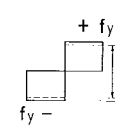
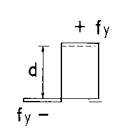
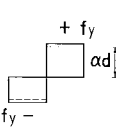
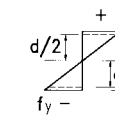
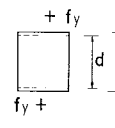
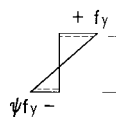
The definition of reliable limitations for the flange and web slenderness that take into account the different performances is a very complex problem both theoretically and experimentally. Besides, the wide range of possible geometries, the influence of the loading conditions and the mechanical characteristics of the steel material have to be considered. Moreover, the interaction with the lateral-torsional buckling mode in the distortional form has to be considered. The buckling problems depend not only on the flange and/or web slenderness but also on the mechanical ratio $f_{y,s}/E_s$; since the elasticity modulus E_s is constant for all steel grades, the yield strength $f_{y,s}$ can be assumed as the reference parameter taking into account steel grade. As a rule, the higher the yield strength, the lower the upper limit slenderness for a given class.

The complexity of the problem and the still limited knowledge available force code specifications to be based on rather conservative assumptions.

The classification limits specified by Eurocode 4 are reported in Tables 6.3 and 6.4. The four different behaviors are defined as “plastic – class 1”, “compact – class 2”, “semi-compact – class 3”, and “slender – class 4”. The limitations accounting for the fabrication processes are different for rolled and welded shapes; also, the presence of web encasement is allowed for by different limitations, which take into account the beneficial restraint offered by the encasing concrete.

The AISC specifications define only three classes. However, a fourth class is suggested for seismic use, due to the higher overall structural ductility required to dissipate seismic energy. The cross-sections are then classified as “seismic”, “compact”, “non compact”, and “slender”. The seismic sections guarantee a plastic rotation capacity (i.e., a rotational ductility defined as the ratio between the ultimate plastic rotation and the rotation at the onset of yield) in the range of 7 to 9, while the compact sections have a rotational ductility of at least 3. With reference to steel rolled I sections in

TABLE 6.3 Eurocode 4 Maximum Width-to-Thickness Ratios for Steel Webs

Webs: elements perpendicular to axis of bending				
				
Class	Web subject to bending	Web subject to compression	Web subject to bending and compression	
Stress distribution				
(compression positive)				
1	$d/t \leq 72 \epsilon$	$d/t \leq 33 \epsilon$	when $\alpha > 0.5$ $d/t \leq 396 \epsilon / (13 \alpha - 1)$ when $\alpha < 0.5$ $d/t \leq 36 \epsilon / \alpha$	
2	$d/t \leq 83 \epsilon$	$d/t \leq 38 \epsilon$	when $\alpha > 0.5$ $d/t \leq 456 \epsilon / (13 \alpha - 1)$ when $\alpha < 0.5$ $d/t \leq 41.5 \epsilon / \alpha$	
Stress distribution				
(compression positive)				
3	$d/t \leq 124 \epsilon$	$d/t \leq 42 \epsilon$	when $\psi > -1$ $d/t \leq 42 \epsilon / (0.67 + 0.33 \psi)$ when $\psi \leq -1$ $d/t \leq 62 \epsilon (1 - \psi) / \psi$	
$\epsilon = 235 / f_y$	f_y (N/mm ²)	235	275	355
	ϵ	1.0	0.92	0.81

pure bending moment, and using the same symbols as in Tables 6.3 and 6.4, the AISC slenderness limitations are given in Table 6.5, where $f_{y,s}$ represents the nominal strength of steel in ksi. The values associated with $f_{y,s}$ in N/mm² are also provided in brackets. The values provided by Eurocode 4 and AISC provisions show a good agreement when both Class 1 and Class 2 sections are compared to seismic and compact sections, respectively. The comparison between Class 3 and non-compact sections highlights that the values provided by Eurocode 4 are more restrictive.

6.4.4 Elastic Analysis of the Cross-Section

Cross-sectional behavior in sagging bending has been treated in Section 6.3.3 to which reference can be made.

In the negative moment regions, where the concrete slab is subject to tensile stresses, two main states of the composite beam can be identified with reference to the value of moment M_{cr} at which cracks start to develop. When the bending moment is lower than M_{cr} , the cross-section is in the “state 1 uncracked” and its uncracked moment of inertia I_1 can be evaluated by the same procedure of the section subjected to positive moment (see Section 6.3.3). When M is greater than M_{cr} the cross-section enters the “state 2 cracked”, characterized by the moment of inertia I_2 . In this phase, the elastic neutral axis x_e usually lies within the steel section, so that concrete does not collaborate

TABLE 6.4 Eurocode 4 Maximum Width-to-Thickness Ratios for Steel Outstanding Flanges in Compression

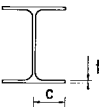
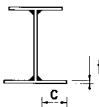
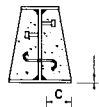
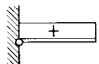

				
Rolled		Welded		Encased web
Class	Type	Web not encased		Web encased
Stress distribution (compression positive)				
1	Rolled Welded	$c/t \leq 10\epsilon$ $c/t \leq 9\epsilon$		$c/t \leq 10\epsilon$ $c/t \leq 9\epsilon$
2	Rolled Welded	$c/t \leq 11$ $c/t \leq 10\epsilon$		$c/t \leq 15\epsilon$ $c/t \leq 14\epsilon$
3	Rolled Welded	$c/t \leq 15\epsilon$ $c/t \leq 14\epsilon$		$c/t \leq 21\epsilon$ $c/t \leq 20\epsilon$
$\epsilon = 235 / f_y$	f_y (N/mm ²)	235	275	355
	ϵ	1.0	0.92	0.81

TABLE 6.5 Limitation to the Local Slenderness of AISC: Rolled I Sections

	c/t (flange)	d/t (web)
Seismic	$52 / \sqrt{f_{y,s}}$	$520 / \sqrt{f_{y,s}}$
	$(137 / \sqrt{f_{y,s}})$	$(1365 / \sqrt{f_{y,s}})$
Compact	$65 / \sqrt{f_{y,s}}$	$640 / \sqrt{f_{y,s}}$
	$(171 / \sqrt{f_{y,s}})$	$(1680 / \sqrt{f_{y,s}})$
Non-compact	$141 / \sqrt{f_{y,s} - 10}$	$970 / \sqrt{f_{y,s}}$
	$(370 / \sqrt{f_{y,s} - 10})$	$(2547 / \sqrt{f_{y,s}})$

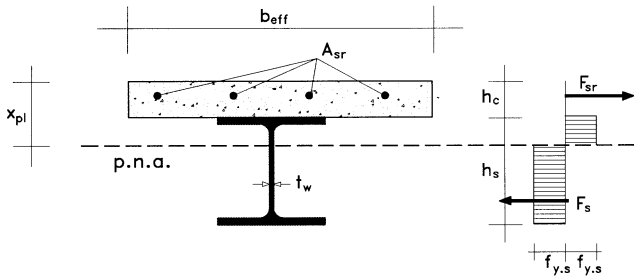


FIGURE 6.20: Plastic stress distribution under hogging moment.

to the stiffness and strength of the composite section. As a consequence, the effective cross-section of the composite beams consists only of steel (reinforcement bars and steel section). The moment of inertia I_2 and the stresses can be computed straightforwardly. The same general considerations apply to elastic verification of cracked composite beams, already discussed in Section 6.3.3 with reference to beams in sagging bending.

6.4.5 Plastic Resistance of the Cross-Section

In most cases, as already discussed, sections in positive bending have the neutral axis within the slab. The steel section is hence fully (or predominantly) in tension and plastic analysis can be applied, i.e., sections are in class 1 or 2 (compact). The stress block model, presented in Section 6.3.4 may be adopted for determining the plastic moment of resistance of the cross-section. Plastic analysis under hogging moment requires a preliminary classification of the cross-section as plastic or compact. The fully plastic stress distribution of the composite cross-section under hogging moments is shown in Figure 6.20: the location of the plastic neutral axis (i.e., the depth x_{pl}) is determined by imposing the equilibrium to the translation in the direction of the beam axis. Usually the neutral axis lies in the steel web, and the value of x_{pl} is given by the following expression:

$$x_{pl} = \frac{h_s}{2} + h_c - \frac{F_{sr}/2}{t_w f_{y.s}} \quad (6.33)$$

where F_{sr} is the plastic strength of the reinforcement:

$$F_{sr} = A_{sr} \cdot f_{y.sr} \quad (6.34)$$

The evaluation of the plastic moment is then carried out by imposing the equilibrium of the cross-section to the rotation respect to the neutral axis:

$$M_{pl} = M_{pl.s} + F_{sr} \cdot \left(\frac{h_s}{2} + h_c - c \right) - \frac{F_{sr}^2}{4t_w f_{y.s}} \quad (6.35)$$

where c is the concrete cover. It can be observed that the form of Equation 6.35 giving the hogging moment resistance M_{pl} is very similar to one Equation 6.25a obtained for the section in sagging bending, i.e., the plastic bending capacity of the composite section may be seen as the sum of the two contributions: the plastic moment of the steel section and the moment of the steel reinforcement.

The design value of M_{pl} can be obtained as:

- Eurocode 4:

$$M_{pl.d} = \frac{M_{pl.s}}{\gamma_s} + \frac{F_{sr}}{\gamma_{sr}} \cdot \left(\frac{h_s}{2} + h_c - c \right) - \frac{\gamma_s}{\gamma_{sr}^2} \frac{F_{sr}^2}{4t_w f_{y.s}} \quad (6.36)$$

- AISC

$$M_{pl.d} = 0.85 \cdot M_{pl} \quad (6.37)$$

The AISC specifications also cover the case of continuous members, where composite action is developed only in sagging moment, while the steel section alone resists in negative moment regions. In this case, consistently with specifications for steel members, the hogging design plastic resistance would be computed as:

$$M_{pl.d} = 0.90 M_{pl.s} \quad (6.38)$$

In the region of negative moment, the ultimate bending resistance might be reduced by “high” vertical shear. In the usual design model, which neglects the contribution of the slab to the vertical shear resistance (see Equation 6.26), the same upper limit value may be assumed for the applied shear as in steel sections, which exceeded the ultimate moment of resistance reduced by shear force. When shear buckling of the steel section web is not critical, this limit value is defined as a percentage of the plastic shear resistance V_{pl} .

The Eurocode 4 specifies it as $0.5V_{pl}$, with V_{pl} defined as in Equation 6.26: if the design shear V is higher than $0.5V_{pl}$, a part of the web is assumed to carry the shear force, therefore, a fictitious

reduced yield strength $f_{y,s,r}$ is used in the determination of the web contribution to the bending resistance:

$$f_{y,s,r} = f_{y,s} \cdot \left[1 - \left(\frac{2 \cdot V}{V_{pl}} - 1 \right)^2 \right] \quad (6.39)$$

where

$f_{y,s}$ = the yield strength of the web material

When $V = V_{pl}$, the bending resistance of the cross-section is equal to the plastic moment capacity of the part of the cross-section remaining after deduction of the web.

6.4.6 Serviceability Limit States

Global Analysis

Elastic calculation of the bending moment distribution under service load combinations is the preliminary step of the design analysis aimed at checking the member against serviceability limit states. As already mentioned, this verification, for continuous composite beams, has to consider many different aspects. A problem arises in performing the elastic analysis, due to change in stiffness of the hogging moment region caused by slab cracking. This problem is different than in reinforced concrete members: the stiffness reduction of a composite member, due to concrete cracking, takes place only in the hogging moment zone and it is very important resulting in a significant redistribution of moments, while in reinforced concrete continuous beam cracking occurs in positive moment zones as well; hence, the associated moment redistribution is usually not so remarkable.

In order to determine the bending moment distribution, the following three procedures may be adopted, which are presented in order of decreasing difficulty:

1. A non-linear analysis accounting for the tension stiffening effect in the cracked zone, and the consequent contribution to the section stiffness of the concrete between two adjacent cracks due to transferring of forces between reinforcement and concrete by means of bond. The effect of the slip between steel and concrete should also be taken into account in the case of partial shear connection.
2. An elastic analysis that assumes the beam flexural stiffness varies as schematically shown in model “a” of Figure 6.21: in the negative moment zone of the beam, where the moment is higher than the cracking one, the “cracked” stiffness $E I_2$ is used, while the “uncracked” stiffness $E I_1$ characterizes the remainder of the beam. In order to further simplify the procedure, the length of the cracked zone can be pre-defined as a percentage of α of the span l . Eurocode 4 recommends a cracking length equal to $0.15 l$.
3. An elastic uncracked analysis based on model “b” shown in Figure 6.21, which considers for the whole beam the “uncracked” stiffness $E I_1$ and accounts for the effect of cracking by redistributing the internal forces between the negative and positive moment regions; the redistribution allowed by the codes ranges from 10 to 15%.

The choice of the stiffness distribution model is a key design issue; in fact, a model that underestimates the beam stiffness over-estimates both the deflections and the moment redistribution, i.e., the procedure is on the safe side for the deformability control, but on the unsafe side for the resistance verification of the cross-sections.

The refined non-linear analysis (method 1 in the above) is particularly complex, and it is not covered in this chapter. Reference can be made to the literature (see for example [11, 12, 31]).

If method 2 is adopted, the analysis can be performed in a simple way by usual computer programs: an intermediate node should be added at the location of the cross-section where the moment is equal to the cracking moment and the beam state changes from the uncracked state (inertia I_1) to the

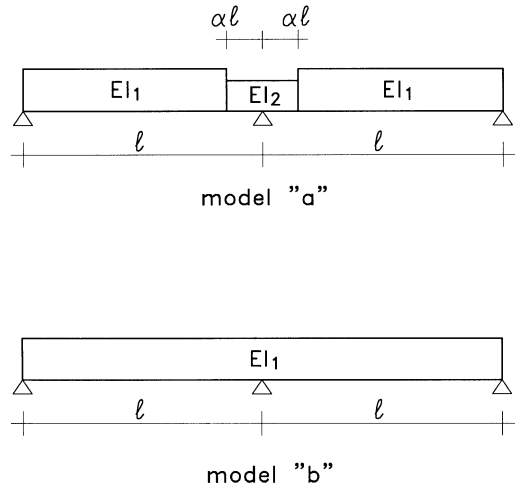


FIGURE 6.21: Stiffness distribution models for composite continuous beam design analysis.

cracked state (inertia I_2). When the value of the cracked length is not pre-defined, the position of this intermediate node varies with the applied load, due to the redistribution of moments.

As an alternative, a beam element can be used, the stiffness matrix of which takes into account the influence of cracking [13].

If this last approach is used, it is possible to develop simplified formulations for assessing the design value of moment redistribution to be adopted in associated uncracked analysis. By means of an example based on a continuous beam with two equal spans, Cosenza and Pecce [13] pointed out that the moment redistribution on the central support could be calculated by means of the following expression:

$$\frac{M_r}{M_e} = \frac{0.890 + 0.110i}{0.614 + 0.386i} \quad (6.40)$$

where

M_r = the moment after the redistribution

M_e = the elastic moment computed for the “uncracked” beam (Figure 6.22)

i = the ratio I_1/I_2

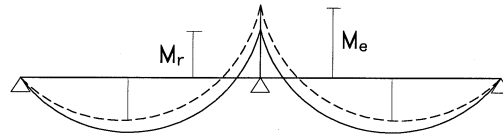


FIGURE 6.22: Bending moment diagram before and after redistribution.

This moment redistribution ratio, which is based on a value of α equal to 0.15, can be compared to the following formula:

$$\frac{M_r}{M_e} = i^{-0.35} \quad (6.40a)$$

provided by Eurocode 4.

The good agreement between Equation 6.40 and 6.40a is shown in Table 6.6.

TABLE 6.6 Evaluation of the Moment Redistribution Due to Cracking

		I_1/I_2			
		1	2	3	4
M_r/M_e	Equation 6.40	1	0.801	0.688	0.616
	Equation 6.40a	1	0.785	0.681	0.616

Stress Limitation

As already mentioned in Section 6.3.6, high stresses in the materials under service loads have to be prevented. High compression in concrete could cause microcracking and, consequently, durability problems; moreover, the creep effect can be very high, and even exceed the range of applicability of the linear theory with an unexpected increase of deflections. Analogously, yielding of steel in tension may lead to excessive beam deformation and increase crack widths in the hogging moment regions, resulting in a greater importance of rebars corrosion. Some codes provide limit stress levels for steel and concrete⁴, which should be considered as reference values to be appraised against specific design conditions.

Deflections

The most advantageous feature of composite continuous beams is the lower deformability with respect to simply supported beams. The greatest overall stiffness enables use of more slender floor systems, which meet serviceability deflection requirements due to continuity effect. The problem arises as to the accuracy of the determination of the beam deflection, which depends on the model adopted in the analysis. Some indication on the opposite influences of continuity and slab cracking on maximum deflections is useful. Some results are presented here with reference to a two span beam subjected to uniform loading. Spans may be different. By means of simple calculations, the following expressions of the midspan deflection can be obtained:

$$\frac{\delta}{\delta_{ss}} = \frac{0.129 + 0.285i + 0.001i^2}{0.614 + 0.386i} \quad (6.41)$$

$$\frac{\delta}{\delta_{i=1}} = \frac{0.311 + 0.687i + 0.002i^2}{0.614 + 0.386i} \quad (6.42)$$

which link the midspan deflection δ of the continuous beam with δ_{ss} ; which is, the deflection of a simply supported beam with the same mechanical and geometric characteristics; and $\delta_{i=1}$, which is the deflection evaluated considering the inertia I_1 constant along the whole of the beam. The first expression represents the reduction of deformability due to the continuity effect with respect to the simply supported beam; the second provides the increase of deformability due to cracking.

⁴Concrete stress is restricted to 50 to 60% of f_c , and stresses in the structural steel to 0.85 to 1.0 $f_{y.s}$.

Equation 6.42 can be written also in a simplified form: Cosenza and Pecce [13] proposed the following formula:

$$\frac{\delta}{\delta_{i=1}} = i^{0.29} \quad (6.43)$$

The comparison between Equations 6.41, 6.42, and 6.43 is reported in Table 6.7. Despite the significant adverse effect of the concrete cracking (the associated increase of deflection ranges from 27 to 43%), the reduction of deflection due to continuity remains substantial and greater for all cases considered to 40%.

TABLE 6.7 Calculation of Deflections in Continuous Beams

	I_1/I_2			
	1	2	3	4
δ/δ_{ss}	0.415	0.507	0.560	0.588
$\delta/\delta_{i=1}$	1	1.273	1.349	1.432
$i^{0.29}$	1	1.222	1.375	1.494

The influence of cracking should be considered as well in the case of long term effects (creep and shrinkage, see Section 6.3.6). A comparison between different methodologies is provided by Dezi and Tarantino [16, 17].

On the other hand, another effect that reduces the deflection is “tension stiffening”, i.e., the stiffening effect given by the concrete in tension between the cracks. This effect was analyzed in several studies (see for example [12, 26]), and it may be advantageously included in design when the associated additional complexity of calculations is justified by the importance of the design project.

Control of Cracking and Minimum Reinforcement

The width of the cracks caused in the slab by negative moments has to be checked if one or both of the following conditions are present:

- durability problems as in an aggressive environment
- aesthetic problems

Usually in buildings both problems are negligible because the environment internal to the building is rarely aggressive and, furthermore, the finishing of the floor somehow protects the slab against, and hides, the cracks. However, if durability and/or aesthetic problems exist, control is necessary. The crack width can be reduced by the following design criteria:

- using reinforcing bars with small diameters and spaced relatively closely
- restricting the stress in the reinforcement
- choosing the amount of reinforcement adequately, in order to avoid a very critical situation where the cracking moment is greater than the moment that leads to the yielding of the reinforcement

The nominal design value of the crack width is usually restrained to values ranging from 0.1 to 0.5 mm according to the various environmental situations. Direct evaluation of the crack width is obtained by multiplying the crack distance by the average strain in the reinforcement. This approach is recommended in aggressive environments. For its application, reference can be made to Eurocode 2 [1992]. The direct evaluation can be avoided if a minimum reinforcement between 0.4 and 0.6% of the concrete slab is employed. Moreover, the crack width, w , can be restricted to 0.3 (moderately

aggressive environment) or to 0.5 mm (little aggressive environment) if the stress limitations under service loads, reported in Table 6.8 as function of the rebars diameter (in mm), are fulfilled.

TABLE 6.8 Maximum Stress in the Steel Reinforcement to Limit Crack Width

σ_s N/mm ²	Rebar diameter (mm)	
	$w = 0.3$ mm	$w = 0.5$ mm
160	32	36
200	25	36
240	20	36
280	16	30
320	12	22
360	10	18
400	8	14
450	6	12

Additional Techniques to Limit Serviceability Problems

In some cases, the flexural capacity under negative moments cannot be sufficient with reference to serviceability limit states. Consequently, appropriate constructional methods can be adopted to solve these problems. In particular:

- Pre-imposed deformation at the intermediate supports can be applied to modify the moment distribution values of the hogging moment region. As a result, the maximum positive moment in the spans increases and the cross-section under positive moment has to be checked.
- The slab in the negative moment zone of the beam can be prestressed, either by the usual post-tension reinforcement included in a duct or by external prestressing cables.

In both construction techniques, which are generally adopted in bridge construction, creep and shrinkage of concrete reduce the effects of imposed deformations. Therefore, these phenomena should be taken into account in design, also by means of simplified calculation procedures [16, 17]. It is evident that the aforementioned techniques provide benefits with reference to the ultimate limit states as well.

6.4.7 Ultimate Limit State

Different methods can be adopted to analyze the structure in ultimate conditions, the main features of which are summarized in the following.

Plastic Analysis

The requirement that all relevant cross-sections are plastic or compact may not be sufficient for a composite beam to achieve the plastic collapse condition. It has been proven [27] that the rotational capacity is sufficient to develop the collapse mechanism only if further particular limitations are met as to the structural regularity, the loading pattern, and the lateral restraint. The limitations, more in detail, are the following:

- Adjacent spans do not differ in length by more than 50% of the shorter span, and end spans do not exceed 15% of the length of the adjacent span.

- In any span in which more than half of the total design load is concentrated within a length of one-fifth of the span, at any hinge location under sagging moment, no more than 15% of the overall depth of the member is in compression.
- The steel flange under compression at a plastic hinge location is laterally restrained.

If these requirements are fulfilled, the limit design approach can be applied in design analysis. In this case, at the ultimate limit condition in the external spans, there is the following relation between the total applied load, p , and the negative and positive plastic moment of resistance of the beam (Figure 6.23a):

$$M_{pl}^{(+)} + \frac{1}{2} M_{pl}^{(-)} \cong \frac{pl^2}{8} \quad (6.44)$$

Whereas in the intermediate spans, it is (Figure 6.23b)

$$M_{pl}^{(+)} + M_{pl}^{(-)} = \frac{pl^2}{8} \quad (6.45)$$

The static advantages are remarkable with respect to the case of a simply supported beam. For

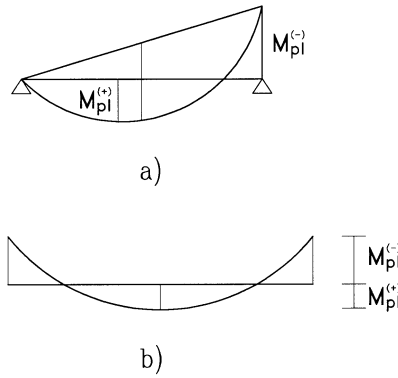


FIGURE 6.23: Structural model for plastic analysis. (a) External span. (b) Internal span.

example, Equation 6.44 suggests for a beam with one fixed end and one supported end that has the same type of behavior of a continuous beam with two symmetrical spans, an increment of the ultimate load capacity of approximately $0.5 M_{pl}^{(-)}$. However, the redistribution of bending moment required to cause the formation of the plastic mechanism is very large; the degree of redistributions is defined as the reduction of the elastic negative moment necessary to obtain the final moment in the mechanism situation, i.e., $M_{pl}^{(-)}$ divided by the initial value of elastic moment:

$$r = \frac{pl^2/8 - M_{pl}^{(-)}}{pl^2/8} = 1 - \frac{M_{pl}^{(-)}}{pl^2/8} \quad (6.46)$$

The degree of redistribution also depends on the ratio, m , between the negative and positive plastic moments of resistance of the beam:

$$m = \frac{M_{pl}^{(-)}}{M_{pl}^{(+)}} \quad (6.47)$$

In the case of a symmetrical two-span continuous beam under uniform loading, the use of Equations 6.44 through 6.46 enables the following relation to be established between r and m :

$$r = \frac{2 - m}{2 + m} \quad (6.48)$$

This relation provides the value of the redistribution, r , necessary to achieve the full mechanism condition in a continuous beam as a function of the ratio, m , between the plastic moments. The values of r associated with selected values of m are presented in Table 6.9. Since m is always less than 1,

TABLE 6.9 Relationship Between Redistribution Degree and Plastic Moment Ratio to Achieve the Plastic Mechanism Condition

m	0.1	0.2	0.3	0.4	0.5	0.6	0.7	0.8	0.9	1
r	90%	82%	74%	67%	60%	54%	48%	43%	38%	33%

except if very large amounts of reinforcement are placed in the slab (the practical values of m vary between 0.4 and 0.7), r results between 50% and 70%. Thus, in many instances, the development of a full plastic mechanism requires such a high moment redistribution that the corresponding service loads would almost cause problems of excessive stress, deflections, cracking, i.e., the serviceability limit states would govern design.

Non-Linear Analysis

If the limitation on the regularity and loading conditions required for applying the plastic analysis are not met, a large redistribution can still be considered up to the formation of a mechanism, if a refined non-linear analysis is performed. As already mentioned, refined methods of analysis are available in the literature [11, 14, 31], while detailed recommendations for use in practice are not yet available. As a general step-by-step procedure, the following approach can be outlined:

1. Cracking of the negative moment zone is accounted for and inelasticity is concentrated in the relevant locations. The plastic rotations associated with the ultimate design load combination, or the mechanism formation, are then determined.
2. The required plastic rotations are compared to the allowable ones.

A refined analysis also allows performance in the serviceability conditions to be checked, since the response of the beam is followed by a step-by-step procedure.

Linear Analysis with Redistribution

The simplified design approach, which combines elastic linear analysis with redistribution of internal forces, can be adopted also for the verifications at ultimate. The amount of redistribution allowed depends on:

- The type of linear analysis: if an uncracked analysis has been performed, the allowable redistribution is higher, since it also has to take into account the effect of cracking.
- The class of the sections: the available plastic rotations are different for plastic, compact, or semi-compact sections, so the allowable redistribution is also different.

Eurocode 4 specifies maximum allowed degrees of the redistribution shown in Table 6.10. The differences between the redistribution accepted in uncracked analysis and the redistribution accepted in cracked analysis is the estimated redistribution due to cracking. This difference varies between

10 and 15%. It is worth noticing that the maximum redistribution is 40% in the uncracked analysis and 25% in the cracked analysis. These values may appear very high, but as already observed in Section 6.4.7 for attaining the plastic sagging moment at midspan (which is usually much higher than the negative one), an even larger redistribution is necessary; on the other hand, higher values of the redistribution are not compatible with the verifications at the serviceability condition.

TABLE 6.10 Allowable Redistribution in Linear Analysis

	class 1	class 2	class 3	class 4
Cracked analysis	25%	15%	10%	-
Uncracked analysis	40%	30%	20%	10%

6.4.8 The Lateral-Torsional Buckling

Under hogging moments, a substantial part of the steel cross-section is stressed in compression, and lateral-torsional buckling can occur. The restraint offered by the concrete slab, which is usually very stiff and continuously connected to the steel section through the shear connectors, prevents this type of buckling from developing in the usual mode characterized by the lateral and torsional displacement of the member. Lateral-torsional buckling in composite beams takes the form of “lateral-distortional” buckling, as described in Figure 6.24.

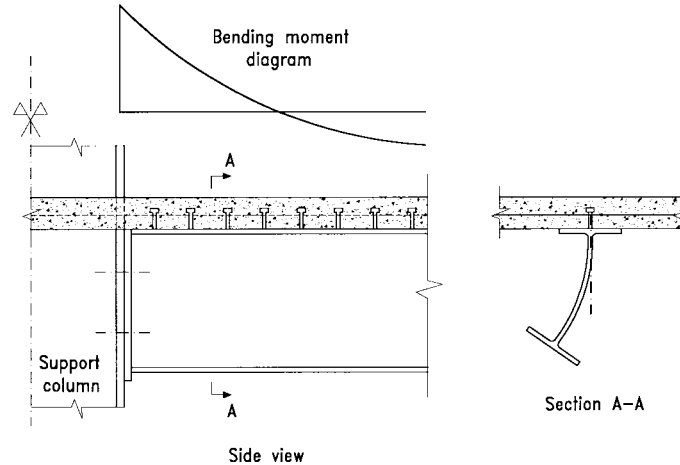


FIGURE 6.24: Distortional buckling of composite beam in a hogging moment zone.

This very complex problem received attention by a few researchers, who developed sophisticated methods of analysis [6, 22, 37, 48].

From a practical point of view, the usual formulations for lateral-torsional buckling can be applied with appropriate modifications to account for the restraint offered by the slab. For example, Eurocode 4 provisions suggest the same approach of the usual lateral-torsional buckling varying the buckling length of the beam in a suitable way. Such a simplified approach is not applicable to sections

with high depth for which a numerical analysis is necessary. In most instances the critical load associated with distortional buckling is usually higher than the “lateral-torsional” one and this problem is often negligible for the shapes commonly used in building structures. A parametric analysis [ECCS, 1993] showed that IPE and HE types, characterized by depths higher than the values provided by Table 6.11, have to be checked against distortional buckling.

TABLE 6.11 Limit Values of Steel Section Depth to Avoid Distortional Buckling

Steel member	$d_{s,lim}$ (mm)	
	$f_{y,s} < 240 \text{ N/mm}^2$	$f_{y,s} < 360 \text{ N/mm}^2$
IPE	600	400
HEA	800	650
HEB	900	700
Encased beam	1000	1000

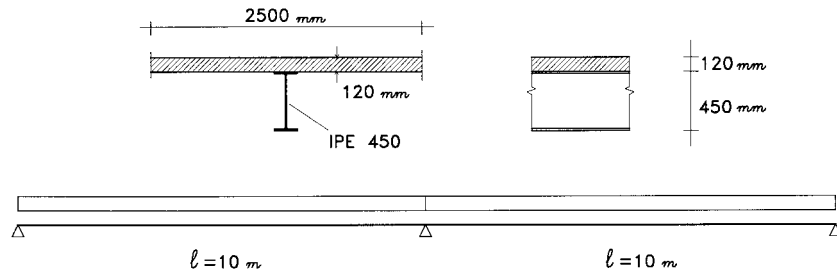


FIGURE 6.25: Cross-section of a continuous beam with two equal spans.

6.4.9 Worked Examples

EXAMPLE 6.3:

In Figure 6.25 it is reported that the cross-section of a continuous beam with two equal spans has a span length of l equal to 10 m; the steel profile (IPE 450) is characterized by $A_s = 9880 \text{ mm}^2$, $I_s = 3.37 \cdot 10^8 \text{ mm}^4$, $t_w = 9.4 \text{ mm}$, $t_f = 14.6 \text{ mm}$. The solid slab has a thickness of 120 mm; the spacing with adjacent beams is 5000 mm. The reinforcement of slab in the negative moment zone is realized by bars of diameter 14 mm with interspacing 250 mm. The beam is subjected to a uniform load $p = 40 \text{ kN/m}$ (16 kN/m of dead load, 24 kN/m of live load) at the serviceability condition. The material has the following design strength:

- concrete 14.2 N/mm^2 (including the coefficient 0.85)
- structural steel 213.6 N/mm^2
- reinforcement steel 365.2 N/mm^2

For the service state, the design load is

$$p = 16 + 24 = 40 \text{ kN / m}$$

For the ultimate limit state, considering a factor of 1.35 for the dead load and 1.5 for the live load, it is

$$p = 1.35 \cdot 16 + 1.5 \cdot 24 = 57.6 \text{ kN / m}$$

1. Determination of design moment:

Considering the “uncracked analysis”, the negative design moment for service conditions is

$$M^{(-)} = \frac{40 \cdot 10^2}{8} = 500 \text{ kNm}$$

At the ultimate state it is

$$M^{(-)} = \frac{57.6 \cdot 10^2}{8} = 720 \text{ kNm}$$

• Ultimate limit state

1. Evaluation of the effective width (Section 6.4.2):

Applying Equation 6.4, it results:

$$b_{\text{eff}} = 2 \cdot \frac{1}{8} = 2 \cdot \frac{10000}{8} = 2500 \text{ mm}$$

Thus, only 2500 of 5000 mm are considered as effective and $A_{sr} = 1540 \text{ mm}^2$.

2. Plastic negative moment resistance:

The plastic resistance of the section in the negative moment is evaluate according to Section 6.4.5

$$\begin{aligned} F_{sr} &= 1540 \cdot 365.2 = 5.62 \cdot 10^5 \text{ N} \\ x_{pl} &= \frac{450}{2} + 120 - \frac{5.62 \cdot 10^5}{2 \cdot 9.4 \cdot 213.6} = 205 \text{ mm} \\ M_{pl.s} &= 363.5 \cdot 10^6 \text{ N} = 363.5 \text{ kNm} \\ M_{pl}^{(-)} &= 363.5 \cdot 10^6 + 5.62 \cdot 10^5 \cdot \left(\frac{450}{2} + 120 - 30 \right) \\ &\quad - \frac{(5.62 \cdot 10^5)^2}{4 \cdot 9.4 \cdot 213.6} = 501 \cdot 10^6 \text{ Nm} = 501 \text{ kNm} \end{aligned}$$

3. Plastic shear resistance of the cross-section:

$$\begin{aligned} A_v &= 1.04 \cdot 450 \cdot 9.4 = 4399 \text{ mm}^2 \\ V_{pl} &= 4399 \frac{213.6}{\sqrt{3}} = 542494 \text{ N} = 542 \text{ kN} \end{aligned}$$

Safely the maximum shear at the ultimate state is evaluated by the uncracked analysis without considering the redistribution of bending moment; it is

$$V = \frac{57.6 \cdot 10}{2} + \frac{720}{10} = 360 \text{ kN}$$

Thus, the shear verify is satisfied.

4. Bending-shear interaction:

V results greater than $V_{pl}/2$; thus, the strength of the web is reduced by the following factor:

$$-\left(2 \cdot \frac{V}{V_{pl}} - 1\right)^2 = 1 - \left(2 \cdot \frac{360}{542} - 1\right)^2 = 0.892$$

thus leading to a design reduced strength:

$$f_{y.s.d.r} = 0.892 \cdot 213.6 = 190 \text{ N / mm}^2$$

The evaluation of the reduced moment resistance results:

$$x_{pl} = \frac{450}{2} + 120 - \frac{5.62 \cdot 10^5}{2 \cdot 9.4 \cdot 191} = 188 \text{ mm}$$

$$M_{pl}^{(-)} = 363.5 \cdot 10^6 + 5.62 \cdot 10^5 \cdot \left(\frac{450}{2} + 120 - 30\right) - \frac{(5.62 \cdot 10^5)^2}{4 \cdot 9.4 \cdot 190} = 497 \text{ kNm}$$

5. Check of the section class (Section 6.4.3):

- for the flange

$$c/t_f = 69.3/14.6 = 4.7 < 10 \cdot 1 \rightarrow \text{class 1}$$

- for the web

$$\alpha = \frac{450 - 205 - 35.6}{378.8} = 0.55$$

$$d/t_w = 378.8/9.4 = 40.3 < 396/(13 \cdot 0.55 - 1) = 64.4 \rightarrow \text{class 1}$$

Thus, the steel profile is in class 1 (Tables 6.3 and 6.4).

6. Plastic positive moment resistance:

By means of Equations 6.13 and 6.14 it is

$$F_{c.\max} = 2500 \cdot 120 \cdot 14.2 = 4260000 \text{ N} = 4260 \text{ kN}$$

$$F_{s.\max} = 9880 \cdot 213.6 = 2110368 \text{ N} = 2110 \text{ kN}$$

Consequently, it is assumed:

$$F_c = F_s = 2110 \text{ kN}$$

and, considering the design strength in Equation 6.17:

$$x_{pl} = \frac{9880 \cdot 213.6}{2500 \cdot 14.2} = 59.4 \text{ mm}$$

the neutral axis lies on the slab. The internal arm is (Equation 6.18):

$$h^* = \frac{450}{2} + 120 - \frac{59.4}{2} = 315 \text{ mm}$$

and the design plastic moment results (Equation 6.19):

$$M_{pl}^{(+)} = 2110 \cdot 0.315 = 665 \text{ kNm}$$

7. Required redistribution:

To satisfy the verify to plastic negative resistance, the following redistribution is required:

$$r = 1 - \frac{497}{720} = 31\%$$

that is, less than the value 40% that is possible for class 1 sections and uncracked analysis (Table 6.10). In the midspan the maximum positive moment, by equilibrium, is

$$M_d^{(+)} = 238 \cdot 4.1 - \frac{57.6 \cdot 4.1^2}{2} = 492 \text{ kNm}$$

assuming the reaction of the support and the abscissa of maximum moment the following values:

$$R = \frac{57.6 \cdot 10}{2} - \frac{497}{10} = 238 \text{ kN} \quad z_{M_{\max}} = \frac{238}{57.6} = 4.1 \text{ m}$$

It results:

$$M_d^{(+)} = 492 \text{ kNm} < M_{pl}^{(+)} = 665 \text{ kNm}$$

8. Flexural-torsional buckling:

In this case the control is not necessary because the steel profile depth is lower than the limit depth provided in Table 6.11 for IPE sections ($h_s = 450 \text{ mm} < d_{s,\text{lim}} = 600 \text{ mm}$).

- Serviceability limit state.

The following assumptions are made:

$$\begin{aligned} E_c &= 30500 \text{ N / mm}^2 \\ E_s &= 210000 \text{ N / mm}^2 \end{aligned}$$

Therefore, at the short time the modular ratio results:

$$n = \frac{210000}{30500} = 6.89$$

Neglecting the contribution of the reinforcement, the state 1 uncracked is characterized by the following parameters:

$$\begin{aligned} A^* &= \frac{9880 \cdot 2500 \cdot 120/6.89}{9880 + 2500 \cdot 120/6.89} = 8053 \text{ mm}^2 \\ I_1 &= \frac{1}{6.89} \frac{2500 \cdot 120^3}{12} + 3.37 \cdot 10^8 + 8053 \frac{(450 + 120)^2}{4} = 1.04 \cdot 10^9 \text{ mm}^4 \end{aligned}$$

After concrete cracking in the negative moment zone, it is necessary to consider the cracked state, leading to:

$$\begin{aligned} x_e &= 30 + \frac{9880 \cdot (450/2 + 120 - 30)}{9880 + 1540} = 302 \text{ mm} \\ I_2 &= 1540 \cdot (302 - 30)^2 + 9880 \cdot (302 - 120 - 450/2)^2 + 3.37 \cdot 10^8 \\ &= 4.69 \cdot 10^8 \text{ mm}^4 \end{aligned}$$

Thus, the parameter i given in Section 6.4.6 is:

$$i = \frac{1.04 \cdot 10^9}{4.69 \cdot 10^8} = 2.2$$

For the long term calculation, a creep coefficient $f = 2$ is assumed obtaining the following modular ratio:

$$n_{ef} = 6.89 \cdot 3 = 20.67$$

and then, in the uncracked state:

$$\begin{aligned} x_e &= \frac{120}{2} + \frac{9880}{9880 + 120 \cdot 2500/20.67} \frac{450 + 120}{2} = 175 \text{ mm} \\ A^* &= \frac{9880 \cdot 2500 \cdot 120/20.67}{9880 + 2500 \cdot 120/20.67} = 5878 \text{ mm}^2 \\ I_1 &= \frac{1}{20.67} \frac{2500 \cdot 120^3}{12} + 3.37 \cdot 10^8 + 5878 \frac{(450 + 120)^2}{4} = 8.32 \cdot 10^8 \text{ mm}^4 \end{aligned}$$

In the cracked state, the section has no variation, thus, leading to:

$$i = \frac{8.32 \cdot 10^8}{4.69 \cdot 10^8} = 1.8$$

1. Redistribution due to cracking

At short term ($t = 0$), according to Equation 6.40, it results:

$$\frac{M_r}{M_e} = \frac{0.890 + 0.110 \cdot 2.2}{0.614 + 0.386 \cdot 2.2} = 0.77$$

Using the simplified Equation 6.40a it is

$$\frac{M_r}{M_e} = i^{-0.35} = 2.2^{-0.35} = 0.76$$

obtaining very similar results. In the case of long term condition ($t = \infty$), the results are

$$\begin{aligned} \frac{M_r}{M_e} &= \frac{0.890 + 0.110 \cdot 1.8}{0.614 + 0.386 \cdot 1.8} = 0.83 \\ \frac{M_r}{M_e} &= i^{-0.35} = 1.8^{-0.35} = 0.81 \end{aligned}$$

2. Stress control

In the negative moment zone, considering the redistribution due to cracking, it is
 $t = 0$

$$\begin{aligned} \sigma_s &= \frac{500 \cdot 10^6 \cdot 0.77}{4.69 \cdot 10^8} \cdot (450 + 120 - 302) = 220 \text{ N / mm}^2 \\ \sigma_{sr} &= \frac{500 \cdot 10^6 \cdot 0.77}{4.69 \cdot 10^8} \cdot (302 - 30) = 223 \text{ N / mm}^2 \end{aligned}$$

$$t = \infty$$

$$\begin{aligned}\sigma_s &= \frac{500 \cdot 10^6 \cdot 0.83}{4.69 \cdot 10^8} \cdot (450 + 120 - 302) = 237 \text{ N / mm}^2 \\ \sigma_{sr} &= \frac{500 \cdot 10^6 \cdot 0.83}{4.69 \cdot 10^8} \cdot (302 - 30) = 240 \text{ N / mm}^2\end{aligned}$$

3. Control of deflections:

Considering Equation 6.41, it follows: $t = 0$

$$\begin{aligned}\frac{\delta}{\delta_{ss}} &= \frac{0.129 + 0.285 \cdot 2.2 + 0.001 \cdot 2.2^2}{0.614 + 0.386 \cdot 2.2} = 0.52 \\ \delta_{ss} &= \frac{5}{384} \cdot \frac{40 \cdot 10000^4}{210000 \cdot 1.04 \cdot 10^9} = 24 \text{ mm}\end{aligned}$$

and then:

$$\delta(t = 0) = 0.52 \cdot 24 = 12 \text{ mm} \quad \delta = \frac{1}{833} \cdot l$$

The deflection at long term is increased by the creep; the effect of shrinkage in the hyperstatic system is considered negligible. Safely the entire live load is considered as long term load. The following result is obtained ($i = 1.8$):

$$\begin{aligned}\frac{\delta}{\delta_{ss}} &= \frac{0.129 + 0.285 \cdot 1.8 + 0.001 \cdot 1.8^2}{0.614 + 0.386 \cdot 1.8} = 0.49 \\ \delta_{ss} &= \frac{5}{384} \cdot \frac{40 \cdot 10000^4}{210000 \cdot 8.32 \cdot 10^8} = 30 \text{ mm} \\ \delta(t = \infty) &= 0.49 \cdot 30 = 15 \text{ mm} = \frac{1}{680} l\end{aligned}$$

4. Control of cracking and minimum reinforcement:

Using Table 6.8, the crack width results is less than 0.3 mm; the interpolation of the limitations referred to diameter 16 and 12 leads to a stress limit of 300 N/mm² that is higher than the reinforcement stress at the serviceability condition.

6.5 The Shear Connection

The mutual transfer of forces between the steel and concrete components is the key mechanism, which makes composite action possible. This mechanism generally involves a complex combination of forces (or stresses) acting at the steel concrete interface. In design, the main attention is focused on the forces (or stresses) parallel to interface, i.e., on the longitudinal shear forces (and stresses). The components of the interface forces perpendicular to the interface, which may play a significant role in the transfer mechanism, are principally considered through the selection of suitable detailing.

It can be stated that the shear connection is a factor of substantial importance and, in many instances, it permits achievement of the required performance. Therefore, a substantial research effort has been devoted to the development of the fundamental knowledge of the response and

performance of the different shear connections available or proposed for practical use. The basics of this knowledge are presented in this chapter, with main reference to provide design oriented information.

Preliminary to any treatment of the behavioral features and design criteria of the shear connection, it seems convenient to give some useful definitions and classifications based on the key behavioral parameters of stiffness, strength, and ductility:

- Stiffness: a shear connection realizes either full interaction (the connection is “rigid” and no slip occurs under stress at the steel-concrete interface) or partial interaction (the connection is flexible and interface slip occurs).
- Resistance: when the overall resistance of the connection can be conveniently considered as in plastic design, a full connection has the shear strength sufficient to make the composite structural element (beam or slab) to develop its ultimate flexural resistance before collapse is achieved. If this condition is not fulfilled, the connection is a partial connection. A structural element with full shear connection is a fully composite structural element. A structural element with partial shear connection is a partially composite structural element. The ratio $F_c/F_{c,f}$ between the resistance of the shear connection and the minimum resistance required by the full connection condition defines the degree of shear connection.
- Finally, a connection is ductile if its deformation (slip) capacity is adequate for a complete redistribution of the forces acting on the individual connectors. The ductility demand depends on the span and the degree of shear connection.

The behavioral parameters relevant to the type of analysis adopted in design (i.e., elastic, inelastic, or plastic analysis) have to be considered. In particular, connection flexibility should be accounted for in elastic and inelastic analyses, which would make design rather complex. However, the simplified assumption of full interaction is satisfactory for most shear connections used in practice: the effect of slip is in fact negligible.

6.5.1 The Shear Transfer Mechanisms

Various forms of shear transfer can be identified for nature and effectiveness, namely:

- adhesion and chemical bond
- interface friction
- mechanical interlock
- dowel action

Shear transfer via adhesion and bond has the non-negligible advantage of being associated with no steel-concrete slip. However, tests show a rather low maximum shear resistance, which decreases rapidly and, remarkably, in the post-ultimate range of response. Moreover, this form of shear strength is highly dependent on factors, such as the quality of the steel surface and the concrete shrinkage, the control and quantification of which is difficult, if at all possible. Therefore, low values have to be assumed in design for the bond strength. Nevertheless, bond might be sufficient when the demand of interface shear capacity is limited as in composite columns (Figure 6.26a) or in fully encased beams (Figure 6.7d), at least in the elastic range (see also the AISC specifications at clause I1 and I3).

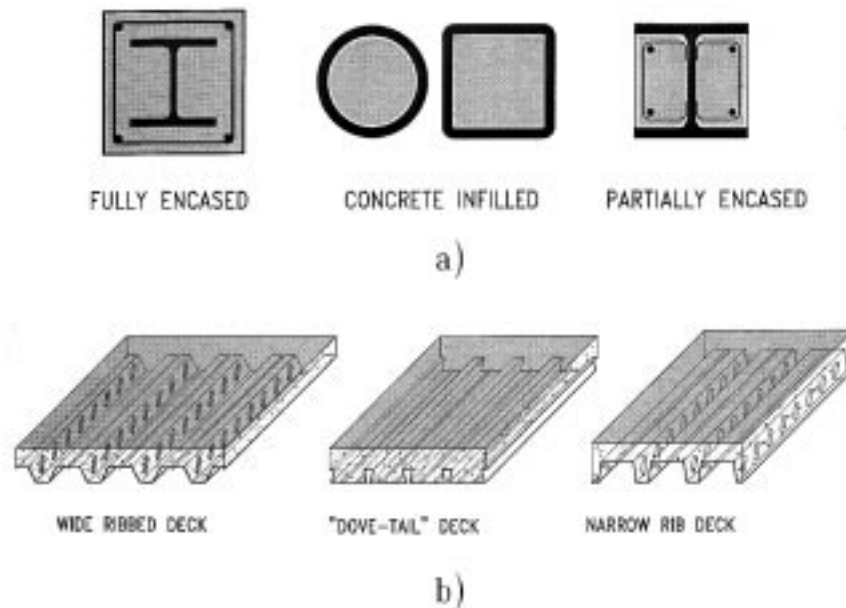


FIGURE 6.26: Composite system. (a) Composite columns. (b) Composite slab.

Eurocode 4 specifies the following values of the bond stress (including the effect of friction) to be considered when checking the connection effectiveness of composite columns:

- completely encased sections 0.6 N/mm^2
- concrete filled hollow sections 0.4 N/mm^2
- flanges in partially encased sections 0.2 N/mm^2
- webs in partially encased sections zero

Friction is often associated to bond in resisting shear. In flexural members, the tendency of steel and concrete elements to separate usually makes frictional action rapidly deteriorate. A suitable geometry of the composite element, as in the composite slab of Figure 6.26b with “dove-tailed” profiled sheeting, prevents separation and allows frictional interlock to develop throughout the response.

Mechanical interlock is obtained by embossing the metal decking so that slip at the interface is resisted by bearing between the steel ribs and the concrete indentations. The effectiveness of the embossments depends on their geometrical dimensions (mainly the height and depth) and shape. Enhancement of the shear transfer capacity in composite slabs is achieved if frictional and mechanical interlock are combined. The complexity of these interlock shear transfer mechanisms dictates that the response of the shear connection is determined by appropriate tests (see Figure 6.27). As discussed in Section 6.7, standard testing procedures are specified in most relevant codes, as in the Eurocode 4 and the ASCE Standard for the Structural Design of Composite Slabs (1991).

The transfer of large shear forces dictates that suitable mechanical connectors are used. New types of connectors have been continuously developing since the early stages of composite construction (see also Figure 6.1). Therefore, an increasing variety of forms of shear connectors is available for practical use. Despite possible significant differences, they all act as steel dowels embedded in concrete, and hence apply a concentrated load to the concrete slab, the diffusion of which requires careful consideration in the design of the slab detailing (Figure 6.28). Figure 6.29 shows some of the connectors more frequently used, for most of which design rules are provided by the relevant codes. The headed stud is by far the most popular connector.

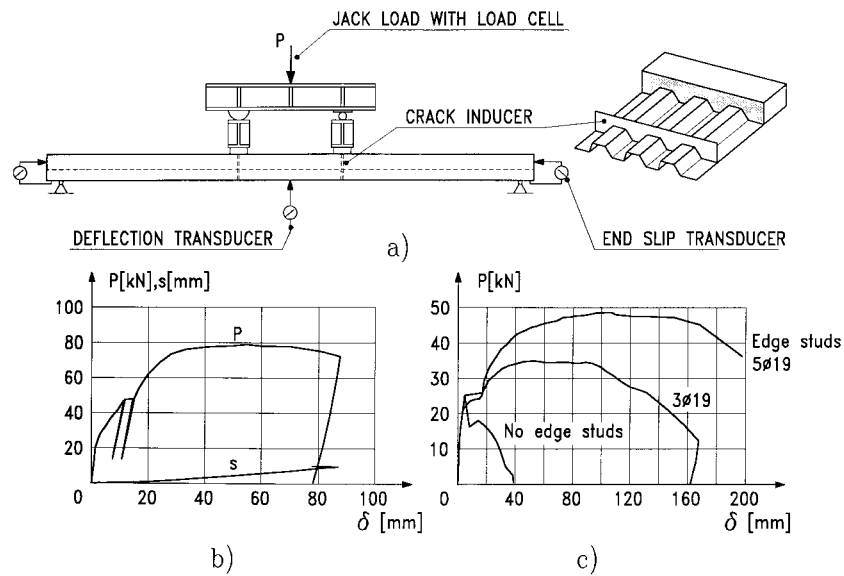


FIGURE 6.27: Slab responses after Bode and Sauerborn [5].

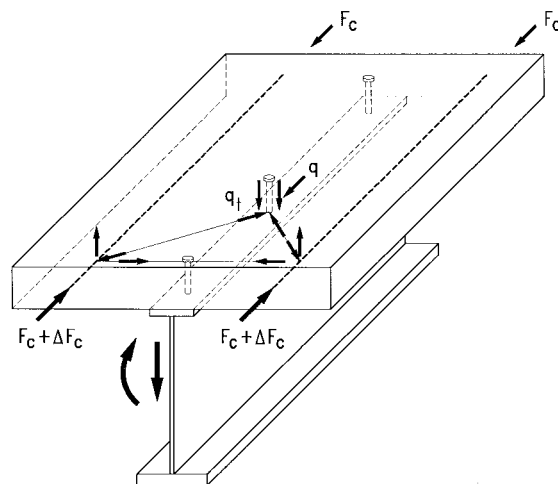


FIGURE 6.28: Shear transfer mechanism.

The behavior and modes of failure of each type of connector highly depend on the local interaction with the concrete, and can only be determined via ad hoc tests: the so-called *push-out tests* schematically shown in Figure 6.30a. Experimental shear force vs. slip curves are plotted in Figure 6.30b for a few connector types. All types of mechanical shear connectors possess a limited deformation capacity. However, in many instances, the associated slip is sufficient to make the design flexural resistance and rotation capacity of the composite section to be developed. If this condition is fulfilled, the connectors (and the connection) can be classified as ductile. As mentioned in the introduction to this section, the ductility requirements depend on the span and the degree of shear connection: the classification of a connector as ductile should hence be associated with a definition of a combination of:

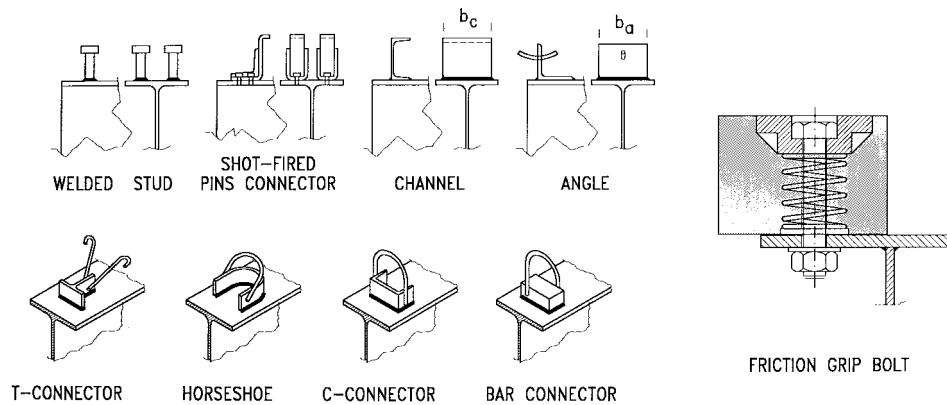


FIGURE 6.29: Typical shear connectors.

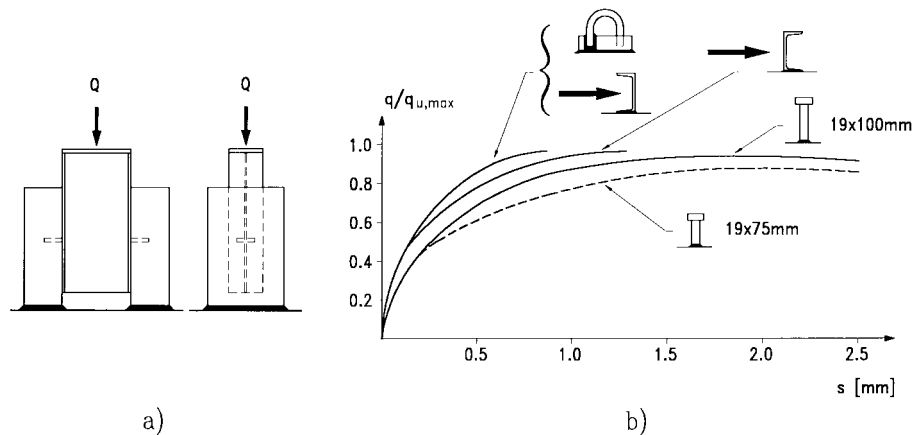


FIGURE 6.30: Test on shear connectors. (a) Push-out specimen. (b) Non dimensional load-slip relationship.

1. a range for these parameters
2. a characteristic value of slip capacity

Eurocode 4 assumes a characteristic slip capacity of 6 mm as the reference parameter in the calibration of the recommendations related to partial composite beams with ductile connectors. On the basis of an assessment of the available experimental data [29], it then classifies as *ductile* for the given ranges of span and degree of shear connection (see Section 6.5.7), only the friction grip bolts and the welded stud connectors meeting the following requirements:

- overall length H_{sc} after welding not less than 4 times the diameter d_{sc}
- $16 \text{ mm} \leq d_{sc} \leq 22 \text{ mm}$

Despite the assumed limitations appearing to be rather strict, most of the shear connections in buildings fall into the ductile category. Therefore, current practice should not be largely affected.

Stud shear connectors may also be used to provide end anchorage in composite slabs: their effect is significant on both the resistance and the ductility of the shear connection as a whole (see Figure 6.27c).

6.5.2 The Shear Strength of Mechanical Shear Connectors

The performance of a mechanical shear connector depends on the numerous factors governing the mutually interactive response of the connector and the surrounding concrete. Despite the number of attempts, a numerical model enabling satisfactory simulation of the many facets of this complex problem has not yet been developed. Design should hence rely on the available sets of experimental data. Besides, due to the inherent difficulty of deducing the resistance of shear connectors from beam tests, most of the usable data come from the push-out tests, which do not entirely reproduce, in terms of loading and confinement from the slab, the more favorable connector's condition in a composite beam. A further problem arises from the lack of consistency among the geometrical and detailing features of push-out specimens designed differently in different research studies. This situation demands for a careful selection of “comparable” data, in the background studies to code specifications [30].

Only the stud connectors were so extensively investigated that a sufficient body of information has been built up to enable a truly statistical determination of the nominal, characteristic, and design values of the resistance. The knowledge of the load-slip response of other types of connector is far more limited and design rules are based also on successful practice.

This situation is well reflected by present codes, which cover shear connectors at a rather different extension. The AISC specifications provide design rules only for studs and channel shear connectors, i.e., to the most popular connectors utilized in buildings. Besides, even when a wide set of shear connectors is covered by a code, as in the case of Eurocode 4, recent types of connectors such as, for example, the shot-fired steel pins in Figure 6.29, cannot be treated. Suitable test programs should be carried out in order to define their performance in terms of design strength and slip capacity. Procedures for conducting and assessing the results of push-out tests are given in many standards as in Eurocode 4.

Stud Connectors Used in Solid Concrete Slabs

Both Eurocode 4 and AISC associate the resistance of a stud with the failure either of the concrete, which crushes in the zone at the lower part of the stud shank, or of the stud shank, which fractures directly above the weld collar under shear, flexure, and tension. Interaction between these two modes of failure is not explicitly accounted for in order to maintain design simplicity. The format of the design rules is the same, although the design values of the resistances are quite different, due partly to the different philosophies on which the two codes are based and partly to the different sets of data on which the adopted strength model was calibrated. The shear resistance q_u of an individual stud is the lesser of

$$q_{u.c} = k_c A_{sc} (f_c E_c)^{0.5} \quad (6.49)$$

$$q_{u.s} = k_s A_{sc} f_{u.sc} \quad (6.50)$$

where A_{sc} represents the cross-sectional area of a stud shear connector. The AISC specifications assume $k_c = 0.5$ and $k_s = 1.0$, while in Eurocode 4 $k_c = 0.36$ and $k_s = 0.8$. Moreover, the Eurocode limits to 500 N/mm^2 the value of the ultimate tensile strength $f_{u.sc}$ to be assumed in Equation 6.50, and it restricts the application of the resistance Equations 6.49 and 6.50 to studs with diameter not greater than 22 mm (7/8 in.).

Experimental results had proven that the height-to-diameter ratio for the stud (H_{sc}/d_{sc}) affects the resistance $q_{u.c}$: the full resistance (Equation 6.49) is developed only when $H_{sc}/d_{sc} \geq 4$. All studs in the study by Ollgaard et al. [38], on which AISC rules are based, satisfy this requirement. The AISC specifications apply only to studs with $H_{sc}/d_{sc} \geq 4$, even if this requirement is not explicitly stated. The European code aims at permitting use of a wider range of studs (studs with lower height may be conveniently used in shallow floor systems). Therefore, it specifies a reduction coefficient of

the resistance $q_{u,c}$ expressed as $\alpha = 0.2[(H_{sc}/d_{sc}) + 1] \leq 1$. In any case, studs with $H_{sc}/d_{sc} < 3$ cannot be used.

A comparison between the two specifications is presented in Figure 6.31 with reference to a 19 mm (3/4 in.) stud with $H_{sc}/d_{sc} \geq 4$. Figure 6.32 illustrates the influence of the concrete density as by the

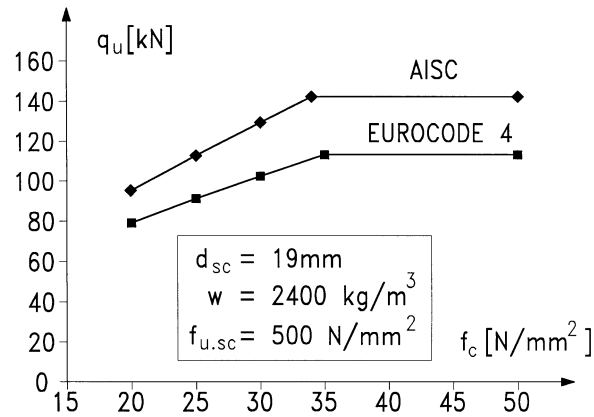


FIGURE 6.31: Stud connector shear resistance–concrete resistance relationship in accordance with AISC and Eurocode 4 provisions.

Eurocode relation between this parameter and the modulus of elasticity E_c .

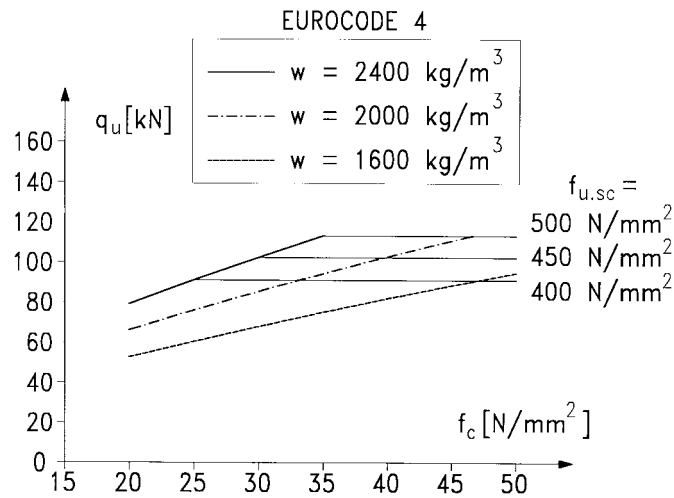


FIGURE 6.32: Influence of the concrete density on the stud connector shear resistance in accordance with Eurocode 4 provisions.

The response and strength of a stud connector welded to a rather thin flange may be affected by the deformation of the flange; a restriction to the stud diameter related to the flange thickness t_f is needed

when the influence of this factor is not appraised experimentally. Both the AISC specifications and the Eurocode restrict d_{sc} to 2.5 times t_f , unless the stud is placed in correspondence to the beam web.

The Eurocode obtains the design resistance q_d by dividing q_u by a safety factor $\gamma_V = 1.25$. In the AISC-LRFD format, the uncertainty related to the stud resistance is included in the resistance factor ϕ_b affecting the beam moment capacity.

Stud Connectors Used with Profiled Steel Decking

The most popular solution for floor systems in composite framed construction makes use of decks where the profiled steel sheeting acts compositely with a concrete “ribbed” slab. The studs are placed within a rib, and their performance is fairly different than in the previous case of solid concrete slab. The concrete stiffness, degree of confinement, and the resistance mechanism of the studs which are loaded by a highly eccentric longitudinal shear force are all different.

The prime parameters affecting the stud behavior are

- the orientation of the ribs relative to the beam span
- the rib geometry as characterized by the b_r / h_r ratio
- the stud height H_{sc} relative to the rib height h_r .

Proposals have been made to account for the influence of the relevant parameters on stud ultimate resistance. However, the available data do not enable a comprehensive design method to be developed. In codes, the effects of the main factors are accounted for via a suitable reduction factor.

Deck Ribs Oriented Parallel to Steel Beams

Studies conducted at Lehigh University in the 1970s [20] provide the sole background to this problem. The results indicated that the resistance of the stud in a rib parallel to the supporting beam can be determined by reducing the resistance in a solid slab Equations 6.49 and 6.50 by the factor

$$k_{rp} = 0.6 \cdot \frac{b_r}{h_r} \left[\frac{H_{sc}}{h_r} - 1.0 \right] \leq 1.0 \quad (6.51)$$

which mainly accounts for the limited restraint provided to the concrete by the sheeting side walls. This restraint is even negligible when the deck is split longitudinally at the beam, as shown in Figure 6.33. Good practice in this case would suggest meeting the requirements set for concrete haunches.

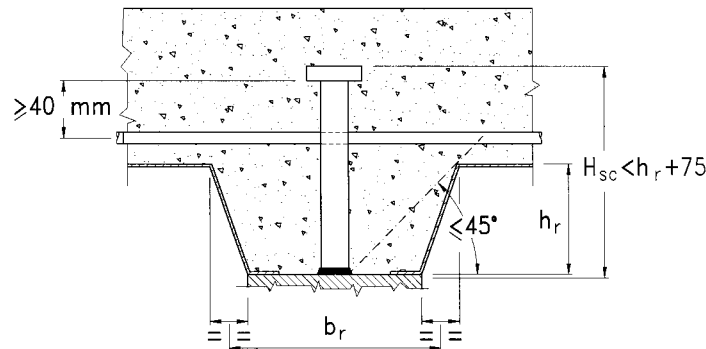


FIGURE 6.33: Geometrical restraint provided to the concrete by sheeting side walls.

Equation 6.51 appears in both codes. However, the AISC specifies that it applies only to very

narrow ribs ($b_r/h_r < 1.5$), while the Eurocode does not give any range of application, but it limits H_{sc} to $h_r + 75\text{mm}$.

Deck Ribs Oriented Perpendicular to Steel Beams

The efficiency of the floor system may require the steel sheeting to be placed with the ribs transverse to the supporting beam. Figure 6.34 schematically illustrates the possible failure modes of the shear connection either by collapse of the stud connector in flexure, tension, and shear or by fracture of the concrete rib associated with local concrete crushing. This deck arrangement apparently involves

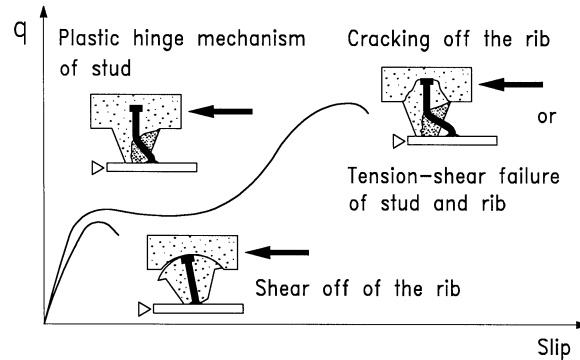


FIGURE 6.34: Failure modes for a stud connector in a deck with transverse ribs.

a concrete rib that is significantly stressed, as it acts as the transfer medium of the longitudinal shear between the concrete slab above the sheeting and the base of the stud. Moreover, the stud connector, subject to a highly eccentric load, tends to be less effective than in solid slabs. Its performance in terms of strength and ductility may be adversely affected by the interaction with other connectors in the same rib (i.e., when the number of studs in a rib, N_r , increases) and/or the reduced efficiency of longitudinal restraint offered by the concrete (i.e., when the studs are placed off center).

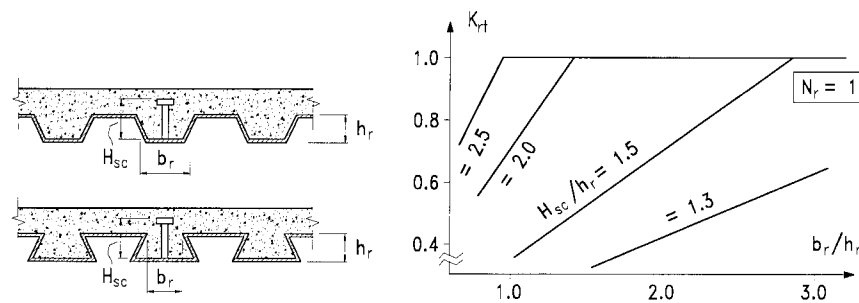


FIGURE 6.35: Reduction factor k_{rt} vs. geometrical parameters.

A comprehensive investigation carried out at Lehigh University [20], which also accounted for the results of previous studies, permitted definition of the general form of the relationship (see figure 6.35) between the main parameters governing the shear connection performance and the reduction factor

k_{rt} to be applied to stud resistance in solid concrete slabs:

$$k_{rt} = \frac{c}{\sqrt{N_r}} \frac{b_r}{h_r} \left[\frac{H_{sc}}{h_r} - 1.0 \right] \leq 1.0 \quad (6.52)$$

The same study proposed for the coefficient c the value 0.85, which was adopted by the AISC-LRFD code.

Further research work conducted mainly to investigate decks with European types of steel sheeting [24, 35] indicated that, in order to avoid unsafe assessment of the shear strength:

1. a lower value should be assumed for coefficient c
2. a range of application of Equation 6.52 should be defined

Therefore, Eurocode 4 assumed $c = 0.7$ and limited application of Equation 6.52 to

- stud diameter $d_{sc} \leq 20$ mm
- studs welded through-deck
- studs with ultimate tensile strength not greater than 450 N/mm²
- ribs with $b_r / h_r \geq 1.$, and $h_r \leq 85$ mm
- $k_{rt} \leq 0.8$ when $N_r \geq 2$

The limited knowledge still available does not allow coverage of the practice, common in a few countries, of welding studs through holes cut in the sheeting.

Neither code takes into account the effect of off center placement of the studs, resulting from the presence of stiffening ribs in the sheeting. This effect may be significant. It would be advisable to locate the stud in the favorable position as shown in Figure 6.36. In the case of symmetrically loaded simply supported beams, the “strong” side is the one nearest to the closest support.

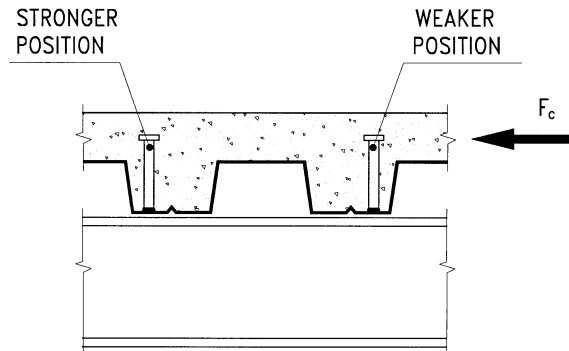


FIGURE 6.36: Different locations of the stud in the rib.

Other Types of Connectors

The knowledge of the performance of other types of connectors is far more restricted, and it is mainly based on research work conducted in the 1970s. This reflects the rather limited use of connectors other than studs both in building and bridge practice. Some new types of shear connector, such as the cold formed “seat element” connected to the steel beam by means of shot fired pins shown in Figure 6.29, are increasingly employed. Their response was found satisfactory in a few studies of

composite beams and joints [4, 15, 33], and comparable to equivalent welded studs. However, no specific rules are currently provided in codes, and their use requires suitable testing to be carried out.

The main code recommendations are reported here, with a few explanatory notes.

Channel Connectors

The Eurocode does not cover channel connectors, while channel connectors are the only connectors other than studs included in the AISC specifications, which are based on the work by Slutter and Driscoll [44]. The strength equation proposed there is modified in order to cover the case of lightweight concrete. Their capacity is then determined as

$$q_u = 0.3 \cdot (t_f + 0.5t_w) \cdot b_c \sqrt{f_c E_c} \quad (6.53)$$

where t_f , t_w , and b_c are the flange thickness, the web thickness, and the length of the channel, respectively.

The effect of the position of the channel flange relative to the direction of the shear force on the connector's strength (see figure 6.30) is not considered, and Equation 6.53 implicitly refers to the weakest position where the flanges are "looking" at the shear force, which was the only one covered by Slutter and Driscoll.

Angle Connectors

Angle connectors were investigated mainly in France, and the Eurocode design formula is based on the French studies:

$$q_u = 10b_a h_{ac}^{3/4} f_c^{2/3} \quad (6.54)$$

where b_a and h_{ac} are the length and the height of the outstanding leg of the connector. The design resistance $q_{u,d}$ is then obtained by applying to q_u a partial safety factor equal to 1.25. Further design requirements relate to:

- the welds fastening the angle to the beam flange, the design of which should be based on a conventional eccentricity of the shear force of $h_{ac}/4$
- the reinforcement bar necessary to resist uplift, whose area should be $\geq 0.1 q_{u,d} \gamma_{sr} / f_{y, sr}$, where γ_{sr} is the partial safety factor for steel reinforcement

The recommended position of the angles with respect to the thrust in the slab is shown in Figure 6.37.

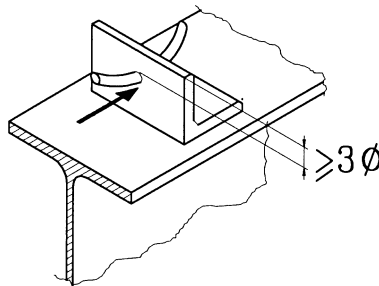


FIGURE 6.37: Recommended position of angle connectors with respect to the thrust in the slab.

Friction Grip Bolts

Friction grip bolts may be advantageously employed to connect precast concrete slabs. The Eurocode 4 recommendations are consistent with the rules for preloaded bolts in Eurocode 3. These should be accounted for, even if not explicitly mentioned: e.g., the standard nominal clearance should be met by the holes in the beam flange, otherwise the reduction factor for the friction resistance as defined in Eurocode 3 must be applied.

The friction resistance is taken as

$$q_u = \mu \frac{F_{b.pr}}{\gamma_V} \quad (6.55)$$

where

μ = the friction coefficient

$F_{b.pr}$ = the preload in the bolt

γ_V = the partial safety factor ($\gamma_V = 1.0$ for serviceability checks and $\gamma_V = 1.25$ for checks at ultimate)

The value of the friction coefficient μ strongly depends on the flexural stiffness of the steel flange. The Eurocode specifies $\mu = 0.50$ for steel flanges with thickness $t_f \geq 10$ mm and 0.55 for $t_f \geq 15$ mm. The surface of the flange should be prepared by blasting and removing loose rust; besides, pitting should not be present.

The bolt preload force is significantly reduced by shrinkage and creep. This effect should be taken into account when determining $F_{b.pr}$. In absence of an accurate determination (by testing or by an evaluation of existing data) a reduction of 40% can be assumed. In many instances, it may not be convenient to ensure that the bolted connection resists by friction the shear force at ultimate. In this case, the ultimate strength of the connector can be by the bolt's shear resistance or by "bearing" against the concrete. The latter resistance can be assumed to be equal to the value specified for studs (see Equation 6.49). Suitable testing may enable use of a further possible design criterion, which combines friction and shear in the bolt to achieve the required ultimate resistance.

Block Connectors, Anchors, and Hoops in Solid Slabs

Block connectors are those connectors with a flat surface opposing the shear force, and whose stiffness is so high that pressure on the concrete may be considered uniformly distributed at least at failure. The connector resistance is determined as

$$q_u = c A_{f1} f_c \quad (6.56)$$

where the coefficient $c = \sqrt{A_{f2}/A_{f1}}$ is ≤ 2.5 for normal weight concrete and ≤ 2.0 for lightweight concrete, and the areas A_{f1} and A_{f2} are defined in Figure 6.38a. Only the part of the area, A_{f2} , which lies within the concrete section, should be taken into account.

If the welds fastening the connector to the beam flange are satisfactorily designed, failure is attained by concrete crushing. The limit to the coefficient c accounts for the effect of the triaxial stress state on the concrete strength, and simultaneously imposes that the lateral restraint is adequate (through its link with the area A_{f2}) and that the distance of the connectors is sufficient to ensure that their full resistance capability is developed.

The design resistance is obtained by dividing q_u by the partial safety factor for concrete γ_c . Ties and hoops should also be present, and designed to resist the uplift force to be assumed as equal to $1/10 q_{u.d}$.

The resistance of each leg of anchors and hoops to longitudinal shear is defined as

$$q_u = A_{sr} \cdot f_{y.sr} \cdot \frac{\cos \beta}{\sqrt{1 + \sin^2 \alpha}} \quad (6.57)$$

where A_{sr} and $f_{y.sr}$ refer to the bar area and yield strength, respectively, and the angles α and β are defined in Figure 6.38b.

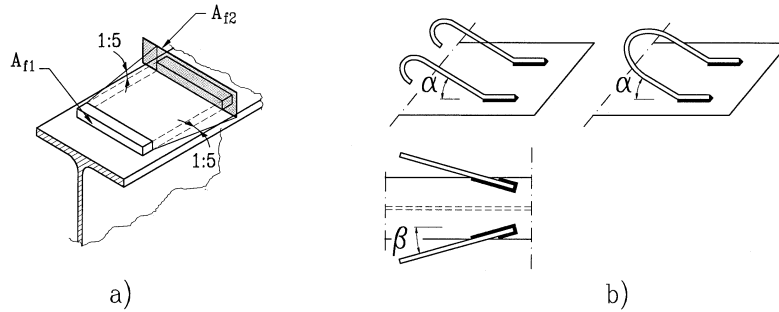


FIGURE 6.38: (a) Definition of areas A_{f1} and A_{f2} . (b) Definition of angles α and β .

The failure is associated to the anchor or hoop. The design resistance is obtained by dividing q_u by the appropriate material partial safety factor: either γ_s or γ_{sr} .

As indicated in the above, block connectors require combination with anchors or hoops in order to ensure adequate resistance to uplift. It may be convenient to use these types of connectors to resist the longitudinal shear force as well. Due to the different stiffness and different failure modes of these connectors, the total resistance $q_{u,tot}$ is less than the sum of the resistances of each of the connectors considered individually; the following expressions may be used in absence of accurate design resistance determination through testing:

$$q_{u,tot} = q_{u,block} + 0.5q_{u,anchors} \quad (6.58)$$

$$q_{u,tot} = q_{u,block} + 0.7q_{u,hoop} \quad (6.59)$$

The welds that connect the system to the beam flange should be designed for a total shear force equal to $1.2 q_{u,block} + q_{u,anchors}$ (or $q_{u,hoop}$).

6.5.3 Steel-Concrete Interface Separation

The analytical model of the composite beam assumes that the curvatures of the concrete and steel elements are the same: i.e., that there is no separation between the concrete flanges and the steel section. However, the shear transfer mechanism implies that forces also arise acting perpendicularly to the interface, which, inter alia, tend to cause steel concrete separation (see also Figure 6.28). Therefore, care should be taken to provide the shear connection with the capacity of resisting such uplift forces. The most efficient solution assigns this additional role to the same shear connectors.

It has been shown that the forces required to maintain full contact are substantially lower than the corresponding shear forces. A ratio of 1 to 10 may usually be assumed in design. As a consequence, no specific strength check is usually required for they can be resisted by connectors with suitable shapes such as headed studs and channels. On the other hand, additional elements resisting uplift should be placed when inadequate connectors are used: for example, anchor bars or hooks are needed in case of angle or block connectors (see Figure 6.29). Moreover, attention should be paid to the detailing. In particular, the spacing of connectors should be limited (the Eurocode recommends the lower value between 800 mm and six times the slab thickness), and, in the case of composite slabs with the ribs transverse to the beam, some form of anchorage should be present in every rib.

In several circumstances it should be considered that other factors may lead to an increased importance of vertical separation, as the loading condition (e.g., suspended loads), the stabilizing role of the concrete flange (typically against lateral buckling), and the cross-sectional variation of the member along its span.

6.5.4 Shear Connectors Spacing

The shear connectors should be suitably distributed among, and spaced along, the various shear spans in which the beam is divided so that the sectional beam capacity is always greater than the design moment. Shear spans, and the correspondent *critical lengths of the steel-concrete interface* to be considered in design verifications can be conveniently defined as the distances between two adjacent *critical cross-sections*, which to that purpose are

- supports
- free ends of cantilever
- sections of maximum bending moment
- sections where heavy concentrated loads are applied
- sections at which a sudden change of the cross-section occurs

The most viable criterion of spacing of connectors distributes them consistently with the longitudinal shear flow determined through an elastic analysis. On the other hand, uniform spacing would commonly be preferred, whenever possible, for it is practically advantageous. This alternative relies on interface slip to fully redistribute the forces within the shear connection, and hence requires an adequate slip capacity of the connectors.

Available information on slip capacity is quite limited, and certainly not sufficient for allowing a reliable assessment of this parameter to be obtained for most types of connector. Therefore, the Eurocode 4 restrains uniform spacing along a critical length l_{cr} to studs and friction grip bolts. Furthermore, this applies to beams that:

- have all critical sections in the span considered in Class 1 or Class 2 (see Section 6.4.3)
- meet the specified limitations as to the degree of shear connection in each critical length
- have a ratio between the plastic moment of the composite section and the plastic moment of the steel section not greater than 2.5

The AISC specifications seem less severe. They cover only studs and channel connectors, and consider their “ductility” sufficient for uniform spacing along the shear span in all cases.

Shear connectors may also ensure the stability of the steel flange. Therefore, an upper limit to their spacing may be associated with their effectiveness as stabilizing elements. The following values are recommended in the Eurocode:

- center-to-center spacing not greater than
slab in contact over the full length (e.g., solid slab)

$$22t_f \cdot \sqrt{\frac{235}{f_{y,s}}}$$

slab not in contact over the full length (e.g., slab with ribs transverse to the beam)

$$15t_f \cdot \sqrt{\frac{235}{f_{y,s}}}$$

- distance to the edge of the steel compression flange not greater than

$$9t_f \cdot \sqrt{\frac{235}{f_{y,s}}}$$

where

t_f = thickness of the flange

$f_{y.s}$ = nominal yield strength of the flange in N/mm^2

6.5.5 Shear Connection Detailing

Quality of a structure always implies a careful selection and sizing of details in design. In composite structures, the large variety of practical situations is combined with the lack of tools enabling a sufficiently accurate appraisal of the three-dimensional complex stress state deriving locally from the composite action. The detailing rules, which are provided by codes, do not have any scientific basis. Rather, they stem from previous successful experience in practice or adequate experimental data. These recommendations should be considered, for their very nature, just as applications rules deemed to satisfy the design principle. Moreover, the practical range of possibilities in composite structures is so broad that no set of rules can cover it in a comprehensive way. Therefore, engineering judgment should be used when applying them in design.

6.5.6 Transverse Reinforcement

Mechanical connectors apply concentrated loads to the concrete slab which disperse into this element through shear and transverse tensile stresses. This complex stress state may result in longitudinal splitting of the slab (tensile stresses) or formation of inclined (herring bone) cracks. Therefore, transverse reinforcement is needed to resist these forces. In most instances, reinforcing bars are already present transversally to the beam as longitudinal rebars of the slab spanning between adjacent beams. However, the capability to resist forces associated with the shear transfer should also be checked.

Transverse rebars play basically the same role as stirrups in reinforced concrete beams. Therefore, background to current design approach are the studies on shear transfer in reinforced concrete by Mattock and Hawkins [32]. Distinction should be made between the shear transfer mechanism in the uncracked slab and in the presence of a longitudinal crack. In the former case, the behavior may be schematically modeled via a strut and tie truss analogy, as shown in Figure 6.28. When the shear is transferred through a cracked plane, three contributions to the resistance can be identified:

1. dowel action of the rebars
2. aggregate interlock
3. friction

Development of the last two contributions requires that transverse rebars are placed, which prevents the crack width from increasing.

The shear transfer capacity in cracked situations is significantly lower than in uncracked slabs. However, the former condition is assumed in design. Besides conservativeness, this approach is simpler, for in this case the shear strength does not depend on the longitudinal stress in the slab. The steel reinforcement resists by bending across the surface of the crack, and its maximum “shear capacity” depends on the steel yield strength and on the relative stiffness and strength of the steel and concrete. Nevertheless, the steel yield resistance remains the main factor. Interlock and friction contributions are limited by fracture of interface protrusions, which is a function of the concrete tensile strength.

The shear transfer capacity per unit length of a shear plane may be written in the following form, which accounts for both resistance contributions

$$v_l = k_1 A_{c.v} f_{ct} + k_2 A_{ef.v} f_{y.sr} \quad (6.60)$$

where

- k_1 and k_2 = factors accounting indirectly for the other parameters affecting v_l
- $A_{c.v}$ = the area per unit length of the concrete shear surface in the failure plane considered
- $A_{ef.v}$ = the area per unit length of the reinforcing bars which can be considered effective
- f_{ct} = the tensile strength of concrete

The experimental data suggest that a lower limit to the reinforcement strength per unit length should be imposed, in order to ensure applicability of Equation 6.60. An upper bound is also necessary because higher reinforcement ratios lead to different failure modes; this limit may be written in the form

$$v_l = k_3 A_{c.v} f_c \quad (6.61)$$

In Eurocode 4, Equations 6.60 and 6.61 are written, respectively, as

$$v_l = 2.5 \eta A_{c.v} \tau_u + A_{ef.v} f_{y.sr} + v_{sd} \quad (6.60a)$$

and

$$v_l = 0.2 \eta A_{c.v} f_c + \frac{v_{sd}}{\sqrt{3}} \quad (6.61a)$$

where the coefficient η is a factor accounting for concrete density: $\eta = 1$ for normal weight concrete and $\eta = 0.3 + 0.7 (w/24)$ for lightweight concrete (with w expressed in kN/m^3), τ_u is the shear strength to be taken as $0.25 f_{ct}$ and v_{sd} is the possible contribution of the steel sheeting of the composite slab. The lowest of the resistances computed by Equations 6.60a and 6.61a has to be taken.

It should be noted that the steel decking can contribute only when its ribs are transverse to the beam, and its value, v_{sd} , should be:

- assumed as $v_{sd} = A_{sd} f_{y.sd}$, if the sheeting is continuous across the beam
- limited by the bearing resistance of the stud against the sheeting, when the sheeting is not continuous, but anchored by studs welded through the sheeting

The shear transfer capacity has to be checked for all the relevant critical shear surfaces shown in Figure 6.39. A value of the total longitudinal shear equal to the design shear force for the connectors is usually considered. However, the variation of the longitudinal shear along the width of the concrete slab may be considered (see [8]) and different values determined for the various shear failure surfaces.

A minimum area of transverse reinforcement equal to $0.002 A_{c.v}$ is prescribed in the AISC specifications, which, on the other hand, do not provide any specific criterion for transverse reinforcement design.

Spacing of the transverse rebars should be consistent with spacing of the shear connectors.

6.5.7 The Shear Connection in Fully and Partially Composite Beams

The methods of analysis and design of composite beams presented in Sections 6.3 and 6.4 are based on the assumption of full interaction. As already mentioned, the effect of interface slip on the performance of a composite beam may generally be neglected in composite beams designed elastically, when the shear connection has adequate resistance in all the critical lengths of the member, and shear connectors are used which proved to possess satisfactory stiffness, as for the ones covered by design codes.

In the case of plastic design, a distinction has to be made between fully and partially composite beams as defined in the introduction to this section. In fully composite beams, i.e., if the requirement

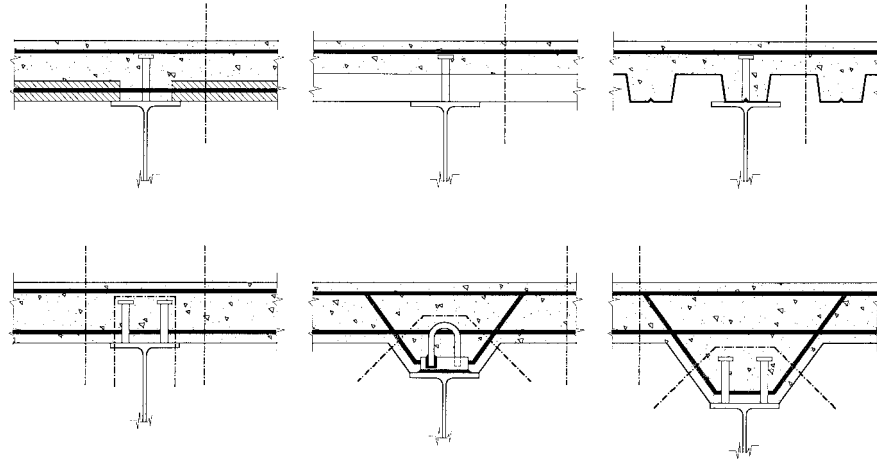


FIGURE 6.39: Relevant shear surface for the evaluation of the shear transfer capacity.

of full shear connection is fulfilled, the deformation of the connectors can be neglected in design analyses. The shear connection design does not differ remarkably from the elastic case, however, the level of strength to be considered in each critical length does differ. The spacing and ductility requirements of the connectors are the same. In many instances, fully composite beams are not the optimal solution, and partially composite beams may better suit the requirements in service and at ultimate, and at a lower cost. The high redistribution in partial shear connection implies that the ductility demand to connectors becomes significant. Furthermore, it sharply increases with the decrease of the degree of shear connection. The performance of partially composite beams depends dramatically on the ductility of the connectors and this is a key design parameter. The main aspects of partially composite beam design are presented in this section. The design of the shear connection in fully composite beams is also treated, as a necessary preliminary step.

Fully Composite Beams

Fully composite beams can develop by definition the full plastic moment in positive and negative bending. The collapse mode is by formation of a plastic beam mechanism. The design of a full shear connection refers to this collapse condition, and is based on the overall longitudinal shear to be transferred at the steel-concrete interface in each beam length between two adjacent plastic hinges or between a plastic hinge and the nearest support (i.e., generally in a half span).

Such an overall longitudinal shear V_l can be determined straightforwardly by imposing the equilibrium to longitudinal translation to the slab:

$$V_l = F_{c.f} + F_{t.f} \quad (6.62)$$

where

$F_{c.f}$ = the compression force in the slab in the section where the sagging moment is maximum (see Equation 6.13)

$F_{t.f}$ = the tensile force in the slab in the section where the negative bending moment is maximum (see Equation 6.34; $F_{t.f}$ is zero in a simply supported beam)

The minimum number of connectors required to transfer V_l is obtained as

$$N_f = \frac{(F_{c.f} + F_{t.f})}{q_u} \quad (6.63)$$

where

q_u = the ultimate shear resistance of the chosen shear connector type

The connectors may be uniformly spaced along the half span. However, a critical cross-section may be located between the plastic hinges considered (or between the plastic hinge in sagging moment and a support), and a further check is needed to suitably distribute the total number of connectors between the critical length. To this purpose, the force in the slab has to be computed at the intermediate critical cross-section (usually by an elastic analysis), and the total change in longitudinal force V_l can then be subdivided between the two critical lengths and the total number of connectors shared accordingly.

Partially Composite Beams

Fully composite beams are not always the most efficient solution. Moreover, the condition of full shear connection is normally difficult to achieve when composite slabs are used with metal decking with the ribs parallel to the beam axis. As to the efficiency, it may be noted, among other aspects, that:

- The design of the slab and the steel section is often governed by criteria other than strength.
- In a building, only a limited number of steel sections will commonly be selected and used. As a result, several beams will be oversized, if fully composite.
- This possible beam over-strength is paid in terms of cost of placement of connectors and detailing (mainly the required amount of transverse reinforcement in the slab).

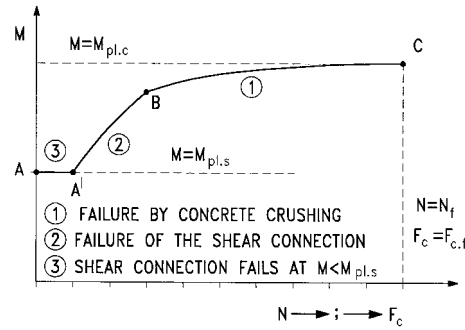
Therefore, the use of connectors in numbers lower than that required by the condition of full shear connection appears advantageous, for it enables the ultimate capacity of the beam to be “tailored” to the design value of the moment. This approach, the so-called partial shear connection design, was recently developed and refined through numerous experimental and numerical studies.

The influence of the reduction of the number N of connectors (i.e., of the allowable compressive force F_c in the slab) on the moment resistance of the beam is schematically illustrated in Figure 6.40a, where representative stress distributions are also shown for the different ranges of behavior. The reduction in moment capacity is moderate until the mode of failure is associated with concrete crushing (line BC in the figure). A further decrease of shear connectors makes the shear connection to fail first, and the moment capacity reduces sharply (line A'B). Failure of the shear connection may happen even before the plastic moment $M_{pl,s}$ of the steel section is attained (line AA'). There is no particular reason to consider differently, in design practice, the two modes of failure, at least when ductile shear connectors are used. The shear connection failure in this case is not more sudden than the flexural mode. On the contrary, a greater conservativeness is necessary in case of non-ductile connectors.

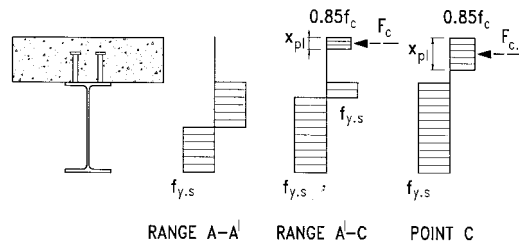
The relationships $M - N$ ($M - F_c$) and, therefore, the location of points A' and B depend on the type of loading and the beam span, and are affected by the strain hardening of the structural steel. Accurate determination of these relations is too burdensome in routine design. Approximate approaches were then developed, and are included in several codes. They are briefly presented here. Besides, deflections of partially composite beams have to be computed allowing for the effect of interface slip. These calculations represent an additional design difficulty; simplified methods are covered as well.

The Moment Resistance

As already underlined, the redistribution of forces on connectors required to exploit the flexural resistance of a partially composite beam is significant. The deformation capacity of the shear connectors (ductile or non-ductile connectors) is the key parameter for the selection of the design method.



a)



b)

FIGURE 6.40: Influence of the reduction of shear connectors. (a) Moment resistance of beam-shear capacity. (b) Possible stress redistribution in the cross-section.

A. Ductile Connectors

If plastic theory can be applied (i.e., all critical cross-sections may be classified as compact) and the deformation capacity of the connectors is sufficient to assume that a complete redistribution can take place within the shear connection in the shear span considered, then the ultimate strength of the partially composite beam at a critical cross-section can be computed rather easily via the same equilibrium approach based on simple plastic theory as for fully composite beams. Due to the occurrence of slip, the slab and the steel beam will have different neutral axes, as shown in Figure 6.40b. The depth $x_{pl} < h_c$ of the concrete slab contributing to the flexural strength is determined by equating the stress block and the shear connection resistance; that is, by posing

$$0.85 f_c x_{pl} b_{eff} = \sum q_u \quad (6.64)$$

The equilibrium of the full composite section to the translation enables calculation of the plastic neutral axis of the steel section, which may lie within the top flange or the web. The determination of the moment capacity M_u is then straightforward (see Section 6.3.4).

As an alternative to the equilibrium approach, the moment capacity of a partially composite beam can be determined via the interpolation method, as illustrated in Figure 6.41:

$$M_w = M_{pl,s} + \frac{F_c (M_{pl,c} - M_{pl,s})}{F_{c,f}} \quad (6.65)$$

In most instances, the accuracy of this method is satisfactory. Besides, it enables a direct assessment

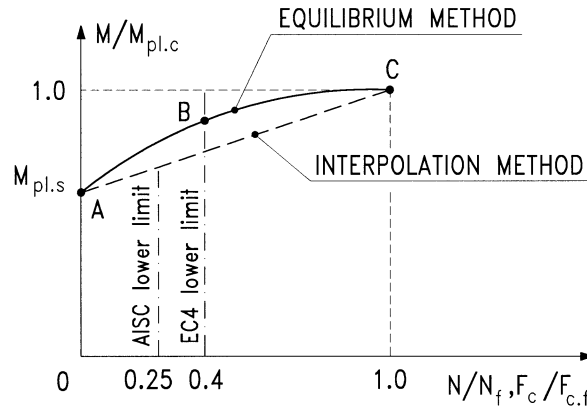


FIGURE 6.41: Non-dimensional relationship between moment resistance of beam and shear connector capacity for partially composite beams.

of the value of F_c required to resist the design moment, M , being

$$F_c = F_{c,f} \frac{(M_w - M_{pl,s})}{(M_{pl,c} - M_{pl,s})} \quad (6.66)$$

Several studies were recently devoted to the appraisal of the “ductility” requirement of the connectors to be associated with partial connection plastic design [3, 29]. They confirmed the substantial deformation capacity needed to allow redistribution for low degrees of shear connection and long spans. The main outcomes provided the background to the Eurocode relations between the beam span and the minimum degree of shear connection allowed for application of Equations 6.65 and 6.66, which are illustrated in Figure 6.42. The cases specifically covered are

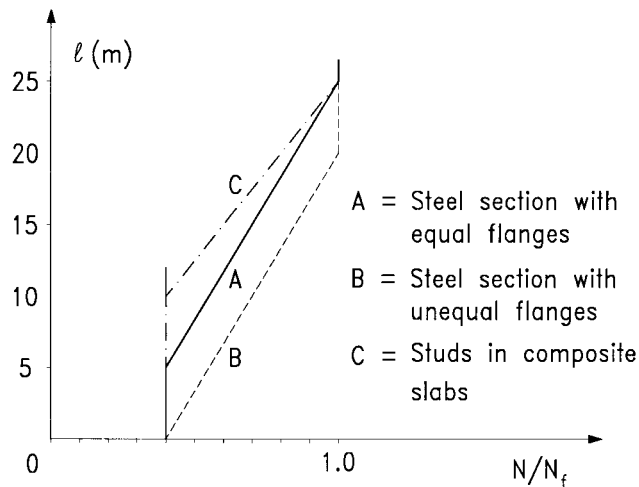


FIGURE 6.42: Relationship between the beam span and the minimum degree of shear connection.

- steel sections with equal flanges (line A)
- steel section with unequal flanges (line B valid for bottom flanges with area not greater than 3 times the upper flange area), for which a more strict limitation is specified
- composite beams with studs connectors in composite slabs with profiled steel sheeting and ribs transverse to the beam (line C), for which tests by Mottram and Johnson [35] indicated the possible availability of higher slip capacities, at least when certain conditions are met by the connectors, the steel section, and the deck sheeting

These relationships are consistent with the definition of ductile connectors given in the same code, which classifies as ductile stud connectors, friction grip bolts, and all connectors having a characteristic slip capacity, determined from push tests, not lower than 6 mm.

B. “Non-Ductile” Connectors

When the condition of full redistribution within the shear span cannot be attained, elastic-plastic calculations should, in principle, be performed to determine the M vs. F_c curve, accounting for the influence of slip (curve A' B' C in Figure 6.43). Such calculations are too complex for usual design practice, even if full interaction is assumed in the consideration of the need to limit the slip and the fact that slip reduces the longitudinal shear force for a given moment distribution. A substantial

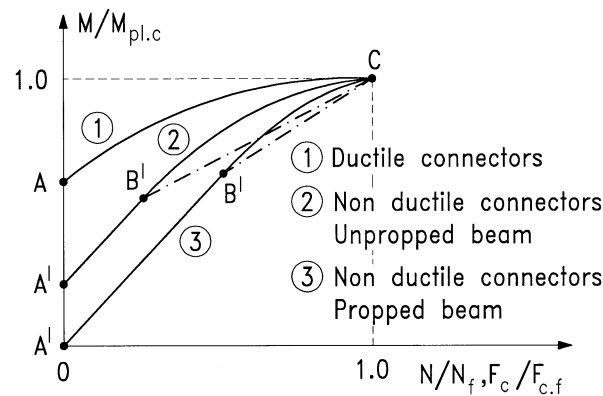


FIGURE 6.43: Non-dimensional relationship between moment resistance of beam and shear connector capacity for different connector behaviors.

simplification is made possible by the relatively easy determination of the three key points A', B', and C and by the nature of the curve linear up to point B' and convex-upwards in the range B'C, which enables use of a straight line also in this range. Point A' is associated with the condition of no composite action ($F_c = 0$); in the case of unshored construction, the coordinate of point A' is the bending moment M_s resisted by the steel section alone. Point B' is associated with the moment M_{el} for which the steel bottom flange achieves its yield strength. Computation of M_{el} should account for the method of construction, i.e., M_{el} should include, for unshored beams, the moment M_s . At point C, the full moment capacity of the composite section is achieved.

The Deflections

The effect of interface slip on beam deflections may be neglected in many instances, even in case of partial shear connection, as shown by several experimental studies [28]. Besides, design criteria usually aim to reduce the importance of longitudinal slip, and shear connections are designed accordingly. However, such an effect tends to become significant as the degree of shear connection

N/N_f decreases and/or the forces on the shear connectors increase, and should be considered when N/N_f is “low”.

The recent parametric studies conducted in view of the preparation of Eurocode 4 supported the proposal by Johnson and May [28]. The approach, included in the Eurocode, accounts for the effect of incomplete interaction in the calculation of the beam deflection δ_p by the simple relation

$$\delta_p = \delta_f + k (\delta_s - \delta_f) \left[1 - \frac{N}{N_f} \right] \quad (6.67)$$

where

δ_f = the deflection for the fully composite beam

δ_s = the deflection of steel beam acting alone

k = a factor allowing for the influence of construction type: $k = 0.5$ for shored construction and $k = 0.3$ for unshored construction

The Eurocode also defines the requirements to be met in order to neglect the slip effect in unshored beams. They are

- $N/N_f \geq 0.5$, or force q on a shear connector $\leq 0.7 q_u$
and in the case of slabs with profiled steel decking transverse to the beam
- height of the ribs $h_r \leq 80$ mm

6.5.8 Worked Examples

EXAMPLE 6.4:

With reference to Example 6.1, the verification of the shear connection is proposed in the following. It is assumed that the connection is full interaction, with headed stud connectors (Figure 6.44), having $H_{sc} = 100$ mm and $d_{sc} = 19$ mm. The ultimate strength of the connectors is $f_{u.sc.B} = 450$ N/mm² and a partial safety factor γ_v equal to 1.25 is considered.

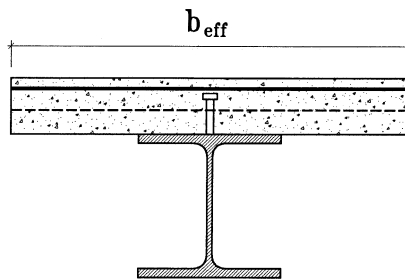


FIGURE 6.44: Cross-section of the composite beam.

1. Longitudinal shear force — In accordance with the hypothesis of full shear connection, the total design longitudinal shear V_1 to transfer by shear connectors, spaced between the point of maximum sagging moment and the end support is:

$$V_1 = \min (F_{s,max}, F_{c,max})$$

where $F_{s,\max}$ and $F_{c,\max}$ are the steel beam and the concrete slab limit resistance, respectively. Therefore, neglecting the contribution offered by the longitudinal slab reinforcement and with reference to the steel beam (see Equation 6.14):

$$F_{s,\max} = \frac{A_a \cdot f_{y.s.k}}{\gamma_s} = \frac{11600 \cdot 235}{1.1} \cdot 10^{-3} = 2478.2 \text{ kN}$$

and with reference to the concrete (see Equation 6.13):

$$\begin{aligned} F_{c,\max} &= \frac{0.85 A_c \cdot f_{c.k}}{\gamma_c} = \frac{0.85 \cdot b_{\text{eff}} \cdot h_c \cdot f_{c.k}}{\gamma_c} \\ &= \frac{0.85 \cdot 2500 \cdot 120 \cdot 25}{1.5} \cdot 10^{-3} = 4250 \text{ kN} \end{aligned}$$

Then, $V_1 = 2478.2 \text{ kN}$

2. Design resistance of shear connection (see Section 6.5.2) — It is necessary to make reference to the lower value between

- the resistance of concrete (Equation 6.49):

$$q_{u.c} = \frac{k_c \cdot A_{sc} \cdot \sqrt{f_{c.d} \cdot E_c}}{\gamma_v} = \frac{0.36 \cdot \frac{\pi \cdot 19^2}{4} \sqrt{25 \cdot 30500}}{1.25} \cdot 10^{-3} = 71.27 \text{ kN}$$

- the resistance of stud connectors (Equation 6.50):

$$q_{u.s} = k_s \cdot f_{u.sc.d} \cdot \frac{A_{sc}}{\gamma_v} = 0.8 \cdot 450 \cdot \frac{\pi \cdot 19^2}{4} \frac{1}{1.25} \cdot 10^3 = 81.7 \text{ kN}$$

Then, $q_{u.d} = q_{u.c} = 71.27 \text{ kN}$

3. Design of the connection

- Minimum number of connectors:

$$N_f = 2 \cdot \frac{V_1}{q_{u.d}} = 2 \cdot \frac{2478.2}{71.27} = 69.54$$

It is assumed

$$N = 2 \cdot 35 = 70 \text{ headed stud connectors}$$

- Spacing of the connectors (see Section 6.5.4)

The stud connectors are spaced uniformly, being:

- all critical sections are in class 1
- $\frac{N}{N_f} = \frac{70}{69.54} = 1.001 \geq 0.25 + 0.03 \cdot l = 0.25 + 0.03 \cdot 10 = 0.55$
- $\frac{M_{pl}}{M_{pl.s}} = \frac{M_{pl.c}}{W_s \cdot f_{y.s.k} / \gamma_s} = \frac{830}{2194 \cdot 235 / 1.10} \cdot 10^{-6} = 1.77 < 2.5$

It is assumed a uniform spacing between studs:

$$i = \frac{l}{N} = \frac{10000}{70} = 143 \text{ mm}$$

It is hence assumed 80 headed stud connectors, spacing of 125 mm.

4. Detailing of the shear connection (see Section 6.5.4)

- Spacing:

$$i \leq 22 \cdot t_f \sqrt{\frac{235}{f_{y.s.k}}} = 22 \cdot 16 \cdot \sqrt{\frac{235}{235}} = 352 \text{ mm}$$

- Overall height:

$$6H_{sc} < i < 5d_{sc} \quad 6 \cdot 100 < 125 < 5 \cdot 19 = 95 \text{ mm}$$

5. Reinforcement in the slab — The area of the reinforcement in a solid slab must not be less than 0.002 times the concrete area being reinforced and should be uniformly spaced. Referring to a width of 1000 mm, minimum amount of reinforcement is:

$$0.002 \cdot A_c = 0.002 \cdot 120 \cdot 1000 = 240 \text{ mm}^2/\text{m}$$

It is assumed a double layers of reinforcement $\phi 10 \text{ mm}/200 \text{ mm}$

$$A_{ef.v} = 2 \cdot 392.7 = 785.4 \text{ mm}^2/\text{m}$$

6. Longitudinal shear in the slab (see Section 6.5.6) — In accordance with Eurocode 4, the shear surfaces are presented in Figure 6.45.

- Section a-a — The design resistance is determined from the smaller value between (Equations 6.60a and 6.61a):

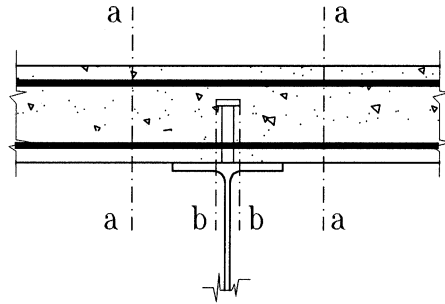


FIGURE 6.45: Longitudinal shear surfaces.

$$\begin{aligned} v_1 &= 2.5\eta A_{cv}\tau_{u.d} + A_{ef.v}f_{y.sr.d} + v_{sd} \\ &= 2.5 \cdot (1000 \cdot 120) \cdot 1 \cdot 0.30 + 2 \cdot 392.7 \cdot \frac{420}{1.15} = 376842 \text{ N/m} \cong 377 \text{ kN/m} \end{aligned}$$

and

$$\begin{aligned} v_1 &= 0.2\eta A_{cv}0.85 \frac{f_{c.k}}{\gamma_c} + \frac{v_{sd}}{\sqrt{3}} \\ &= 0.2 \cdot (1000 \cdot 120) \cdot \frac{0.85 \cdot 25}{1.5} = 340000 \text{ N/m} \cong 340 \text{ kN / m} \end{aligned}$$

where

$$\begin{aligned}\tau_{u.d} &= 0.30 \text{ N/mm}^2 \\ A_{cv} &= 120 \cdot 1000 = 120000 \text{ mm}^2 \\ \eta &= 1.0 \quad (\text{normal concrete}) \\ v_{sd} &= 0 \quad (\text{contribution of the profiled steel sheeting})\end{aligned}$$

The design longitudinal shear force per unit length is:

$$v = \frac{q_u}{i} = \frac{71.27}{125} = 0.570 \text{ kN / mm} = 570 \text{ kN / m}$$

Referring to only one section of the headed stud connector it is assumed:

$$\frac{v}{2} = 285 \text{ kN / m} < 340 \text{ kN / m}$$

- Section b-b — It is preliminary to calculate the length of the shear surface. In accordance with Eurocode 4 and assuming a width of 1000 mm, it is assumed:

$$A_{cv} = (2 \cdot H_{sc} + d_{sc}) \cdot 1000 = (2 \cdot 100 + 19) \cdot 1000 = 219000 \text{ mm}^2 / \text{m}$$

then:

$$\begin{aligned}v_1 &= 2.5\eta A_{cv}\tau_{u.d} + A_{ef.v} \frac{f_{y.sr.k}}{\gamma_{sr}} + v_{sd} \\ &= 2.5 \cdot 219000 \cdot 1 \cdot \frac{0.30}{1.10} + 2 \cdot 392.7 \cdot \frac{420}{1.15} = 451092 \text{ N / m} \simeq 451 \text{ kN/m}\end{aligned}$$

Being v less than v_1 , the section b-b will be safe.

EXAMPLE 6.5:

With reference to Example 6.1, the design of the shear connection is proposed. It is assumed Partial shear connection with ductile connectors. In particular, 19 mm diameter stud connectors with ultimate tensile strength $f_{u.sc.k} = 450 \text{ N/mm}^2$ are used.

It is also assumed that the headed stud connectors have an overall length after welding not less than 4 times the diameter and with a shank of diameter not less than 16 mm and not exceeding 22 mm (see Eurocode 4 – 6.1.2).

1. Connection design — The connection is considered ductile if:

$$\frac{N}{N_f} \geq 0.25 + 0.03l$$

where

l = total length of the beam

N = number of shear connectors

N_f = number of shear connectors for total shear connection

Then

$$\frac{N}{N_f} \geq 0.25 + 0.03 \cdot 10.00 = 0.55$$

The stud design shear resistance is evaluated as the lesser value between

- the resistance of the concrete (Equation 6.49):

$$q_{u.c} = \frac{k_c \cdot A_{sc} \cdot \sqrt{f_{c.d} \cdot E_c}}{\gamma_v} = 71.27 \text{ kN}$$

- the resistance of the connectors (Equation 6.50):

$$q_{u.s} = k_s \cdot A_{sc} \frac{f_{u.sc.k}}{\gamma_v} = 0.8 \cdot \frac{\pi \cdot 19^2}{4} \frac{450}{1.25} \cdot 10^{-3} = 81.7 \text{ kN}$$

Then, $q_u = q_{u.c} = 71.27 \text{ kN}$

According to Examples 6.1 and 6.2, the shear force between the section at midspan and the one at the support is

$$V_1 = F_{s\max} = 2478.2 \text{ kN}$$

In the hypothesis of total shear connection the minimum number of stud connectors is:

$$N_f = \frac{V_1}{q_u} = \frac{2478.2}{71.27} = 34.97$$

Therefore, it is possible to evaluate N.

$$N = 0.55 \cdot N_f = 0.55 \cdot 34.77 = 19.12$$

Hence, 20 connectors are selected for the half beam. The corresponding force F_c is

$$F_c = N \cdot q_u = 20 \cdot 71.27 = 1425.4 \text{ kN}$$

As a consequence, the connection system on the beam is made with 40 headed stud connectors.

2. Connection check — In accordance with the interpolation method, it is:

$$\begin{aligned} M_{pl.s} &= W_s \cdot \frac{f_{y.s.k}}{\gamma_s} = 2194 \cdot \frac{235}{1.1} = 468.7 \text{ kNm} \\ M_{pl.c} &= 830 \text{ kNm} \\ M &= 720 \text{ kNm} \\ \frac{N}{N_f} &= \frac{F_c}{F_{c.f}} = \frac{M - M_{pl.s}}{M_{pl.c} - M_{pl.s}} = \frac{720 - 468.7}{830 - 468.7} = 0.696 \end{aligned}$$

The number of headed stud connectors is then evaluated.

$$N = 0.696 \cdot N_f = 0.696 \cdot 67.8 = 47.2$$

Hence, 50 headed stud connectors along the beam are required.

3. Detailing of the connection (see Section 6.5.4)

- Spacing of the connectors

The stud connectors are spaced uniformly, being:

- all critical sections are in class 1
- $\frac{N}{N_f} = \frac{40}{67.8} = 0.59 \geq 0.25 + 0.03 \cdot 10 = 0.55$
- $\frac{M_{pl,c}}{M_{pl,s}} = \frac{M_{pl,c}}{W_s \cdot f_{y,s,k} / \gamma_s} = \frac{830}{2194 \cdot 235 / 1.10} \cdot 10^{-6} = 1.77 < 2.5$

It is assumed a uniform spacing between studs:

$$i = \frac{l}{N} = \frac{10000}{40} = 250 \text{ mm} < 22t_f \sqrt{\frac{235}{f_{y,s,k}}} = 22 \cdot 16 \cdot \sqrt{\frac{235}{235}} = 352 \text{ mm}$$

It is assumed 40 headed stud connectors, spacing of 250 mm.

- Overall height:

$$6H_{sc} < i < 5d_{sc} \quad 600 \text{ mm} = 6 \cdot 100 < 250 < 5 \cdot 19 = 95 \text{ mm}$$

The evaluation of the minimum reinforcement in the slab and the check of the longitudinal shear in the slab must be carried out as indicated in the previous example.

4. Maximum beam deflection — In accordance with Eurocode 4, it is

$$\frac{\delta}{\delta_f} = 1 + 0.3 \cdot \left(1 - \frac{N}{N_f}\right) \cdot \left(\frac{\delta_s}{\delta_f} - 1\right)$$

$\delta_f = 24.4 \text{ mm}$ (see Example 6.1 in Section 6.3.7)

$$\delta_s = \frac{5 \cdot p \cdot l^4}{384 \cdot E \cdot I} = 51.46 \text{ mm}$$

Hence:

$$\begin{aligned} \frac{\delta}{\delta_f} &= 1 + 0.3 \cdot \left(1 - \frac{40}{70}\right) \cdot \left(\frac{51.46}{24.1} - 1\right) = 1.1426 \\ \delta &= 27.88 \text{ mm} \cong \frac{1}{359} l \end{aligned}$$

6.6 Composite Columns

6.6.1 Types of Sections and Advantages

The most common types of steel-concrete composite columns are shown in Figure 6.46. The cross-sections can be classified in 3 groups:

- fully encased
- partially encased
- concrete filled

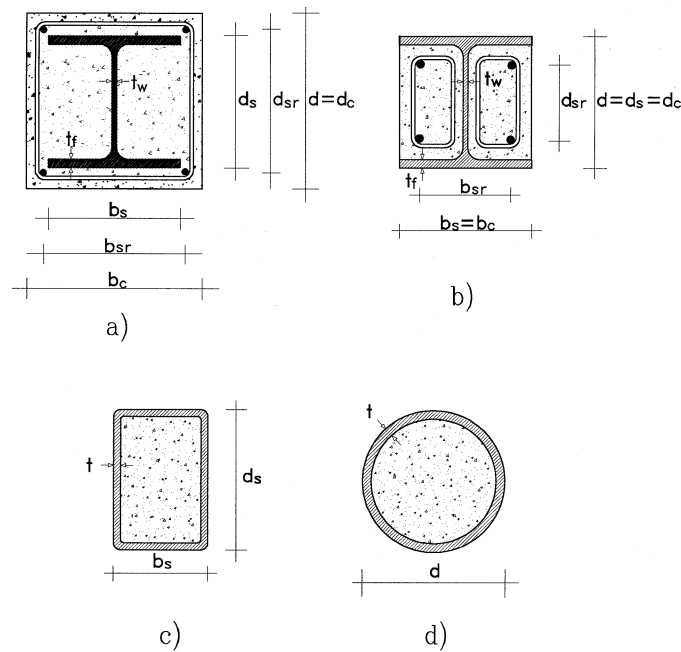


FIGURE 6.46: Typical steel concrete composite columns. (a) I steel profile fully encased in concrete. (b) I steel profile partially encased in concrete. (c) Hollow steel section filled of concrete. (d) Circular steel section filled of concrete.

The first type of cross-section, which is illustrated in Figure 6.46a, is characterized by I-steel profiles fully encased in concrete. In the second type of cross-section (See Figure 6.46b), the steel profile is partially encased in concrete while the external surface of the steel flanges is uncovered. In the third type, the concrete completely fills a steel hollow section. In this case, the column behavior is different when rectangular steel sections (Figure 6.46c) or circular steel sections (Figure 6.46d) are considered.

Composite columns embody several advantages. In general, the two limit cases of a composite section are the reinforced concrete section, when the steel area is small, and the steel section, when concrete is not introduced. Thereby, the composite system is a more complete structural system than simple reinforced concrete or steel elements.

When adopting a composite section, the amount of structural steel, reinforcing steel and concrete area, and the geometry as well as the position of the three materials represent relevant design parameters. Indeed, a number of different combinations is possible thus leading to a flexible design. From a technical viewpoint, the fully encased and partially encased columns offer good fire and corrosion resistance properties, owing to the protection offered by concrete. On the other hand, the most important benefit of the concrete filled type owing to the cross-section is that the steel tube also serves as form-work for concrete even if adequate additives have to be used for reducing the concrete separation from the steel section due to shrinkage.

Further advantages are associated with the constructional techniques: for instance, it is possible to set up entirely the steel part of the structure and then to complete it with concrete at alternate levels reducing erection time. It is also possibly a convenient precast of partially encased columns. In particular, the steel profile can be filled with concrete in a horizontal position and then the column can be turned 180° and completed with the remaining concrete.

Moreover, structural benefits can be identified. One important aspect is that concrete prevents local buckling, more effectively in fully encased sections but also in partially encased ones. Also,

for concrete filled sections this problem is reduced. Indeed, concrete represents an effective bound for steel in order to prevent or delay the critical warping. Thereby, the elements are generally characterized by a compact behavior while the section reaches full plastic state. In the concrete filled type, the steel provides benefits to concrete. In detail, the confinement effect due to steel is high for the rectangular sections and very high for circular sections, resulting in the increasing of strength with a great enhancement of ductility. The aforementioned last advantage appears to be more relevant to seismic countries, in which composite columns are largely used (see, as an example, Japan).

Clearly, the performances of composite columns require a proper design of connections, both between the two materials (i.e., concrete and steel) and between the two elements (i.e., beams and/or columns and base columns). The problem of steel-concrete connection is analyzed in this section while connections between elements are analyzed in Chapter 23 of this Handbook.

6.6.2 Failure Mechanisms

Composite columns are characterized by several typical failure mechanisms. Collapse due to combined compression and bending could occur, together with the phenomena that characterizes the behavior of slender beam-columns (i.e., geometrical imperfections, erection imperfections, and residual stresses). The shear interaction mechanism could also be present, especially for stocky elements. Local buckling is usually prevented.

A problem relevant to composite systems is represented by the force transfer mechanism between the two components. The force transferring and/or the load introduction have to be developed along a short part of the column in order to consider the element as composite, i.e., full interaction between concrete and steel arises. Reference to bond is possible, but in most cases mechanical connectors are necessary to produce mechanical interlock. The evaluation of connector strength can be made by means of the rules in Section 6.5.

6.6.3 The Elastic Behavior of the Section

All the sections reported in Figure 6.46 are characterized by the centroid of steel profile, reinforcement, and concrete that are coincident, owing to the symmetry about both axes; other cases are more complex [42] and are out of the scope of this chapter.

Due to the aforementioned symmetry, the geometrical characteristics can be evaluated in a simple manner. If concrete is uncracked, the overall full section must be considered, and as a result, the area, A , and the inertia, I , of the composite section can be evaluated as the sum of the area and the inertia of the two components by introducing the modular ratio, n :

$$A = A_s + A_{sr} + A_c/n \quad (6.68)$$

$$I = I_s + I_{sr} + I_c/n \quad (6.69)$$

The long term effects can be taken into account by the EM (Effective Modulus) method. In detail, Equation 6.9 can be adopted to introduce the creep effects caused by dead loads. Both the maximum and minimum stress in concrete, steel profile, and steel rebars can be computed by means of the following expressions:

$$\sigma_{c.\max(\min)} = \frac{N}{n \cdot A} \pm \frac{M}{nI} \cdot \frac{d_c}{2} \quad (6.70)$$

$$\sigma_{s.\max(\min)} = \frac{N}{A} \pm \frac{M}{I} \cdot \frac{d_s}{2} \quad (6.71)$$

$$\sigma_{sr.\max(\min)} = \frac{N}{A} \pm \frac{M}{I} \cdot \frac{d_{sr}}{2} \quad (6.72)$$

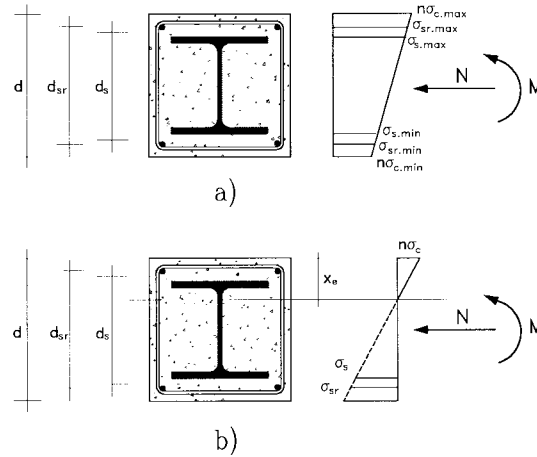


FIGURE 6.47: Beam-column composite element. (a) Composite section fully effective. (b) Cracked composite section.

where M and N represent the design values (see Figure 6.46 and 6.47a). If the section is in a cracked condition, only the concrete in compression has to be considered (Figure 6.47b), and the approach is similar to the one used for reinforced concrete sections. The elastic neutral axis, x_e , can be evaluated by means of the following equation:

$$I - S \left(\frac{M}{N} - \frac{d}{2} + x_e \right) = 0 \quad (6.73)$$

where

S = the first moment of the cross-section effective area (steel and concrete assumed to be under compression) with respect to the elastic neutral axis

I = the inertia of the effective section respect to the same line

d = the overall dimension of the cross-section

Finally, concrete contributions are divided by the modular ratio, n .

Moreover, stresses can be computed by means of similar expressions that are typical of reinforced concrete sections:

$$\sigma_c = \frac{N}{n \cdot S} \cdot x_e \quad (6.74)$$

$$\sigma_s = \frac{N}{S} \cdot \left(\frac{d + d_s}{2} - x_e \right) \quad (6.75)$$

$$\sigma_{sr} = \frac{N}{S} \cdot \left(\frac{d + d_{sr}}{2} - x_e \right) \quad (6.76)$$

The stress control follows the same indications as the ones adopted for composite beams (see Section 6.3.4).

6.6.4 The Plastic Behavior of the Section

Resistance of the Section Under Compression

First, the uniaxial compression case is considered in order to highlight the main aspects of the problem. Experimental results showed that the resistance of the section can be evaluated as the sum

of the strength of the three components (i.e., concrete, structural steel, and reinforcing steel). This approach is allowed if the maximum stress in concrete is reached when steel is yielded (Figure 6.48). Since the concrete strain at the maximum stress is about 0.2%, and by assuming the elastic modulus of steel is about 210000 N/mm², maximum stress is reached simultaneously in the two materials

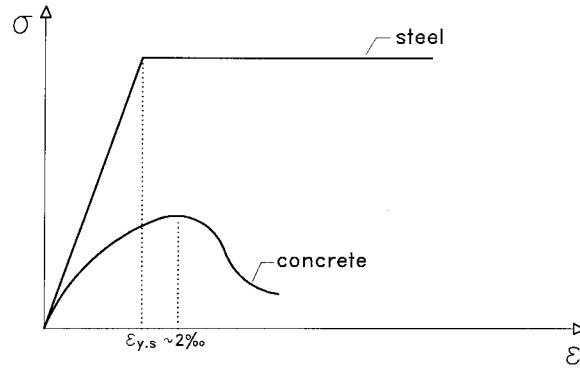


FIGURE 6.48: Stress-strain relationship for concrete and steel.

if the steel stress at yielding is lower than $2/1000 \times 210000 = 420$ N/mm². On the basis of the aforementioned consideration, AISC provisions specify a maximum yield stress of 55 ksi (about 380 N/mm²). Thereby, high strength steel is excluded as steel yield strain could be higher than the peak strain of concrete. As a result, the yield stress of steel could be reached when concrete behaves in the softening range so as to get the section resistance lower than the sum of the resistance of the two components. However, the sum of the two resistances can still be obtained only if concrete is well confined: in such conditions, concrete is ductile and stress remains practically constant even for high strain values.

According to Eurocode 4 provisions, the “design” plastic axial resistance of the section N_{pl} is evaluated by dividing the “characteristic” strength of material $f_{y,s}$, $f_{y,sr}$, and f_c by means of the partial safety factors as follows:

- encased sections:

$$N_{pl} = \frac{f_{y,s} \cdot A_s}{1.10} + \frac{f_{y,sr} \cdot A_{sr}}{1.15} + \frac{0.85 \cdot f_c \cdot A_c}{1.50} \quad (6.77)$$

- rectangular concrete filled sections:

$$N_{pl} = \frac{f_{y,s} \cdot A_s}{1.10} + \frac{f_{y,sr} \cdot A_{sr}}{1.15} + \frac{f_c \cdot A_c}{1.50} \quad (6.78)$$

Additional corrective factors are introduced for circular concrete-filled sections to take into account the confinement action, which is both very effective and beneficial in concrete and reduces the normal bearing capacity of steel that is subjected to biaxial tension and compression.

According to the AISC provisions, the resistance of the section is computed as the product of the “nominal strength” of the materials $f_{y,s}$, $f_{y,sr}$, and f_c times the resistance factor $\phi_c = 0.85$. As a result,

$$N_{pl} = 0.85 \cdot (f_{y,s} \cdot A_s + c_1 \cdot f_{y,sr} \cdot A_{sr} + c_2 \cdot f_c \cdot A_c) \quad (6.79)$$

in which the strength of materials has to be considered as a “nominal value”, while the numerical factors, c_i , assume the following values:

- encased sections

$$c_1 = 0.70; c_2 = 0.60 \quad (6.80a)$$

- concrete-filled sections

$$c_1 = 1.00; c_2 = 0.85 \quad (6.80b)$$

A comparison between the code approaches can be performed by deriving AISC formulation in the EC4 format. One obtains the following quantities:

- encased sections:

$$N_{pl} = \frac{f_{y,s} \cdot A_s}{1.18} + \frac{f_{y,sr} \cdot A_{sr}}{1.68} + \frac{0.85 \cdot f_c \cdot A_c}{1.67} \quad (6.81)$$

- concrete-filled sections:

$$N_{pl} = \frac{f_{y,s} \cdot A_s}{1.18} + \frac{f_{y,sr} \cdot A_{sr}}{1.18} + \frac{f_c \cdot A_c}{1.38} \quad (6.82)$$

A comparison between Equations 6.77 and 6.78 and Equations 6.81 and 6.82 mirrors differences that are not very remarkable, especially if the different procedures are considered, which are then applied to evaluate the strength of the material (characteristic values vs. nominal values). It should be noted that AISC provisions remarkably reduce the reinforcement contribution in encased sections.

Resistance of a Section to Combined Compression and Bending

The behavior of composite cross-sections under compression and bending actions is determined by the interaction curves M–N. The relevant codes provide methods quite different for defining the interaction curves. For example, the Japanese provisions (based on the method of Wakabaishi) are reported in [AIJ, 1987] and the AISC provisions are reported in [AISC, 1994]. The Eurocode 4 approach is based on the study of Roik and Bergman [41, 42].

The general procedure consists of defining some points of the interaction curve by means of the solution of both translational and rotational equilibrium equations of the section. These are based on Bernoulli's hypothesis and by introducing the constitutive relationships of materials, which are described in Section 6.2. The method is theoretically simple, but it requires a considerable effort and it is not used in practice. Thereby, simplified methods are required.

The ductility of the materials allows a full plastic analysis to be used. With reference to the interaction curve of Figure 6.49, point A defines the uniaxial plastic resistance ($N = N_{pl}$, $M = 0$) and it can be determined by means of the formulation reported in the previous paragraph. Point B represents the plastic moment resistance ($M = M_{pl}$, $N = 0$).

AISC code suggests a simple procedure in order to draw the interaction curve, which consists of approximating the curve by means of two linear segments with the evaluation of N_{pl} and M_{pl} only.

The studies of Roik and Bergman [41, 42] suggest a piecewise linear curve on the safe side with respect to the actual interaction curve to be drawn. The minimum number of points necessary to obtain a realistic multi-linear curve ranges between four or five. These points can be determined by assuming a full plastic stress distribution (i.e., stress block) in all the materials (concrete, structural steel, and reinforcing steel). The result of the method is schematically shown in Figure 6.50. It can be observed that point C is sufficient to obtain a simplified, but conservative, approximation. Point C, which can be readily defined without any additional evaluation, is determined by the same moment M_{pl} that characterizes the condition $N = 0$. This consideration allows $N_{pl,c}$ to be easily identified as

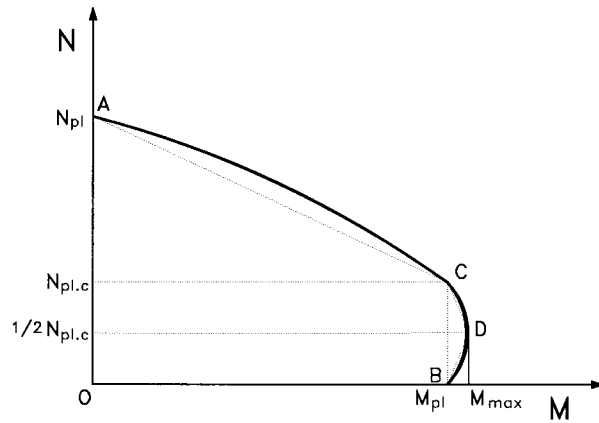


FIGURE 6.49: M–N interaction curve.

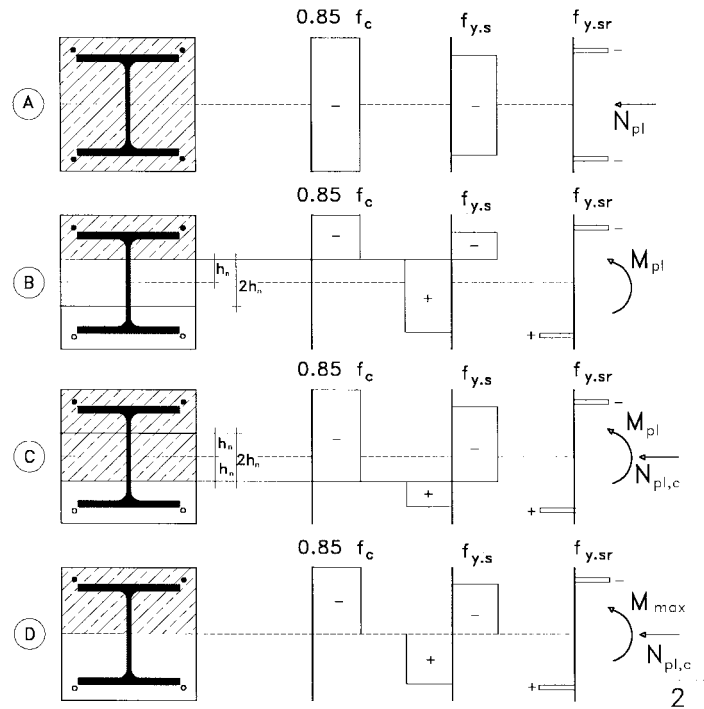


FIGURE 6.50: Stress distributions corresponding to an interaction curve.

the resistance of the concrete area, by comparing the stress pattern to the one of point B:

$$N_{pl,c} = \frac{c_3 \cdot f_c \cdot A_c}{1.5} \quad (6.83)$$

($c_3 = 1.0$ for filled and $c_3 = 0.85$ for encased sections, respectively)

Point D is identified through the coordinates ($N = N_{pl,c}/2$ and $M = M_{max}$). Point D can be safely neglected, leading to a slightly conservative interaction curve. In general, the interaction curve A –

C – D is convex and, as a result, on the safe side.

In order to evaluate M_{\max} and M_{pl} , by means of the stress pattern of Figure 6.50, the following equations can be defined:

$$M_{\max} = W_s \cdot f_{y.s} + W_{sr} \cdot f_{y.sr} + \frac{W_c}{2} \cdot 0.85 \cdot f_c \quad (6.84)$$

$$M_{pl} = (W_s - W_{s.n}) \cdot f_{y.s} + (W_{sr} - W_{sr.n}) \cdot f_{y.sr} + \frac{1}{2} \cdot (W_c - W_{c.n}) \cdot 0.85 \cdot f_c \quad (6.85)$$

where

W_s , W_{sr} , and W_c = the plastic moduli of the steel profile, reinforcement, and concrete
 $W_{s.n}$, $W_{sr.n}$, and $W_{c.n}$ = the plastic moduli of the part of steel profile, reinforcement, and concrete in the height of section $\pm h_n$, where h_n is the distance between the plastic neutral axis line and the centroid line in correspondence of $M = M_{pl}$

In Example 6.6, applications of Equations 6.84 and 6.85 will be analyzed. In Equations 6.84 and 6.85, the strength of materials should be considered as “unfactored” strength. In order to obtain the design values of Eurocode 4, it is necessary to introduce the partial safety factors. Clearly, the interaction curve characterizes the sole section behavior or the behavior of a very stocky element. The actual behavior of members is analyzed in the next paragraph.

6.6.5 The Behavior of the Members

Resistance of Members to Compression

As far as buckling problems are concerned, both AISC and Eurocode 4 extend the approach of the steel columns to the composite ones

According to Eurocode 4, the design ultimate bearing capacity of the composite column N_u has to be determined by considering the imperfection effects and residual stresses. The influence of these effects on the axial resistance of the section N_{pl} , evaluated by means of Equation 6.77 or 6.78, are introduced by means of the factor χ of the buckling curves, in order to evaluate the ultimate axial load of column N_u :

$$N_u = \chi \cdot N_{pl} \quad (6.86)$$

$$\chi = \frac{1}{\phi + \sqrt{\phi^2 - \lambda^2}} \quad (6.87)$$

$$\phi = 0.5 \cdot \left[1 + \alpha \cdot (\lambda - 0.2) + \lambda^2 \right] \quad (6.88)$$

where

λ = the relative slenderness of the column that shall be defined in the following
 α = the imperfection factor that is equal to 0.21, 0.34, and 0.49 for three different curves named a, b, and c, respectively (Figure 6.51)

In particular, these three buckling curves a, b, and c refer to concrete-filled cross-sections, encased cross-sections loaded along the strong axis, and encased sections loaded along the weak axis, respectively.

AISC code allows the critical stress σ_{cr} (F_{cr} according to the symbols of AISC) to be evaluated, which has to be multiplied by the steel area A_s as a function of a conventional value of steel yield stress f_{my} , modified in order to account for the other components of the section. The buckling curve comprises two branches represented by the following equations:

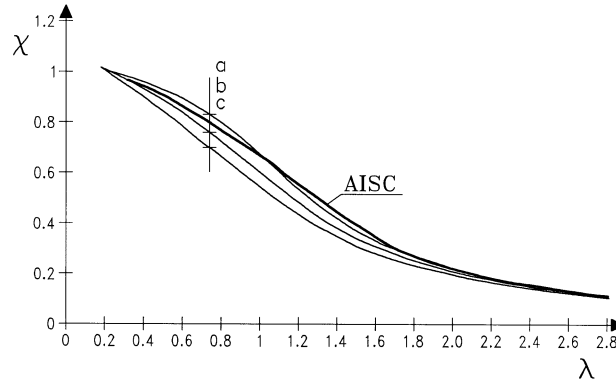


FIGURE 6.51: Buckling curves for Eurocode 4 and AISC provisions.

$$\sigma_{cr} = (0.658^{\lambda^2}) \cdot f_{my} \text{ if } \lambda \leq 1.5 \quad (6.89a)$$

$$\sigma_{cr} = \left(\frac{0.877}{\lambda^2} \right) \cdot f_{my} \text{ if } \lambda \geq 1.5 \quad (6.89b)$$

The comparison among the three buckling curves of Eurocode 4 and the one of AISC is shown in Figure 6.51. In order to draw the AISC curve, the following relations are adopted:

$$\chi = (0.658^{\lambda^2}) \text{ for } \lambda \leq 1.5 \quad (6.90a)$$

$$\chi = \left(\frac{0.877}{\lambda^2} \right) \text{ for } \lambda \geq 1.5 \quad (6.90b)$$

Eurocode 4 defines the “relative slenderness” by means of the following expression:

$$\lambda = \sqrt{\frac{N_{pl}}{N_{cr}}} = \frac{k \cdot l}{\pi} \cdot \sqrt{\frac{f_{y,s} \cdot A_s + f_{y,sr} \cdot A_{sr} + 0.85 \cdot f_c \cdot A_c}{E_s \cdot I_s + E_{sr} \cdot I_{sr} + 0.8 \cdot E_c \cdot I_c / 1.35}} \quad (6.91)$$

Since N_{pl} is expressed by means of Equations 6.77 or 6.78, by assuming the characteristic values of the strength without the partial safety factors:

$$N_{pl} = f_{y,s} \cdot A_s + f_{y,sr} \cdot A_{sr} + c_3 \cdot f_c \cdot A_c \quad (6.92)$$

($c_3 = 1.0$ filled $c_3 = 0.85$ encased)

The critical bearing capacity N_{cr} is calculated as follows:

$$N_{cr} = \frac{\pi^2 \cdot (EI)_e}{(kl)^2} \quad (6.93)$$

where

kl = the effective length

$(EI)_e$ = the effective flexural stiffness of the composite section

$$(EI)_e = E_s \cdot I_s + E_{sr} \cdot I_{sr} + 0.59 E_c \cdot I_c \quad (6.94)$$

The factor $0.8 / 1.35 = 0.59$ that reduces the elasticity modulus of concrete considers a secant modulus owing to the non-linear behavior of concrete and it allows a good agreement of the theoretical and experimental results to be achieved [41]. The creep influence can be remarkable for slender columns; therefore, in such a case, an additional reduction of the elasticity modulus of concrete that leads to an effective elasticity modulus:

$$E_{c.ef} = E_c \cdot \left(1 - 0.5 \cdot \frac{N_p}{N} \right) \quad (6.95)$$

where the ratio between the axial load owing to the dead load, N_p , and the total axial load, N , is considered to weight the creep effect. As an example, if the dead load is 2/3 and the live load is 1/3 of the total axial load, the effective modulus of concrete is obtained by a reduction factor equal to $1 - 0.5 \cdot 2/3 = 0.67$.

The slenderness definition of AISC is quite different since the following expression is introduced:

$$\lambda = \frac{kl}{\pi \cdot r_m} \cdot \sqrt{\frac{f_{y.s} \cdot A_s + c_1 \cdot f_{y.sr} \cdot A_{sr} + c_2 \cdot f_c \cdot A_c}{E_s \cdot A_s + c_4 \cdot E_c \cdot A_c}} \quad (6.96)$$

where

$r_m = (I_s/A_s)^{0.5}$ = the gyration radius of the steel part

The factors c_1, c_2 have already been used to define Equation 6.79, while c_4 assumes the following values:

- encased cross-sections:

$$c_4 = 0.20$$

- concrete cross-filled:

$$c_4 = 0.40$$

Also, in this case the comparison between the two codes can be affected by changing the format of AISC slenderness according to the Eurocode 4 expression:

$$\lambda = \frac{kl}{\pi} \cdot \sqrt{\frac{f_{y.s} \cdot A_s + c_1 \cdot f_{y.sr} \cdot A_{sr} + c_2 \cdot f_c \cdot A_c}{E_s \cdot I_s + c_4 \cdot E_c \cdot I_s \cdot A_c / A_s}} \quad (6.97)$$

The conceptual difference between Equations 6.91 and 6.97 is that the reinforcement contribution to the effective inertia is neglected and the concrete contribution is evaluated in a simplified manner in Equation 6.97.

The reduction factor χ allows the interaction curve of the section to be reduced by obtaining the interaction curve of the member. Under a pure compression regime, the column design is satisfied if:

$$N < \chi \cdot N_{pl} \quad (6.98)$$

Resistance of Members to Combined Compression and Bending

The check of a column subject to combined compression and bending has to be carried out by means of the following steps:

- The interaction curve of the section has to be evaluated.

- The interaction curve of the member shall be drawn reducing the interaction curve of the section to take into account the geometrical non-linearity related both to the axial compression (axial buckling) and to bending (flexural-torsional buckling). Moreover, it has to be considered the influence of geometrical imperfections (by the fabrication of the elements as well as the erection procedure), mechanical imperfections, (i.e., residual stresses), bending moment pattern along the element, the presence of lateral restraints, etc.
- The external actions have to be increased in a simplified way (in particular, the bending moment owing to the load has to be increased) to evaluate the stress introduced by the geometrical non-linearity that can influence the slender elements.

By considering the procedure of Eurocode 4, one assumes that no bending moment, M , can be applied in correspondence of $N_u = \chi N_{pl}$. However, when the axial compression is null, the moment M_{pl} can be applied entirely. As a result, for a generic value of N , Eurocode 4 suggests referral to the line between these two limiting values. For the design value of the axial force, N_d , the plastic moment, M_{pl} , reported in Figure 6.52 can be carried by the column. Moreover, what follows can be

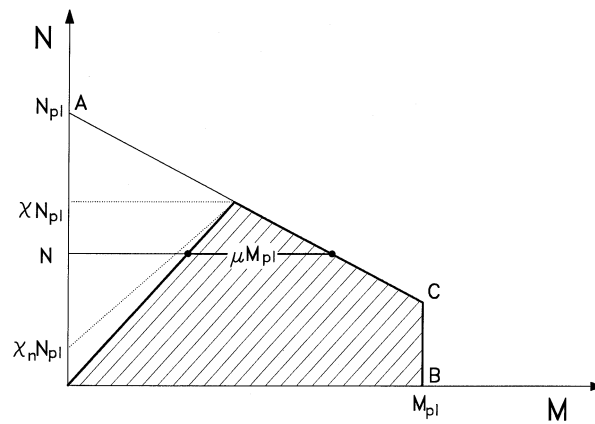


FIGURE 6.52: M–N design interaction diagram.

observed:

- The use of stress blocks for the materials is unsafe to a certain extent because it implies infinite ductility of concrete. As a result, Eurocode 4 suggests reduction of M_{pl} by a factor of 0.9.
- The geometrical imperfections of the column which are taken into account in the buckling curves are considered in the most unfavorable combination: constant along all the element. Thus, the method previously explained is referred to as a constant distribution of the bending moment. If the moment is variable along the column, the procedure is much safer. It is possible to consider the interaction curve marked by the dotted line in Figure 6.52 that intersects the points $M = 0$; $N = \chi_n N_{pl}$ where

$$\chi_n = \chi \cdot \frac{1 - r}{4} \quad (6.99)$$

where r is limited between -1 and 1 and represents the ratio between the values of bending moments at the member ends. The design bending moment, M , that has to be considered in the check is an equivalent moment, owing to the variability along the element.

A number of studies dealt with this aspect; in particular, Eurocode 4 takes into account the second order moment multiplying the first order bending moment by means of a factor, a :

$$a = \frac{c}{1 - N/N_{cr}} \geq 1.0 \quad ; \quad c = 0.66 + 0.44 \cdot r \geq 0.44 \quad (6.100)$$

where r is already defined in Figure 6.53. In the factor, a , the term above takes into account the moment distribution along the column. In detail, c equals 1 if the moment is constant, the term

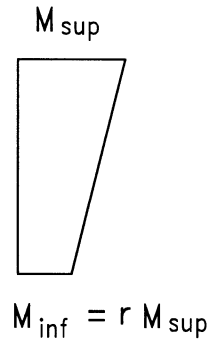


FIGURE 6.53: Definition of r factor in accordance with Eurocode 4.

below is lower than 1, and increases the equivalent moment introducing the effect of the second order moment (this term approaches 1 if N is much lower than N_{cr} , while it approaches 0 if N tends to N_{cr}). Finally, the check of the column requires that the moment M is lower than the ultimate value M_u equal to $0.9 \mu M_{pl}$; i.e.:

$$M \leq M_u = 0.9 \cdot \mu \cdot M_{pl} \quad (6.101)$$

The aforementioned numerical procedure is developed by means of the examples to follow regarding fully encased columns, partially encased columns, and concrete-filled columns reported in Section 6.6.9.

6.6.6 Influence of Local Buckling

The elastic approach of Section 6.6.3 has to be applied to evaluate the stress condition under the serviceability loading; conversely, the full plastic bearing capacity of the section can be reached almost always at failure. In fact, as mentioned previously, the presence of the concrete reduces the local buckling phenomena; in particular, in fully encased sections local buckling is definitely prevented if a certain minimum concrete cover is used. In the other cases, local buckling can be excluded if limit ratios of depth-to-thickness for the steel section are respected. By considering Eurocode 4, it follows that:

- partially encased I-sections:

$$b_s/t_f \leq 44 \cdot \sqrt{235/f_{y,s}} \quad (6.102)$$

- circular hollow steel sections:

$$d_s/t \leq 90 \cdot \sqrt{235/f_{y.s}} \quad (6.103)$$

- rectangular hollow steel sections:

$$b_s/t \leq 52 \cdot \sqrt{235/f_{y.s}} \quad (6.104)$$

where $f_{y.s}$ is the characteristic strength in N/mm². These restrictions are loose with respect to the case of simple profiles analyzed in Section 6.4.3.

The AISC approach is slightly different by considering the following restrictions:

- circular hollow steel sections:

$$t \geq d_s \sqrt{\frac{f_{y.s}}{8 \cdot E_s}} \quad (6.105)$$

- rectangular hollow steel sections:

$$t \geq b_s \sqrt{\frac{f_{y.s}}{3 \cdot E_s}} \quad (6.106)$$

where

$f_{y.s}$ = the nominal strength in N/mm²

In order to compare different codes, the AISC provisions can be expressed in the same format of Eurocode 4 by assuming $E_s = 210000$ N/mm² and are reported in the following:

- circular hollow steel sections:

$$d_s/t \leq 85 \cdot \sqrt{\frac{235}{f_{y.s}}} \quad (6.107)$$

- rectangular hollow steel sections:

$$b_s/t \leq 52 \cdot \sqrt{\frac{235}{f_{y.s}}} \quad (6.108)$$

One can observe that the restrictions of the two codes are similar.

6.6.7 Shear Effects

In stocky members, or in the case of high horizontal loads, the shear influence can be remarkable. In this case, the interaction curve N–M–V has to be drawn both for the section and for the member. To analyze this problem in a general manner, the constitutive relationships of materials and appropriate resistance criteria are required. Moreover, all the geometrical and mechanical non-linearities and imperfections of the element have to be considered in the computation.

Usually, the provisions suggested for the continuous beam (see Section 6.4.5), where interaction between shear and bending takes place, apply to the columns. In detail, the approximate procedure assumes that shear is carried out by means of the web of the steel profile and only a part of the web is considered able to resist the combined compression and bending moment.

6.6.8 Load Introduction Region

The connection between horizontal (beams) and vertical (beam columns) usually requires complex systems that are analyzed in Chapter 23 of this Handbook. However, when the joints are set, it is necessary to ensure the load introduction along a short length of the members out of the nodal zone. As an example, Eurocode 4 suggests that the load introduction length should not exceed twice the overall dimensions of the cross-section. The transfer of the shear forces can be guaranteed by steel-concrete bond only if the bond stress is lower than prescribed limits. As already stated in Section 6.2 bond stress has to satisfy the following limits:

- 0.6 N/mm^2 for encased cross-sections
- 0.4 N/mm^2 for concrete-filled cross-sections

Otherwise, mechanical shear connectors must be used. Analogous rules of the connections to beams have to be used. Moreover, in the case of fully encased beams, Eurocode 4 provisions allow an increase of the shear capacity of stud connectors owing to the friction between concrete and steel flange, using a frictional coefficient of 0.5.

Another aspect of the problem regards the load introduction to the members. When the supporting concrete area is wider than the loaded area, the restrained lateral expansion offered by the remaining concrete provides a strength increase; AISC provisions consider this phenomenon increasing of the design strength of the concrete with a factor of 1.7.

6.6.9 Restrictions for the Application of the Design Methods

The rules explained in the previous paragraphs according to both Eurocode 4 and AISC are effective if some restrictions are fulfilled. Indeed, the simplified procedures are based on large experimental and numerical analyses that, however, cannot take into account all design conditions. Thereby, though it is always possible to apply a general procedure introducing the constitutive relationships of materials, the rules suggested by Eurocode 4 can be used only if the following restrictions are satisfied:

- the cross-sections are symmetric about the two axes and the cross-section is constant along the member
- the factor δ_s

$$\delta_s = \frac{A_s \cdot f_{y,s} / 1.1}{N_{pl}} \quad (6.109)$$

that represents the contribution of structural steel in the plastic axial load capacity varies between 0.2 and 0.9; otherwise, the member has to be designed as a reinforced concrete element corresponding to a lower restriction or as a steel element corresponding to a higher restriction.

- The relative slenderness λ shall be lower than 2.
- If the longitudinal reinforcement is considered in the design, the minimum share of 0.3% and maximum share of 4% of the concrete area shall be provided.
- In the fully encased cross-sections, a minimum concrete clear cover of 40 mm shall be provided.

Moreover, the additional restrictions must be considered: maximum clear cover along the axis direction of $0.3 d$; maximum clear cover along the weak axis of $0.4 b_s$. Likewise, the AISC provisions require the following restrictions:

- The steel profile area has to be at least 4% of the composite cross-section area.

- In the case of encased sections, longitudinal reinforcement shall be continuous at framed levels; the spacing of ties shall be not greater than $2/3$ the minimum dimension of the cross-section.
- The cross-sectional area of the transverse and longitudinal reinforcement shall be at least 1.8 mm^2 per millimeter of bar spacing (0.007 in.^2 per inch of bar spacing). The clear cover of both longitudinal and transversal reinforcement shall be at least 38.1 mm (1.5 in.).
- The concrete, reinforcing steel, and structural steel shall follow the requirements of par 2.1, 2.2, and 2.3.
- In the case of concrete-filled sections, the restrictions expressed by Equations 6.107 and 6.108 reported in Section 6.6.6 have to be taken into account.
- The gyration radius of the steel profile r_m (see Section 6.6.5) shall not be less than 0.3 times the overall dimension of the cross-section in the plane of buckling.

6.6.10 Worked Examples

In what follows, the Eurocode 4 procedure is developed with reference to two beam columns characterized by the same length, bending moment pattern, and axial load, but different type of cross-section. In Example 6.6, the case of a fully encased cross-section is analyzed; in Example 6.7, a rectangular concrete-filled cross-section is analyzed. In both cases, the column is characterized by the following conditions:

- length $l = 4000 \text{ mm}$
- restraints: fixed at the lower end and simply supported at the top end in both vertical planes
- axial load: $N = 850 \text{ kN}$
- bending moment: linear pattern as illustrated in Figure 6.54 characterized by $M = 140 \text{ kNm}$ at the top end and $M = -70 \text{ kNm}$ at the bottom end ($r = -0.5$ as shown in Figure 6.53)

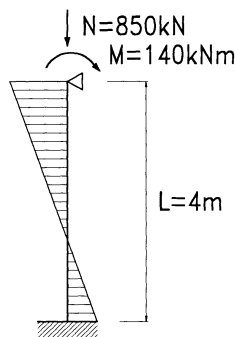


FIGURE 6.54: Distribution of bending moment in the column.

Materials are characterized by the following characteristic strength, design strength, and elasticity modulus:

- structural steel: $f_{y.s} = 355 \text{ N/mm}^2$, $f_{y.s.d} = 322.7 \text{ N/mm}^2$; $E_s = 210000 \text{ N/mm}^2$
- reinforcing steel: $f_{y.sr} = 420 \text{ N/mm}^2$, $f_{y.sr.d} = 365.2 \text{ N/mm}^2$; $E_{sr} = 210000 \text{ N/mm}^2$
- concrete: $f_c = 20 \text{ N/mm}^2$; $f_{c.d} = 13.3 \text{ N/mm}^2$; $E_c = 29000 \text{ N/mm}^2$

EXAMPLE 6.6: Fully encased cross-section

The section has dimension $300 \text{ mm} \cdot 300 \text{ mm}$; the steel profile is HEA 200; the reinforcement is provided by four bars with diameter 12 mm.

The geometric characteristics of the cross-section are (see Figure 6.55):

$$\begin{aligned} b_c &= 300 \text{ mm}; d_c = 300 \text{ mm}; \\ b_{rs} &= 230 \text{ mm}, d_{rs} = 230 \text{ mm}; \\ b_s &= 200 \text{ mm}, d_s = 190 \text{ mm}; \end{aligned}$$

thus leading to the following area and second order moment of the cross-section:

- steel

$$\begin{aligned} A_s &= 5380 \text{ mm}^2, \\ I_s \text{ (strong axis)} &= 3692 \cdot 10^4 \text{ mm}^4, I_s \text{ (weak axis)} = 1336 \cdot 10^4 \text{ mm}^4 \end{aligned}$$

- rebars:

$$A_{sr} = 4 \cdot 113 = 452 \text{ mm}^2; I_{sr} = 4 \cdot 113 \cdot 115^2 = 598 \cdot 10^4 \text{ mm}^4$$

- concrete

$$\begin{aligned} A_c &= 300 \cdot 300 - 5380 - 452 = 84,168 \text{ mm}^2 \\ I_c &= \frac{300^4}{12} - 3692 \cdot 10^4 - 598 \cdot 10^4 = 6321 \cdot 10^4 \text{ mm}^4 \quad (\text{strong axis}) \\ I_c &= \frac{300^4}{12} - 1336 \cdot 10^4 - 598 \cdot 10^4 = 6557 \cdot 10^4 \text{ mm}^4 \quad (\text{weak axis}) \end{aligned}$$

1. Application of simplified rules and shear interaction — The plastic axial resistance of the cross-section according to Equation 6.77 is

$$N_{pl} = \frac{355 \cdot 5380}{1.10} + \frac{420 \cdot 452}{1.15} + \frac{0.85 \cdot 20 \cdot 84168}{1.50} = 2855 \cdot 10^3 \text{ N} = 2855 \text{ kN}$$

The steel contribute as given by Equation 6.109 is

$$\delta_s = \frac{5380 \cdot 355/1.1}{2855 \cdot 10^3} = 0.608$$

The other limitations given by Section 6.6.9 are satisfied; thereby the simplified method of Eurocode 4 can be applied. It should be observed that there are no problems of local buckling that is typical of fully encased elements (see Section 6.6.6). It should also be observed that:

- the design value of shear is

$$V = \frac{140 + 70}{4} = 52.5 \text{ kN}$$

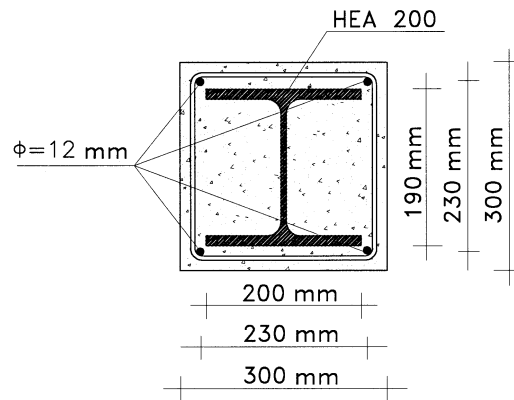


FIGURE 6.55: Geometric characteristics of the cross-section.

- the plastic shear resistance is

$$V_{pl} = 1.04 \cdot 6.5 \cdot 200 \cdot \frac{355}{1.1\sqrt{3}} = 252 \cdot 10^3 \text{ N} = 252 \text{ kN}$$

thus not leading to interaction between bending moment and shear ($V < 0.5 V_{pl}$; Section 6.6.7).

2. Determination of the M - N interaction curve — With reference to Section 6.6.4, the general evaluation of the interaction N - M curve requires a number of couples (N, M) using the two equations of equilibrium and Bernoulli assumption to be evaluated. The full interaction curve of the cross-section defined in this example, evaluated point by point by means of a numerical procedure, is illustrated in Figure 6.56. It is evident that point A, B, C, and D provide a quite good approximation of the actual curve.

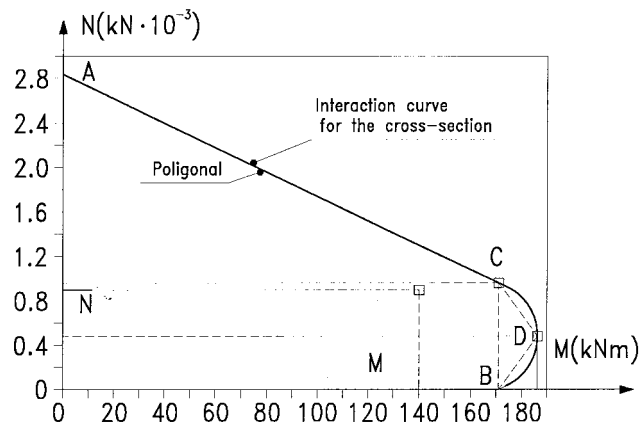


FIGURE 6.56: Cross-section interaction curve.

The points are defined as follows:

- point A: ($N = N_{pl}$, $M = 0$)

- point B: ($N = 0$, $M = M_{pl}$)
- point C: ($N = N_{pl.c}$, $M = M_{pl}$)
- point D: ($N = N_{pl.c}/2$, $M = M_{\max}$)

By means of Equation 6.83, one obtains what follows:

$$N_{pl.c} = 0.85 \cdot 13.3 \cdot 8416 = 953 \cdot 10^3 \text{ N} = 953 \text{ kN}$$

M_{\max} and M_{pl} are evaluated by Equations 6.84 and 6.85:

$$\begin{aligned} M_{\max} &= W_s \cdot f_{y.s.d} + W_{sr} \cdot f_{y.sr.d} + \frac{W_c}{2} 0.85 \cdot f_{c.d} \\ M_{pl} &= (W_s - W_{s.n}) \cdot f_{y.s.d} + (W_s - W_{sr.n}) \cdot f_{y.sr.d} + \frac{1}{2} \cdot (W_c - W_{c.n}) \cdot 0.85 \cdot f_{c.d} \end{aligned}$$

where:

$$\begin{aligned} W_s &= 407 \cdot 10^3 \text{ mm}^3 \\ W_{sr} &= 4 \cdot 113 \cdot 115 = 52 \cdot 10^3 \text{ mm}^3 \\ W_c &= \frac{b_c h_c^2}{4} - W_s - W_{sr} = \frac{300 \cdot 300^2}{4} - 407 \cdot 10^3 - 52 \cdot 10^3 = 6291 \cdot 10^3 \text{ mm}^3 \end{aligned}$$

and

$$\begin{aligned} h_n &= \frac{953 \cdot 10^3 / 2}{300 \cdot 0.85 \cdot 13.33 + 6.5 \cdot (2 \cdot 322.7 - 0.85 \cdot 13.33)} = 63.4 \text{ mm} \\ W_{s.n} &= t_w \cdot h_n^2 = 6.5 \cdot 63.4^2 = 26127 \text{ mm}^3 \\ W_{sr.n} &= 0 \\ W_{c.n} &= b_c \cdot h_n^2 - W_{s.n} = 300 \cdot 63.4^2 - 26127 = 1180 \cdot 10^3 \text{ mm}^3 \end{aligned}$$

It follows that:

$$\begin{aligned} M_{\max} &= 407 \cdot 10^3 \cdot 322.7 + 52 \cdot 10^3 \cdot 365.2 \\ &\quad + \frac{6291 \cdot 10^3}{2} 0.85 \cdot 13.33 = 186 \cdot 10^3 \text{ N} = 186 \text{ kN} \\ M_{pl} &= (407 - 26) \cdot 10^3 \cdot 322.7 + (52) \cdot 10^3 \cdot 365.2 \\ &\quad + \frac{1}{2} (6291 - 1180) \cdot 10^3 \cdot 0.85 \cdot 13.3 = 171 \cdot 10^5 \text{ Nmm} = 171 \end{aligned}$$

3. Ultimate axial load evaluation — In order to evaluate the ultimate axial load, it is necessary to compute the plastic axial resistance, without partial safety factors, i.e.:

$$N_{pl} = 355 \cdot 5380 + 420 \cdot 452 + 0.85 \cdot 20 \cdot 84168 = 3530 \cdot 10^3 \text{ N} = 3530 \text{ kN}$$

It is also necessary to evaluate the effective elastic flexural stiffness, by means of Equation 6.94, both in the planes of the strong axis of the steel profile and of the weak axis of the steel profile:

- strong axis:

$$(EI)_e = 210000 \cdot 3692 \cdot 10^4 + 210000 \cdot 598 \cdot 10^4 + \frac{0.8 \cdot 29000 \cdot 6557 \cdot 10^5}{1.35} = 1.987 \cdot 10^{13} \text{ N} \cdot \text{mm}^2$$

- weak axis:

$$(EI)_e = 210000 \cdot 1336 \cdot 10^4 + 210000 \cdot 598 \cdot 10^4 + \frac{0.8 \cdot 29000 \cdot 6321 \cdot 10^5}{1.35} = 1.492 \cdot 10^{13} \text{ N} \cdot \text{mm}^2$$

By considering a value of the effective length factor $k = 0.7$ in both planes, the slenderness and the buckling curve factor are according to Equation 6.91:

- strong axis:

$$\lambda = \frac{0.7 \cdot 4000}{\pi} \cdot \sqrt{\frac{3530 \cdot 10^3}{1.987 \cdot 10^{13}}} = 0.376$$

In this plane it shall be considered the stability curve b and the value of the imperfection factor α is 0.34. It follows by means of Equation 6.88:

$$\phi = 0.5 \left[1 + 0.34 \cdot (0.376 - 0.2) + 0.376^2 \right] = 0.60$$

The stability curve factor is given by means of Equation 6.87:

$$\chi = \frac{1}{0.601 + \sqrt{0.601^2 - 0.376^2}} = 0.935$$

- weak axis

$$\lambda = \frac{0.7 \cdot 4000}{\pi} \cdot \sqrt{\frac{3530 \cdot 10^3}{1.492 \cdot 10^{13}}} = 0.433$$

In this plane it shall be considered the stability curve c and the value of the imperfection factor $\alpha = 0.49$; it follows by means of Equation 6.88:

$$\phi = 0.5 \left[1 + 0.49 \cdot (0.433 - 0.2) + 0.433^2 \right] = 0.65$$

The stability curve factor is given by means of Equation 6.87:

$$\chi = \frac{1}{0.651 + \sqrt{0.651^2 - 0.433^2}} = 0.879$$

It is evident that the minimum value of the stability curve factor is given by the weak axis, thus leading to (Equation 6.86):

$$N_u = 0.879 \cdot 2855 = 2510 \text{ kN}$$

4. Member check — By means of Equation 6.98, we get:

$$\chi_n = 0.879 \cdot \frac{1 + 0.5}{4} = 0.330$$

Being:

$$\frac{N}{N_{pl}} = 0.298 < 0.330$$

In Figure 6.57, the procedure for the evaluation of the factor μ (Equation 6.101 and Figure 6.52) is shown; the check point is under the point C; thus, it is on the safe side to consider a value of $\mu = 1$. Consequently, the value of the ultimate moment of the column is the following:

$$M_u = 0.9 \cdot 1 \cdot 171 = 154 \text{ kNm}$$

It is evident that the magnification factor, a , of Equation 6.100 is equal to 1. Thus, it follows that:

$$M = 140 \text{ kNm} < M_u = 154 \text{ kNm}$$

and the column check is satisfied.

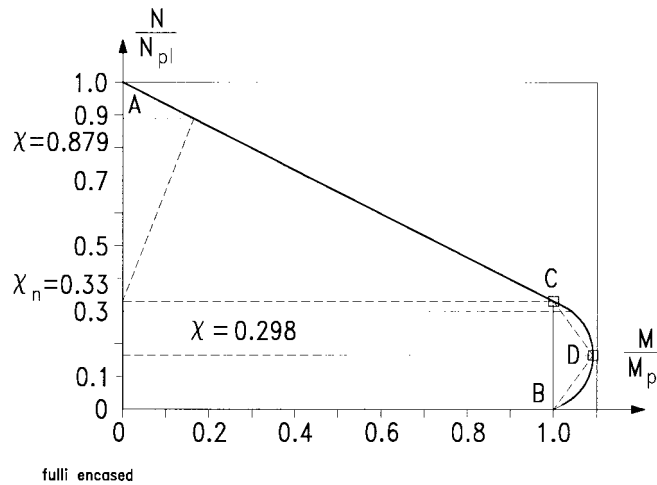


FIGURE 6.57: Procedure for the evaluation of the factor μ .

EXAMPLE 6.7: Square steel section filled of concrete

The section is characterized by the dimension 220 mm · 220 mm; the steel section has a square shape with a constant thickness t equal to 7.1 (Figure 6.58). Thus, the area and second order moment of the cross-section are

- steel:

$$A_s = t \cdot 2 \cdot (b - t) = 7.1 \cdot 2 \cdot (220 - 7.1) = 6046 \text{ mm}^2$$

$$I_s = \frac{b^4}{12} - \frac{(b - 2 \cdot t)^4}{12} = \frac{220^4}{12} - \frac{(220 - 2 \cdot 7.1)^4}{12} = 4573 \cdot 10^4 \text{ mm}^4$$

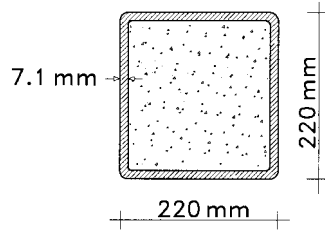


FIGURE 6.58: Geometric characteristics of the cross-section.

- concrete

$$A_c = (b - 2 \cdot t)^2 = (220 - 2 \cdot 7.1)^2 = 42354 \text{ mm}^2$$

$$I_c = \frac{(b - 2 \cdot t)^4}{12} = \frac{(220 - 2 \cdot 7.1)^4}{12} = 14949 \cdot 10^4 \text{ mm}^4$$

1. Application of the simplified rules and shear interaction — The plastic axial resistance of the cross-section is according to Equation 6.77:

$$N_{pl} = \frac{355 \cdot 6046}{1.10} + \frac{20 \cdot 42354}{1.50} = 2515 \cdot 10^3 \text{ N} = 2515 \text{ kN}$$

The steel contribution is given by Equation 6.109 and it is equal to:

$$\delta_s = \frac{6046 \cdot 355 / 1.1}{2515 \cdot 10^3} = 0.776$$

The local slenderness is according to (Section 6.6.6):

$$\frac{d}{t} = \frac{220}{7.1} = 30.98 < 52 \sqrt{\frac{235}{355}} = 42.12$$

Thus, the simplified method of Eurocode 4 can be applied. However, it should be observed that:

- the design value of shear is

$$V = \frac{140 + 70}{4} = 52.5 \text{ kN}$$

- while the plastic shear resistance is

$$V_{pl} = 1.04 \cdot 2 \cdot 7.1 \cdot 220 \cdot \frac{355}{1.1\sqrt{3}} = 605 \cdot 10^3 \text{ N} = 605 \text{ kN}$$

thus not leading to interaction between bending moment and shear ($V_d < 0.5 V_{pl}$; see Section 6.6.7).

2. Determination of the M – N interaction curve — With reference to Section 6.6.4, the evaluation of interaction N – M curve requires the definition of a number of couple (N,M) by using the two equations of equilibrium and the Bernoulli assumption. The full interaction curve of the cross-section defined in this example, evaluated point by point by means of a numerical procedure, is illustrate in Figure 6.59. In this case, the linear curve by means of the points A, B, C, and D provide an approximation less accurate; therefore, additional couple of points E and F should be considered. The points are defined as follows:

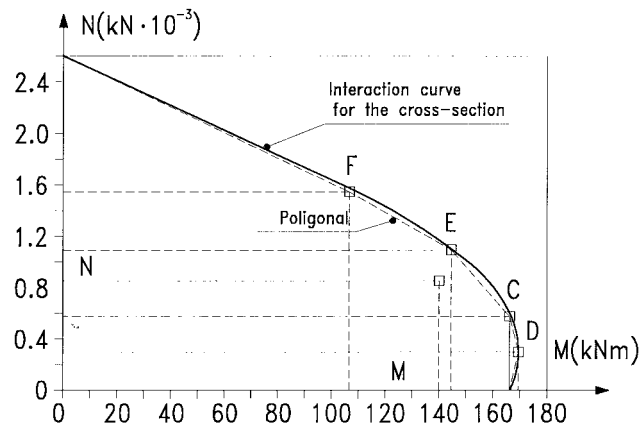


FIGURE 6.59: Interaction curve of the cross-section.

- point A: ($N = N_{pl}$, $M = 0$)
- point B: ($N = 0$, $M = M_{pl}$)
- point C: ($N = N_{pl.c}$, $M = M_{pl}$)
- point D: ($N = N_{pl.c}/2$, $M = M_{max}$)
- point E: ($N = N_E$, $M = M_E$)
- point F: ($N = N_F$, $M = M_F$)

By means of Equation 6.83:

$$N_{pl.c} = f_{c.d} \cdot A_c = 13.3 \cdot 42354 = 563 \cdot 10^3 \text{ N} = 563 \text{ N}$$

M_{max} and M_{pl} are evaluated by means of Equations 6.84 and 6.85 where:

$$\begin{aligned} W_s &= 2 \left[b \cdot t \cdot \left(\frac{b-t}{2} \right) + \left(\frac{b-t}{2} \right)^2 \cdot t \right] \\ &= 2 \left[220 \cdot 7.1 \cdot \left(\frac{220-7.1}{2} \right) + \left(\frac{220}{2} - 7.1 \right)^2 \cdot 7.1 \right] = 483 \cdot 10^3 \text{ mm}^3 \\ W_{sr} &= 0 \\ W_c &= \frac{(b-2 \cdot t)^3}{4} = \frac{(220-2 \cdot 7.1)^3}{4} = 2179 \cdot 10^3 \text{ mm}^3 \end{aligned}$$

and

$$\begin{aligned} h_n &= \frac{563 \cdot 10^3 / 2}{206 \cdot 13.3 + 2 \cdot 7.1 \cdot (2 \cdot 322.7 - 13.3)} = 24 \text{ mm} \\ W_{c.n} &= (b-2 \cdot t) \cdot h_n^2 = (220-2 \cdot 7.1) \cdot 24^2 = 118.5 \cdot 10^3 \text{ mm}^3 \\ W_{s.n} &= b \cdot h_n^2 - W_{c.n} = 220 \cdot 24^2 - 118.5 \cdot 10^3 = 8220 \text{ mm}^3 \\ W_{sr.n} &= 0 \end{aligned}$$

It follows that:

$$M_{\max} = 483 \cdot 10^3 \cdot 322.7 + 2179 \cdot 10^3 \cdot \frac{13.3}{2} = 170 \cdot 10^3 \text{ N} = 170 \text{ kN}$$

$$M_{pl} = (483 \cdot 10^3 - 8220) \cdot 322.7 + \frac{1}{2}(2179 - 118.5) \cdot 10^3 \cdot 13.3 = 167 \text{ kNm}$$

By using the same procedure, it is also possible to define points E and F, i.e., it is possible to determine the values h_E and h_F of the position of plastic neutral axis, and then to evaluate N and M by means of the equilibrium equations. The points illustrated in Figure 6.59 are characterized by:

$$h_E = 66.84; N_E = 1077 \text{ kN}, M_E = 143.3 \text{ kNm}$$

$$h_F = 102.9; N_F = 1507 \text{ kN}, M_F = 107.0 \text{ kNm}$$

3. Ultimate axial load evaluation — In order to evaluate the ultimate axial load it is necessary to compute the plastic axial resistance, without partial safety factors, i.e.:

$$N_{pl} = 355 \cdot 6046 + 20 \cdot 42354 = 2993 \cdot 10^3 \text{ N} = 2993 \text{ kN}$$

It is also necessary to evaluate the effective elastic flexural stiffness, by means of Equation 6.94, than in this particular case is equal in both planes:

$$(EI)_e = 210000 \cdot 4573 \cdot 10^4 + \frac{0.8 \cdot 29000 \cdot 14949 \cdot 10^4}{1.35} = 1.217 \cdot 10^{13} \text{ N} \cdot \text{mm}^2$$

By considering a values of the effective length factor $k = 0.7$, the slenderness and the buckling curve factor are equal to (see Equation 6.91):

$$\lambda = \frac{0.7 \cdot 4000}{\pi} \cdot \sqrt{\frac{2993 \cdot 10^3}{1.217 \cdot 10^{13}}} = 0.442$$

In this plane, it shall be considered the stability curve a and the value of the imperfection factor α is 0.21; it follows by means of Equation 6.88 that:

$$\phi = 0.5 \left[1 + 0.21 \cdot (0.442 - 0.2) + 0.442^2 \right] = 0.623$$

The stability curve factor is given by Equation 6.87:

$$\chi = \frac{1}{0.623 + \sqrt{0.623^2 - 0.442^2}} = 0.941$$

$$N_u = 0.941 \cdot 2515 = 2367 \text{ kN}$$

4. Member check — By means of Equation 6.98, one gets:

$$\chi_n = 0.941 \cdot \frac{1 + 0.5}{4} = 0.353$$

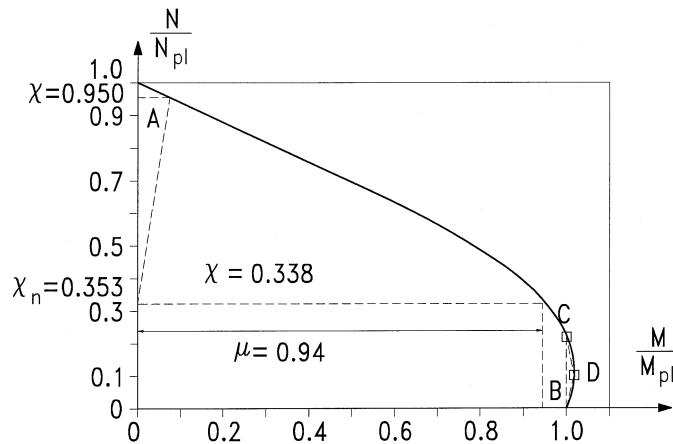


FIGURE 6.60: Procedure for the evaluation of factor μ .

Being:

$$\frac{N}{N_{pl}} = 0.338 < 0.353$$

In Figure 6.60, the check point is above the point C and as a result $\mu = 0.94$. Consequently, the value of the ultimate moment of the column is

$$M_u = 0.9 \cdot 0.94 \cdot 167 = 141 \text{ kNm}$$

It is evident that the magnification factor, a , of Equation 6.99 is equal to 1. Thus, it follows that:

$$M = 140 \text{ kNm} < M_u = 141 \text{ kNm}$$

and the column check is satisfied.

6.7 Composite Slabs

Since its development in North America in the late 1950s, composite floor systems using light gauge metal sheeting proved to be a very efficient solution, which became increasingly popular worldwide (Figure 6.26b). The steel deck serves

- first as a working platform and safety netting system,
- then as a shuttering for the *in situ* casting of concrete,
- and finally as the bottom tensile “reinforcement” of the composite slab.

This capability of efficiently fulfilling different roles during construction and in service conditions is certainly one of the main factors of the success of composite flooring. As already mentioned in the introduction to this section, a second key factor was related to the technological breakthrough provided by the possibility of welding stud connectors through the sheeting by means of a convenient and reliable process.

The designer should suitably consider the diverse aspects and potential problems associated with the different phases of erection and service. These are discussed here, and design criteria and specifications are then provided, which include the recent methodologies also enabling treatment of slabs with

partial shear connection theory. Eurocode 4 includes detailed rules for the design of composite slabs. The AISC-LRFD specifications, on the contrary, do not cover this subject; reference is hence made to the ASCE Standards (1991).

6.7.1 The Steel Deck

The profiled steel sheeting may be seen as a mono-directional structural system whose geometry, depth, and thickness are dictated by the types of load imposed during construction, and by the economical requirement of maximizing the span without need of shoring. This purpose led to an increase of the deck depth from values lower than 50 mm (2") to 70/75 mm (3") and more. Even sheetings 200 mm (8") deep are presently available. The rib width is also important in relation to the composite beam performance: when the composite slab acts together with the steel beam and the ribs are transverse to the beam axis, narrow deck flutes would penalize the stud resistance, often resulting in use of more studs. Wider flutes tend to characterize present deck profiles. Wide-rib profiles have a ratio h_r/b_r between the rib height and average width greater than 2. Sheetting thicknesses range from 0.76 to 1.52 mm (0.3 to 0.6 in.). Deeper decks require greater thickness in order not to have significant out-of-plane deformability, which would reduce the shear transfer capacity in the composite slab. The necessary protection against corrosion is provided by zinc coating. In many instances, the deflection under fresh concrete is the parameter governing deck selection and design. Therefore, the steel resistance is not fully exploited, and use of high strength steels would generally not be advantageous.

The steel sheeting is a structural system consisting of a number of plates subject to in plane and out of plane bending and shear. Even in the elastic range, only a rather refined method, such as the folded plate analysis, would enable an accurate determination of the stresses and deformations [18]. However, when loads are low, the response of the deck under uniform loading is close to that of a beam, and this model can be adopted also when, under increasing loads, local buckling may occur in the compressed parts. This phase of the response requires effective sectional properties to be utilized in design calculations. Buckling is not leading to abrupt failure, which is associated either to extensive sectional yielding or further development of buckles involving folded lines as well.

In the construction stage the sheeting acts as a working platform and shuttering system for the fresh concrete. The concrete is in a liquid state and applies a load normal to each of the plate components. As a result, the sheeting bends transversally due to the variation in lateral restraint from the center to the edge. However, it is acceptable, for design purposes, to model the wet concrete load as a uniform load. Besides, the "ponding" effect of concrete due to the deck deflection imposes an additional load. As a working platform, the deck supports different construction loads, including the ones related to concreting (heaping, pipelines, and pumping). Local overloads as well as vibration and impact effects may be significant, and should be considered, depending on site equipment and operations.

Codes specify minimum construction loads to be used, in addition to the weight of the fresh concrete, for the design checking of the steel deck. In several instances, the designer should assess the construction loads in order to better approximate the actual conditions. Uniform and concentrated live loads are given to simulate the overall and local effects. Differences in value and distribution also reflect the different constructional practices.

The ASCE standards prescribe to consider either a uniform load of 1.0 kN/m^2 (20 psf) or a concentrated load 2.2 kN/m (150 lb per foot of width). The sequence of construction should be accounted for, and several possible loading conditions should be defined for determination of moments, support reactions, and deflections.

Eurocode 4 allows for the local nature of the construction loads and applies a characteristic load of 1.5 kN/m^2 (30 psf) distributed on any area $3 \text{ m} \times 3 \text{ m}$, while the remaining area should be subject to a load of 0.75 kN/m^2 (15 psf). Furthermore, the sheeting should be able to resist, in absence of

concrete, a concentrated load of 1 kN (0.22 kip) on a square area of side 300 mm (11.8 in.), so that a sufficient resistance against crushing of the profile is ensured.

The loads specified by ASCE are nominal loads to be directly utilized in safety and deflection checks. These should be made in accordance to the AISI specifications [1986], which are in the allowable stress format. Partial safety factors should be applied to the characteristic load values given by Eurocode 4 in order to obtain the design load combination.

Elastic methods of analysis should be used to compute the internal forces. The slenderness ratios of the component plates are usually so high (typically about 50) that local buckling governs the resistance of the deck, even when flats are stiffened. However, the effect of local buckling may be neglected in many instances, and the design analysis performed assuming uniform stiffness. A rough account for the loss of effectiveness of some parts of a continuous sheeting may then be obtained via partial moment redistribution. This approach is rather conservative. However, more accurate calculations should involve iterative procedures to determine the effective cross-sectional properties (see for example the methods provided in the AISI specifications or in the part of Eurocode 3 [1994]).

In consideration of the fairly complex response and the many parameters involved (some of which, as the variation of the yield strength in the cross-section due to the forming process and the presence of embossments, are difficult to be accounted for in a simple yet reliable way), a number of design aids were developed and are available to practitioners, mainly providing values of stiffness and resistance based on tests commissioned by the manufacturers.

The verification in service is based on a check of the midspan deflection, δ , under the wet concrete weight: the deflection limit is assumed as $l/180$ or 20 mm, whichever the minimum. The Eurocode prescribes that when this limit is exceeded, the effect of concrete ponding should be allowed for in the design. A uniform load corresponding to an additional concrete thickness of 0.7δ may be assumed for that purpose.

6.7.2 The Composite Slab

When concrete has achieved its full strength, the deck acts as a composite slab, and the steel sheeting serves as the bottom reinforcement under sagging moments. The concrete is continuous over the whole floor span. However, the amount of bottom tensile reinforcement provided by the sheeting is sufficient to make it advantageous to consider and design the slab as simply supported. A design method based on the elastic uncracked analysis with limited redistribution would lead, in fact, to maximum allowable loads for a continuous slab lower than those determined assuming the slab as simply supported. Top reinforcement is present anyway for shrinkage and temperature effects as well as for crack control over the intermediate supports. A minimum amount of reinforcement is specified by Eurocode 4 as 0.2% of the cross-section of the concrete above the steel ribs for unshored construction, and 0.4% for shored construction. Further requirements relate to the minimum values of the total depth, h_t , of the slab and of the thickness of the concrete cover, h_c . These values are similar in the Eurocode and the ASCE specifications (see Table 6.12), for they basically reflect past satisfactory performances and satisfy the need for consistency with other detailing rules. The analysis usually considers a slab strip of unit width, which depends on the system of units adopted: 1 m (SI units) or 1 ft (American units system).

Simply Supported Composite Slabs

The same modes of failure already identified for composite beams (see Section 6.3) may be associated with ultimate conditions of a composite slab: I) flexural resistance, II) longitudinal shear, and III) vertical shear. Critical sections for each of the possible modes are schematically shown in Figure 6.61a with reference to the simply supported case. The type of mechanism for longitudinal shear transfer, which involves bond and frictional interlock as discussed in Section 6.5.1, makes the

TABLE 6.12 Minimum Values of the Slab Depth

Depth	EUROCODE 4	ASCE
h_t [mm]	80 (90) ^a	90
h_c [mm]	40 (50) ^a	50

^a For slabs acting compositely with the beam

condition of complete shear connection difficult to achieve for the slab geometries and spans typical of current design practice. Therefore, collapse is primarily due to the loss of shear transfer capacity at the steel deck — concrete interface (failure mode II). However, the bending capacity may become the critical parameter for slabs with full shear connection (either long slabs or slabs with efficient end anchorage), and vertical shear may govern design of slabs with fairly low span-to-depth ratios.

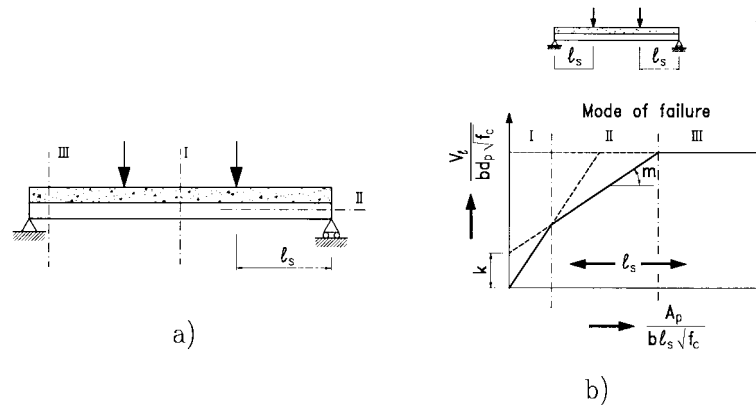


FIGURE 6.61: Composite beams. (a) Typical failure modes: critical sections. (b) Shear-bond line.

The Longitudinal Shear Capacity

Several experimental studies permitted identification of the main features of the shear bond failure with formation of major diagonal cracks at approximately one-quarter to one-third of the span from the supports accompanied by significant slip and vertical separation at the steel-concrete interface. The shear transfer mechanism in composite slabs is fairly complex. Besides material properties, its efficiency depends on many parameters, in particular to those related to the sheeting and to its deformations, such as the geometry (height, shape, and orientation) and spacing of the embossments and the out-of-plane flexibility of the sheeting component plates. Reliable models for the various phenomena involved (i.e., chemical bond, friction, and mechanical interlock) are not yet available. Moreover, end anchorage may be provided over the supports by shear connectors (typically welded studs) or suitable deformation of the sheeting, which prevent slip between the concrete slab and steel deck and enhance the slab resistance to shear bond failure (see Figure 6.27c). In some instances, combined action of in span shear bond and end anchorages should be taken into account. As a consequence of the complexity of the phenomenon and the lack of comprehensive analysis models, the determination of the longitudinal shear capacity of a composite slab is still based on performance tests.

In 1976, Porter and Ekberg [39] proposed the empirical method, on which most design code recommendations are based: the so-called m-k method. This approach conveniently relates the

vertical shear resistance, V_u , at shear bond failure and the shear span, l_s , in which that failure occurs. The factors m and k are the slope and the ordinate intercept of the shear–bond line (Figure 6.62) obtained by linear regression analysis of the test results. Tests are performed on assemblies of the type

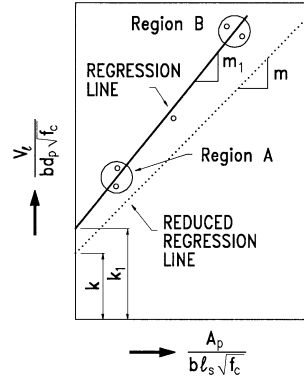


FIGURE 6.62: Shear bond line.

presented in Figure 6.27, with two concentrated line loads applied at a distance, l_s , from the supports. This “shear span” is specified to be equal to one quarter of the total span l in the Eurocode, which also prescribes the use of crack inducers to improve the accuracy of determination of the effective shear span to be utilized in the evaluation of test results. The test program should include two groups of specimens: the first with rather long and shallow slabs (region A in Figure 6.62) and the second with larger depths and smaller shear lengths (region B). Detailing, construction, loading procedure, and assessment of test data are specified in the codes.

The method requires that the maximum vertical shear not exceed the longitudinal shear bond capacity. The unfactored shear bond capacity may be expressed as

$$V_{l,u} = b d_p \left[\left(\frac{m A_p \sqrt{f_c}}{b l_s} \right) + k \sqrt{f_c} \right] \quad (6.110)$$

where

A_p = the cross-sectional area of the steel deck for unit width

b = the specimen width

d_p = the distance of the top fiber of the composite slab to the centroid of the steel deck

Test results by Evans and Wright [18] showed that the influence of the concrete strength is modest and may be neglected. Based on this outcome, formula 6.110 in Eurocode 4 becomes

$$V_{l,u} = b d_p \left[\left(\frac{m A_p}{b l_s} \right) + k \right] \quad (6.111)$$

The moderate effect of the concrete strength is also reflected by the relation provided in the ASCE standards to permit approximation of the shear bond capacity, $V_{l,u,2}$, of a composite slab with concrete strength, $f_{c,2}$, when an identical slab was tested but with concrete strength $f_{c,1}$:

$$V_{l,u,2} = V_{l,u,1} \left(\frac{f_{c,2}}{f_{c,1}} \right)^{1/4} \quad (6.112)$$

The design shear bond strength is obtained by reducing the unfactored resistance:

- by multiplying for the resistance factor $\phi = 0.75$ the ASCE value of $V_{l,u}$ (Equation 6.110)
- by dividing for the safety factor $\gamma_{V_l} = 1.25$ the Eurocode value of $V_{l,u}$ (Equation 6.111).

Application of Equations 6.110 and 6.111 requires preliminary determination of the value of shear span l_s , accounting for the actual loading on the slab, which is, in most instances, different from the two-point loading condition of the test and implies a variation along the shear span of the longitudinal shear force per unit length. A suitable criterion for determining an equivalent l_s to be assumed in design calculations is presented in Figure 6.63 with reference to the uniform loading case: the equivalence of the two cases is imposed by assuming that the support reactions and the areas of the shear diagrams are the same.

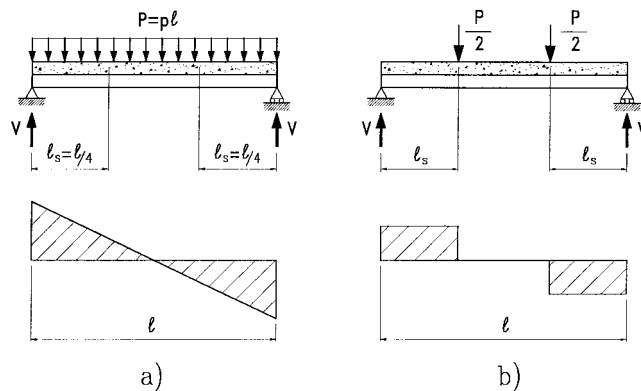


FIGURE 6.63: Suitable criterion for determining the equivalent length l_s . (a) Uniform load. (b) Point loads.

Due to its empirical nature, the m and k factors should be strictly applied only to the slab configuration tested. A limited extension is possible to cover slabs with the same steel deck type, but different for the thickness of the sheeting, slab depth, and steel yield strength. However, some conservativeness is necessary in defining the range of applicability. Furthermore, the method cannot take into account the very different behaviors that may be associated with slab failure, which range from very brittle to fairly ductile. Figure 6.27 shows typical composite slab responses, and points out the effect of end anchorage also on the type of failure.

The conceptual model of flexural composite members with partial shear connection and incomplete interaction can be satisfactorily applied to composite slabs with ductile behavior as demonstrated by recent German studies [5]. This type of approach enables better exploitation of the resistance capacity of composite slabs made with the types of sheeting profiles presently available. Eurocode 4 includes partial connection design, which utilizes the results of the same type of testing specified for the m - k method; for the sake of clarity, this design procedure will be illustrated after having discussed the flexural resistance of partially composite slabs.

The Flexural Capacity

Traditional approaches to the analysis and design of composite slabs adopted and adapted the methods and design criteria developed for reinforced concrete elements. The steel sheeting is hence considered and modeled as the tensile reinforcement, and limitations are imposed to ensure that failure is associated with a “ductile” mode: i.e., that crushing of the concrete in compression is avoided while the “steel reinforcement” may achieve its full plasticity strength. Restrictions are made

on the depth of the concrete in compression or a range is defined, as in the ASCE standards (1991), within which only the “plastic” stress block analysis can be applied. Consistently with the reinforced concrete analogy, the parameter adopted to define the upper boundary of such a range is a suitable “reinforcement” ratio, obtained by modifying the relevant expression in the ACI standards, and hence assumed as the ratio of the steel deck area to the effective concrete area in the unit slab width b :

$$\rho = \frac{A_p}{bd_p} \quad (6.113)$$

The balanced value of it, ρ_b , also defined in accordance to the ACI Standards (1989), is

$$\rho_b = \left(\frac{0.85\beta f_c}{f_{y.p}} \right) \cdot \left[\frac{\varepsilon_c E_s \cdot (h_t - h_p)}{(\varepsilon_c E_s + f_{y.p}) d_p} \right] \quad (6.114)$$

where β is a stress block depth factor depending on concrete strength (β is equal to 0.85 for $f_c \leq 28$ N/mm², and decreases by 0.05 for each increase of f_c equal to 7 N/mm² down to a minimum value of 0.65), ε_c is the maximum allowable concrete strain ($\varepsilon_c = 0.003$ mm/mm in the ASCE standards), and h_t is the overall thickness of the slab.

The ratio ρ_b defined by Equation 6.114 refers to the balanced cross-sectional strain condition involving simultaneous achievement of the maximum concrete strain, ε_c , and full plastification of the steel sheeting. A slab with a reinforcement ratio lower than ρ_b is under-reinforced and the

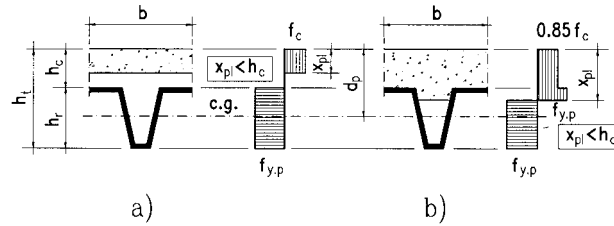


FIGURE 6.64: Simplified calculation method for plastic analysis of slab.

nominal moment resistance can be determined via a stress block analysis (Figure 6.64a), then

$$M_{pl.cs} = A_p f_{y.p} \left(d_p - \frac{x_{pl}}{2} \right) \quad (6.115)$$

where

x_{pl} = the depth of the concrete stress block

$$x_{pl} = \frac{A_p \cdot f_{y.p}}{0.85 \cdot b \cdot f_c} \quad (6.116)$$

b = the unit slab width

Equations 6.115 and 6.116 assume that the plastic neutral axis is in the slab and the whole steel deck yields in tension. Therefore, it is not applicable to deep decks for which the plastic neutral axis would lie within the deck profile, and for decks made of steel grades with low ductility. The latter aspect is covered in the ASCE standards by imposing that the ratio f_u/f_y for the steel deck shall not be lower than 1.08.

Determination of the flexural resistance of over-reinforced slabs (for which $\rho > \rho_b$) requires use of a general strain analysis in order to take account of all the various phenomena that possibly affect the slab performance. Besides including material nonlinearities, a refined analytical model should enable simulation of several events such as fracture of the deck in tension, buckling of the deck parts in compression, presence of additional reinforcing bars, crushing of concrete, and interface slip between steel and concrete. Furthermore, the influence of shoring on strains and stresses should also be accounted for.

The value of the strength reduction factor, ϕ , for the different types of slab recognizes the characteristics of the mode of failure: ϕ is assumed equal to 0.85 for under-reinforced slabs, and decreased to 0.70 for over-reinforced slabs and to 0.65 for under-reinforced slabs for which $f_u/f_y \leq 1.08$ in consideration of the possibility of brittle failure.

Recent research studies [45] pointed out that several features are peculiar of the steel deck acting as “reinforcement”, which cause composite slabs to perform differently from reinforced concrete members. In particular, they are less sensitive to concrete failure.

These features are

- the bending stiffness and strength of the steel deck, which becomes significant for deep decks
- the yield strength of the sheeting, usually substantially lower than that of the reinforcing bars
- the fact that the selfweight of the slab is resisted by the sheeting alone, which is subject to important stresses before acting compositely with the concrete

As a consequence, traditional approaches, based on the behavioral analogy with reinforced concrete members, were found to be rather conservative, in particular with respect to the range of application of plastic analysis. A more general procedure for determining the ultimate flexural resistance of the slab was then proposed. Equations 6.115 and 6.116 implicitly assume that the shear bond is sufficient to cause the full flexural capacity of the composite slab to develop (i.e., the case of a fully composite slab), and that the neutral axis lies in the concrete ($x_{pl} \leq h_c$, Figure 6.64a). For unusually deep decks, the neutral axis lies within the steel section ($x_{pl} > h_c$, Figure 6.64b). In this case, a simplified approach can be used to compute $M_{pl.cs}$ illustrated in Figure 6.65 which neglects the concrete in the rib. The tensile force in the sheeting can be decomposed in two forces: one at the bottom, $N_{pl.pr}$,

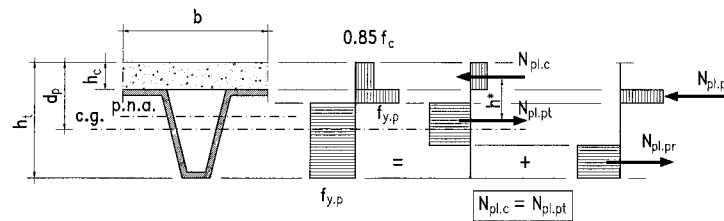


FIGURE 6.65: Additional simplified calculation method for plastic analysis of slab.

while the other, $N_{pl.pt}$, is equal to the compression force $0.85 b h_c f_c$. The contribution of the forces, $N_{pl.pc}$, defines a moment, $M_{pl.pr}$, that may be considered as the plastic moment of the steel deck, $M_{pl,p}$, reduced by the presence of the axial force, $N_{pl.pt}$. The reduced plastic moment, $M_{pl.pr}$, can be obtained from the interaction diagram of the sheeting (see Figure 6.66). A good approximation

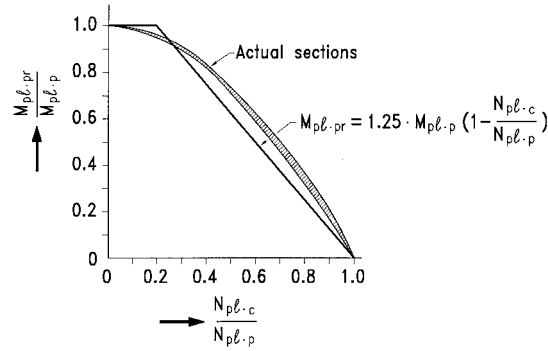


FIGURE 6.66: Interaction curve N-M for profiled sheetings.

is provided by the following expression:

$$M_{pl,pr} = 1.25 M_{pl,p} \left(1 - \frac{N_{pl,c}}{N_{pl,p}}\right) \leq M_{pl,p} \quad (6.117)$$

where $M_{pl,p}$ and $N_{pl,p}$ are the plastic moment and the full plastic axial resistance of the sheeting, respectively.

The plastic moment of resistance of the composite slab is then obtained as

$$M_{pl,cs} = M_{pl,pr} + 0.85 b h_c f_c h^* = M_{pl,pc} + N_{pl,c} \cdot h^* \quad (6.118)$$

The lever arm h^* can be satisfactorily approximated by the relationship [45]

$$h^* = h_t - 0.5 h_c - e_p + \left[(e_p - e) \cdot \frac{N_{pl,c}}{N_{pl,p}} \right] \quad (6.119)$$

where e and e_p are the distances from the bottom of the slab to the centroid and the plastic neutral axis of the steel sheet, respectively (Figure 6.67).

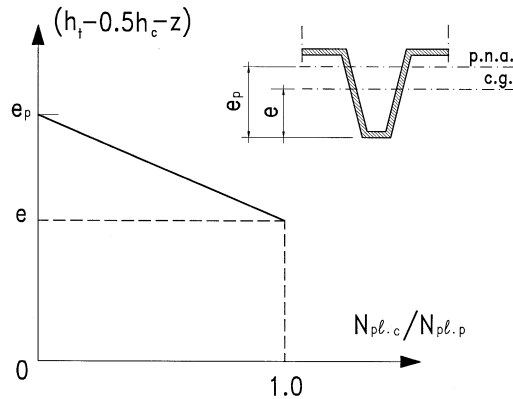


FIGURE 6.67: Plot of the relationship Equation 6.119.

The extension of the method to the case of partially composite slabs is straightforward. The compression force in the concrete, F_c , is lower than the value, $F_{c,f}$, associated with the condition of

full shear connection, and two neutral axes are present in the cross-section: i.e., the first lying in the concrete and the second within the steel sheeting. The depth of the concrete stress block is given by

$$x_{pl} = \frac{F_c}{0.85 \cdot b \cdot f_c} \leq h_c \quad (6.120)$$

By replacing in Equations 6.117 to 6.119 h_c with x_{pl} and $N_{pl,pt}$ with F_c , the moment resistance can be computed as:

$$h^* = h_t - 0.5x_{pl} - e_p + \left[(e_p - e) \frac{F_c}{N_{pl,p}} \right] \quad (6.121)$$

$$M_{pl,pr} = 1.25M_{pl,p} \cdot \left[1 - \frac{F_c}{N_{pl,p}} \right] \leq M_{pl,p} \quad (6.122)$$

$$M_{w.cs} = M_{pl,pr} + F_c h^* \quad (6.123)$$

Slab Design Based on Partial Interaction Theory

A composite slab for which the shear bond failure is ductile may be treated as a partially composite slab. In this condition, the flexural and longitudinal shear capacity of the section are linked, in the sense that the bending resistance of the slab is limited by the maximum shear resistance. A design procedure based on the analytical model of partially composite members was included in Annex E of Eurocode 4. This approach enables the effect of end anchorages to be accounted for in a rather straightforward and efficient way. The procedure, which makes use of the results of standard tests for the determination of the factors m and k presented before, is briefly described here. Ductile behavior is defined as that of a composite slab for which the failure experimental load is at least 10% higher than the load at which end slip is observed. If collapse is associated with a midspan deflection δ greater than $l/50$, the load at $\delta = l/50$ has to be assumed as a failure load.

The partial-interaction design method requires that the mean ultimate shear stress is determined. As a first step, for the slab considered, the curve expressing the relationship between the unfactored moment of resistance and the degree of interaction $\eta = F_c/F_{c,f}$ has to be defined (Figure 6.68). The

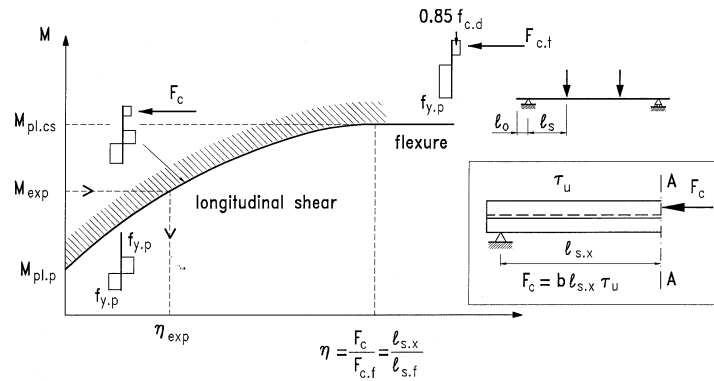


FIGURE 6.68: Composite slab partial interaction diagram.

following must occur:

1. The moment capacity, $M_{pl,cs}$, of the fully composite slab is computed and the corresponding value of the compressive force, $F_{c,f}$, in the concrete slab is determined.

2. A value of h^* is selected, to which the partial-interaction compression force $F_c = \eta F_{c,f}$ corresponds, and the value of the associated moment capacity $M_{pl,cs}$ is computed via Equations 6.121 to 6.123.
3. The calculations at Step 2 are repeated for a number of values of η sufficient to define the $M_{w,cs} - \eta$ curve.

This curve is then used in combination with the experimental ultimate moment to obtain the degree of interaction of the considered slab and then the value of F_c . Finally, under the assumption of uniform shear bond resistance along the shear span l_s and the overhang l_o , the mean ultimate shear stress is obtained as

$$\tau_u = \frac{F_c}{b \cdot (l_s + l_o)} \quad (6.124)$$

A value of τ_u is determined for each test. A statistical treatment of these values then enables definition of a design value $\tau_{u,d}$. The Eurocode first defines a characteristic ultimate shear $\tau_{u,k}$ as the mean value reduced by 10%, and then the design value as $\tau_{u,d} = \tau_{u,k}/1.25$.

It should be noted that while a reduced number of additional tests is sufficient for assessing the influence of the steel deck thickness, the thickness of the slab remarkably affects the partial interaction curve, and results cannot be applied to slabs with higher slab thicknesses than the specimens tested.

In the verification procedure, the partial-interaction diagram is computed using the design values of slab dimensions and material strengths. If $l_{s,x}$ is the distance of a cross-section from the closer support, the assumption of uniform shear strength distribution implies that $F_c = b\tau_{u,d}l_{s,x}$ and allows substitution of the ratio $F_c/F_{c,f}$ with the ratio $l_{s,x}/l_{s,f}$, with $l_{s,f}$ the value of the shear span for which the full shear interaction is achieved. Verification that the design bending moment is lower than the moment of resistance is simply obtained by superimposition as shown in Figure 6.69.

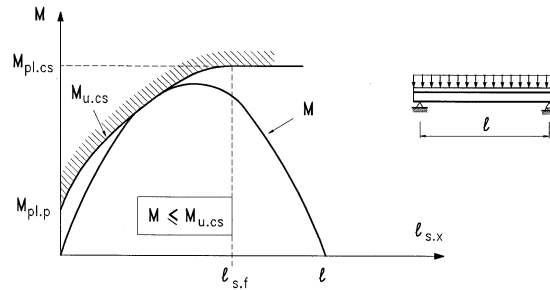


FIGURE 6.69: Verification procedure for simply supported slab under uniform loading.

If end anchorages are used, three additional tests are required to determine their contribution V_{ea} to the longitudinal shear strength. From each test, this contribution can be computed as

$$V_{ea} = \eta F_{c,f} - b(l_s - l_o)\tau_{um} \quad (6.125)$$

where τ_{um} is the mean value of c_u from the tests carried out without end anchorage.

The mean value of V_{ea} reduced by 10% is assumed to be a characteristic value, $V_{ea,k}$. The design resistance is then obtained as $V_{ea,k}/1.25$. When defining the design partial-interaction diagram, the compressive force, F_c , should account for the contribution of the end anchorage:

$$F_c = bl_{s,x}c_{u,d} + V_{ea,d} \quad (6.126)$$

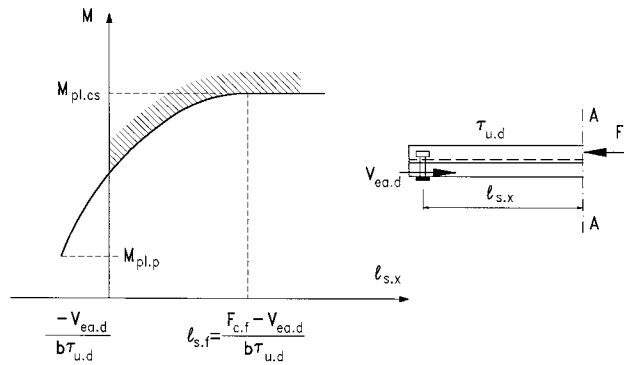


FIGURE 6.70: Design partial interaction diagram for a slab with end anchorage.

This will result in a shifting of the design diagram as illustrated in Figure 6.70.

Reinforcing bars are often provided in the slab ribs to enhance the fire response. The contribution of rebars to the flexural resistance of the slab may also be taken advantage of. The moment capacity can be obtained by adding up the plastic resistances associated with the relevant reinforcing bars (see Figure 6.71).

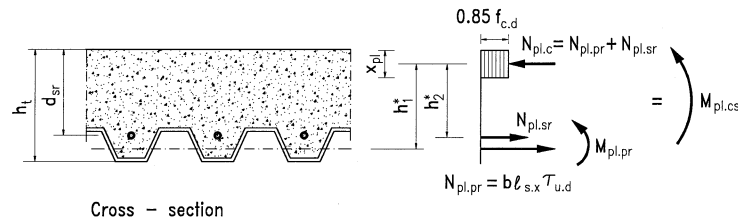


FIGURE 6.71: Contribution of additional longitudinal reinforcement.

Continuous Composite Slabs

Elastic analysis with limited moment redistribution and plastic analysis can both be adopted. In most instances, the latter approach is advantageous. However, it imposes that rotation capacities are checked in the hogging moment regions, which are substantially affected by the ductility of the reinforcing bars. If high ductility rebars are selected, the method can be applied to commonly used slabs for spans up to 5 m [45].

The hogging ultimate moment of resistance can be computed by the stress block theory, also accounting for the contribution of the sheeting when continuous over the support. The possible buckling of plate components should be considered. The restraint offered by the concrete allows for relaxation of the related rules. The Eurocode recommends that the effective widths be taken as twice the values given for class 1 steel webs. When the deck is not continuous over the support, the slab in the hogging moment region should be modeled as a reinforced concrete element.

If elastic design analysis is adopted, the large available sagging moment of resistance makes modeling the slab as independent simple spans the most convenient approach. The elastic analysis with limited redistribution of moments (up to 30% is allowed by the Eurocode) is less advantageous in

terms of load carrying capacity. On the other hand, continuity may become beneficial to reduce deflections and meet serviceability requirements.

When checking the shear bond resistance of the slab portions in sagging moment, an effective simple span equal to the distance between points of contraflexure may be assumed for internal spans, while for end spans the full exterior span length has to be used. The regions in the hogging moment provide a constraint to shear slippage, which is modest for end spans and should be neglected.

Vertical Shear

The resistance to vertical shear is mainly provided by the ribs, and formulae for reinforced concrete T-beams can be applied, if suitably adjusted. Moreover, the shear stresses in the sheeting consequent to it functioning as shuttering during concrete casting can be neglected and the total shear force can be considered as resisted by the composite cross-section.

Reference can be made to a slab width equal to the distance between the centers of adjacent ribs, and the unfactored vertical shear resistance expressed as (Eurocode 4):

$$V_v = b_r d_p \tau_u k_v (1.2 + 40\rho) \quad (6.127)$$

where

τ_u = the shear strength of concrete

b_r = mean width of concrete rib

$k_v = (1.6 - d_p) \geq 1$ (with d_p in m)

$\rho = A_p / b_r d_p$

A_p = the effective area in tension within width b_o

The shear strength for Eurocode should be taken as equal to $0.25 f_{ct}$.

Punching Shear and Two-Way Action

Heavy concentrated loads may be applied to the slab (i.e., by the wheels of fork-lift trucks), which make the slab subject to two-way action and may cause failure by punching shear.

The limited experimental knowledge available is not sufficient to allow for an appraisal of the sheeting contribution to the resistance to punching shear. This resistance is hence generally determined as for reinforced concrete sections. An effective area can be defined accounting for the different stiffnesses of the slab in the two directions. The critical perimeter, C_p , can be obtained by a 45° dispersion of the load down to the centroidal axis of the sheeting in the longitudinal direction and to the top of the sheeting in the transverse direction (see Figure 6.72):

$$C_p = 2\pi h_c + 2(2d_p + a_p - 2h_c) + 2b_p + 8h_f \quad (6.128)$$

where a_p and b_p define the loaded area, and h_f is the height of finishes.

In analogy with vertical shear, and considering the height of concrete over the deck, h_c , as the effective depth, the punching shear resistance can be written as

$$V_p = C_p d_p \tau_u k_v (1.2 + 40\rho) \quad (6.129)$$

The ASCE standards limit the nominal shear stress to $2\sqrt{f_c}$ in inch-pound units ($0.166\sqrt{f_c}$ if f_c in N/mm²) in view of the incomplete two-way action.

The load distribution requires the slab to possess adequate flexural strength in the transverse direction, and suitable transverse reinforcement should be placed in consideration of the negligible bending strength of the steel sheeting transverse to the deck ribs.

Serviceability Limit State

The performance in service is verified mainly with reference to cracking of concrete and to the flexural stiffness (through a limitation of the midspan deflections).

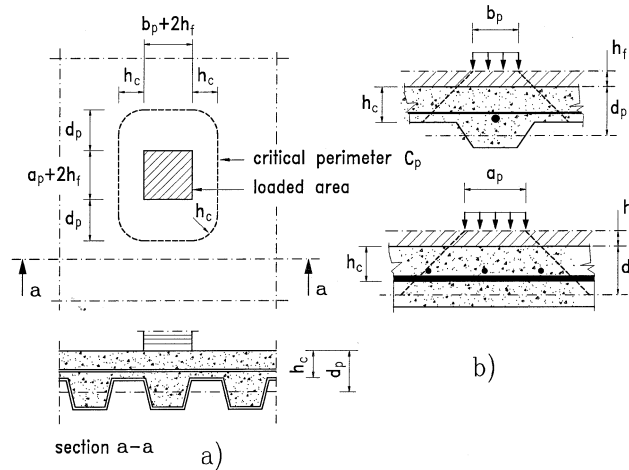


FIGURE 6.72: Critical perimeter for punching shear.

Cracking of Concrete

Cracking of concrete may occur in the regions over the supports where some degree of continuity develops due to the intrinsic continuity of the concrete slab, also when the composite slab is conceived and designed as a series of simply supported elements. Control of the crack width would require that the criteria are used, which were developed and codified for reinforced concrete members. When the environment is not aggressive and the width of the cracks is not critical for the functioning of the structure, placement of nominal anti-crack reinforcement would be sufficient to satisfy serviceability requirements. The Eurocode specifies a minimum amount of reinforcement equal to 0.2% of the concrete area over the deck for unpropped slabs, and 0.4 for propped slabs.

Deflections

The floor deflection has to be limited to the values that ensure that no damage is induced by floor deformation in partitions and other nonstructural elements. Values of maximum deflections are provided in the codes, which can usually be allowed in buildings. Table 6.13 presents the limit values given in the ASCE standards, while the ones in Eurocode 4 are in Table 6.2. Besides, both codes provide limitations to the span-to-depth ratios (Table 6.14), which are related, though in a different way, to in-service conditions. The ASCE span-to-depth ratios refer to the total depth, h_t , of the slab, and intend to provide guidance to obtain satisfactory in-service deflections. Slab deformation should be computed and checked. On the contrary, fulfillment of the Eurocode limitation, which refers to the effective depth of the slab, d_p , allows for deflection calculations to be omitted, at least when slip does not significantly affect the slab response. In some instances, a more accurate assessment is necessary, accounting for the expected type of behavior of nonstructural elements chosen in the specific design project.

In the deflection calculation different components have to be taken into account that are associated with the various facets of the response. In particular, the deformation under short and long term loading and the effect of interface slip need to be considered. Immediate slab deformation, δ_{st} , can be determined via a linear elastic analysis. In continuous slabs, calculations can assume that the slab has a uniform stiffness characterized by a moment of inertia equal to the average of those of the cracked and uncracked section.

The effect of slip may be important in external spans, and it should be accounted for, with reference to the results of the relevant performance tests. It generally may be neglected when the experimental data indicate that end slip greater than 0.5 mm does not occur at loads equal to 1.2 times the service

TABLE 6.13 Limiting Values for Vertical Deflections Recommended by ASCE Standards

Type of composite slab	Type of deflection	Deflection limitation (in.)
Flat roofs	Immediate deflection due to live load	$\frac{l}{180}$
Floors	Immediate deflection due to live load	$\frac{l_f}{360}$
Roofs or floor slabs supporting or attached to non-structural elements likely to be damaged by large deflections	That part of the total deflection which occurs after attachment of the non-structural elements, the sum of the long-time deflection to immediate deflection due to any additional live load	$\frac{l_f}{480}$
Roofs or floor slabs supporting or attached to non-structural elements not likely to be damaged by large deflections		$\frac{l_f}{240}$

TABLE 6.14 Recommended Limiting Values for Span-to-Depth Ratios

	ASCE: l/h_t	EUROCODE 4: l/d_p
Simply supported slabs	22	25
External span of continuous slabs	27	32
Internal spans of continuous slabs	32	35

loads. If this condition is not fulfilled, there are two possible alternatives to the calculation of the deflection including slip:

- suitable end anchorages can be provided, or
- the design service loads are reduced so that the previous limit on end slip is met.

Additional deflections under long-term loading, δ_{lt} , may be approximated, as for reinforced concrete members, as a quota of the elastic deflection under short-term loads, i.e.,

$$\delta_{lt} = k_\delta \delta_{st} \quad (6.130)$$

The ASCE standards specify as k_d the same factor as in the ACI 318 Code:

$$k_\delta = \left[2 - 1.2 \left(\frac{A_{s,c}}{A_{s,t}} \right) \right] \leq 0.6 \quad (6.131)$$

where

$A_{s,c}$ and $A_{s,t}$ = the areas of steel in compression and tension under service loads, respectively

The area, $A_{s,c}$, includes reinforcement and the possible portion of the steel deck in compression. The Eurocode enables a simplified appraisal of the total deflection under sustained loads to be obtained, for slabs with normal density concrete, via a linear elastic analysis performed with a slab stiffness based on an average modular ratio for long and short term effects. In the calculations of total deflections for serviceability checks, loads should be carefully selected. The immediate deformations induced by all the dead loads applied before placement of the relevant nonstructural elements can be neglected. However, the applied forces simulating the effect of shore removal, which contributes to long-term deflections, should be accounted for as well. Finally, in some instances, the shear-bond slip may also cause significant additional deflections under sustained loads. Test data are needed in these cases to provide appropriate input to design calculations.

6.7.3 Worked Examples

EXAMPLE 6.8: Design of a composite slab

With reference to Example 6.2 the design of the composite slab is proposed in the following, which is made by using HiBond 55/100 steel profiled sheeting. A reinforcing steel mesh is placed in the concrete slab with 25 mm top cover, providing $188 \text{ mm}^2/\text{m}$ of reinforcement ($\phi 6 \text{ mm } p = 150 \text{ mm}$). For the check of the longitudinal shear, the m and k parameters for the HiBond 55/100 profiled sheeting are equal to 86 and 0.69, respectively. The analysis is related to a strip of 1000 mm. The stactical system and typical cross-section are given in Figure 6.73.

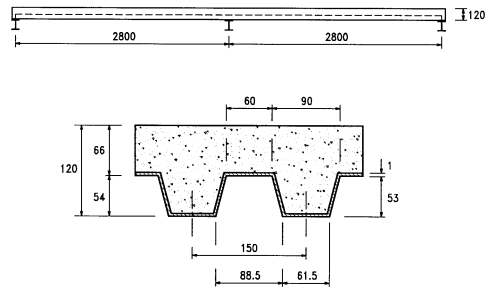


FIGURE 6.73: Stactical system and typical cross-section.

- Characteristic of materials:

The design strength of materials is assumed.

Concrete:	$f_{c.k} = 25 \text{ N/mm}^2$	$\gamma_c = 1.5$
Steel: reinforcement	$f_{y.sr.k} = 235 \text{ N/mm}^2$	$\gamma_s = 1.15$
steel sheeting	$f_{y.p.k} = 320 \text{ N/mm}^2$	$\gamma_p = 1.10$

A. Verification of the profiled sheeting (see Section 6.7.1)

Loads:

Self-weight of the sheet	g_p	0.13	kNm/m^2	$(\gamma_F = 1.35; 1)$
Weight of the wet concrete construction load	g_c	2.27	kNm/m^2	$(\gamma_F = 1.35; 1)$
	q_{m1}	1.5	kNm/m^2	$(\gamma_F = 1.5; 0)$
	q_{m2}	0.75	kNm/m^2	$(\gamma_F = 1.5; 0)$

Stactical system and loading cases are given in Figures 6.74 and 6.75.

1. Ultimate limit states — By elastic calculation of the beam, it follows:

- Maximum positive bending moment $M^{(+)} = 3.62 \text{ kNm/m}$
- Maximum negative bending moment $M^{(-)} = 6.12 \text{ kNm/m}$
- Maximum support reaction $F = 19.10 \text{ kN/m}$

- Cross-section resistance (trade literature):

γ_p		=	1.1
$M_{pl.p}^{(+)}$	$7.41/\gamma_p$	=	6.74 kNm/m
$M_{pl.p}^{(-)}$	$7.48/\gamma_p$	=	6.8 kNm/m
F_p	$68.1/\gamma_p$	=	61.9 kN/m

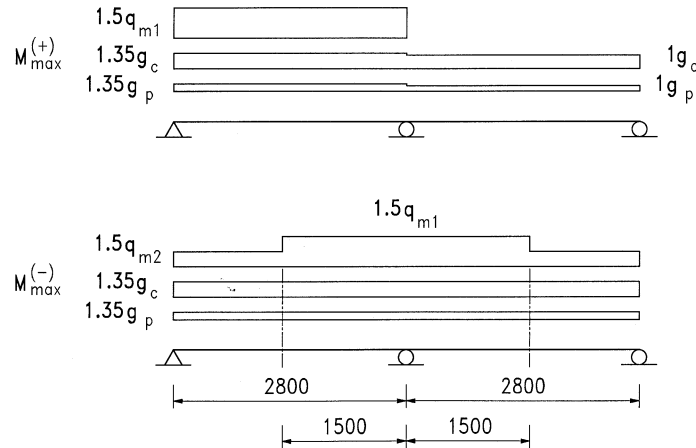


FIGURE 6.74: Stactical system and loading cases for ultimate limit states.

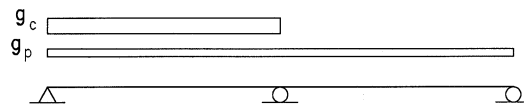


FIGURE 6.75: Loading case for serviceability limit state.

- Safety check:

$$\begin{array}{llll} M^{(+)} & 3.62 \text{ kNm/m} & < & 6.74 \text{ kNm/m} \\ M^{(-)} & 6.12 \text{ kNm/m} & < & 6.8 \text{ kNm/m} \\ F & 19.10 \text{ kN/m} & < & 61.9 \text{ kN/m} \end{array}$$

$$\frac{M^{(-)}}{\frac{M_{pl,p}^{(-)}}{\gamma_p}} + \frac{F}{\frac{F_p}{\gamma_p}} = \frac{6.12}{6.8} + \frac{19.10}{61.9} = 0.9 + 0.31 = 1.21 < 1.25$$

2. Serviceability limit states — The analysis makes with reference to the stactical system in Figure 6.75.

The maximum moment is

$$M = 1.773 \text{ kNm/m}$$

- Deflection control

By means of an elastic analysis (Figure 6.75), it is $\delta = 7.19 \text{ mm}$.

Check:

$$\delta = 7.19 \text{ mm} < l/180 \quad ((2800/180) = 15.56 \text{ mm} < 20 \text{ mm})$$

B. Verification of the composite slab.

It is assumed that the composite slab is designed as a series of a simply supported beams (Figure 6.76).

Loads:

$$\text{Self-weight of the slab and floor finishes} \quad g = 3.05 \text{ kNm/m}^2 \quad (\gamma_g = 1.35)$$

$$\text{Live load} \quad q = 4.8 \text{ kNm/m}^2 \quad (\gamma_q = 1.5)$$

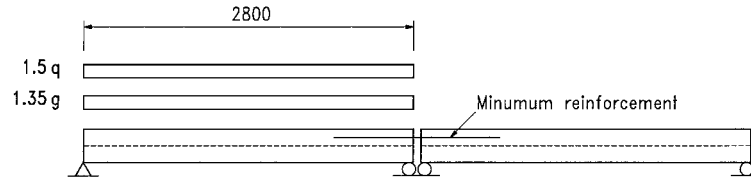


FIGURE 6.76: Composite slab as a series of a simply supported beams.

- Design load

$$p = (\gamma_g g + \gamma_q q) \cdot b = (1.35 \cdot 3.05 + 1.5 \cdot 4.8) \cdot 1.00 = 11.32 \text{ kN/m}$$

- Ultimate limit state

Design bending moment

$$M^{(+)} = \frac{p \cdot l^2}{8} = \frac{11.32 \cdot 2.80^2}{8} = 11.09 \text{ kNm/m}$$

Determination of the design bending resistance.

Calculation of the plastic neutral axis

$$x_{pl} = \frac{A_p \cdot f_{y.p.k} / \gamma_p}{b \cdot 0.85 f_{c.k} / \gamma_c} = \frac{1482 \cdot 320 / 1.10}{1000 \cdot 0.85 \cdot 25 / 1.5} = 30.43 \text{ mm} < 120 \text{ mm}$$

Design bending resistance:

$$\begin{aligned} M_{pl.cs}^{(+)} &= A_p \cdot \frac{f_{y.p.k}}{\gamma_p} \left(d_p - \frac{x_{pl}}{2} \right) \\ &= 1482 \cdot \frac{320}{1.1} \left(120 - 27.5 - \frac{30.43}{2} \right) = 33.3 \text{ kNm/m} \end{aligned}$$

Check

$$M^{(+)} = 11.09 \text{ kNm/m} \leq 33.3 \text{ kNm/m}$$

Longitudinal shear: m-k method (see Section 6.7.2). Calculation of design shear force

$$V_1 = p \cdot \frac{l}{2} = 11.32 \cdot \frac{2.8}{2} = 15.85 \text{ kN}$$

Design shear resistance (Equation 6.111):

$$m = 86, \quad k = 0.069$$

$$V_{1.u} = b \cdot d_p \cdot \frac{(mA_p / b l_s + k)}{\gamma} = 1000 \cdot 92.5 \cdot \frac{\left(\frac{86 \cdot 1482}{1000 \cdot 2800 / 4} + 0.069 \right)}{1.25} = 18.6 \text{ kN}$$

Check

$$V_1 = 15.85 \text{ kN} \leq 18.6 \text{ kN} = V_{1.u}$$

- Vertical shear

Calculation of design vertical shear resistance:

$$V_v = b_0 d_p \tau_{w.d} k_v (1.2 + 40 \rho) \cdot$$

where

$$\begin{aligned}\tau_{w,d} &= 0.30 \text{ N/mm}^2 \\ k_v &= 1.6 - d_p = 1.6 - 0.0925 = 1.51 \text{ mm} \\ 1.2 + 40\rho_0 &= 1.2 + 40 \cdot \frac{A_p}{b_0 \cdot d_p} = 1.2 + 40 \cdot \frac{188}{500 \cdot 92.5} = 1.36\end{aligned}$$

Hence,

$$V_v = 28675 \text{ N} \cong 28.7 \text{ kN}$$

Check

$$V_1 = 15.85 \text{ kN} < 28.7 \text{ kN} = V_v$$

- Serviceability limit state — The deflection of the sheeting under its selfweight and the weight of the concrete is

$$\delta = 7.19 \text{ mm}$$

For the evaluation of the deflection of the composite slab, it is assumed the hypothesis of continuous beam. The deflection under the weight of floor finishes is:

$$\delta_g = 0.132 \text{ mm}$$

The deflection of the composite slab under variable loading of long duration has the value:

$$\delta_p = 1.661 \text{ mm}$$

where the deflection evaluation has been evaluated as the average of the value for the cracked and uncracked section, calculated with an average coefficient $n = \frac{E_s}{E_c} = 15$.

Checks

$$\delta_{\text{tot}} = \delta + \delta_g + \delta_p = 7.19 + 0.132 + 1.661 = 8.983 \text{ mm} < \frac{l}{250} = \frac{2800}{250} = 11.26 \text{ mm}$$

$$\delta_2 = \delta_g + \delta_p = 0.132 + 1.661 = 1.793 \text{ mm} < \frac{l}{300} = 9.3 \text{ mm}$$

- Cracking of concrete — The amount of reinforcement at an intermediate support is:

$$\rho = \frac{A_s}{bh_c} = \frac{188}{1000 \cdot 65} = 0.29\% > 0.2\%$$

This percentage is greater than the minimum recommended by Eurocode 4.

Notations

a	=	amplification factor
b	=	slab width of a composite beam, width of a composite column section, or unit width of a composite slab
b_a	=	length of the outstanding leg of connection
b_c	=	base width of concrete component of a composite column section
b_e	=	effective width of the portion of the concrete flange on each side of the steel web
b_{eff}	=	effective width of the concrete flange of a composite beam
b_r	=	average width of concrete rib or haunch
b_s	=	base width of structural steel component of a composite column section

b_{sr}	=	base width of reinforcement component of a composite column section
c	=	outstanding flange of the steel profile, numerical factor
c_i	=	numerical factors
d	=	overall depth of member, clear distance between flanges of the steel profile
d_b	=	beam depth
d_c	=	depth of concrete component of a composite column section
d_p	=	distance between the top fiber of a composite slab to the centroid of the steel deck
d_{inf}	=	distance between centroid of structural steel profile and centroid of composite beam
d_{sc}	=	diameter of stud shear connector
d_s	=	depth of structural steel component of a composite column section
d_s, d_i	=	distances between centroid of concrete slab and centroid of composite beam
d_{sr}	=	depth of reinforcement component of a composite column section
f	=	fundamental frequency of a beam
f_c	=	nominal compressive strength of concrete
$f_{c,d}$	=	design cylinder strength of concrete under compression
$f_{c,k}$	=	characteristic cylinder strength of concrete under compression
f_{ct}	=	tensile strength of concrete
f_{my}	=	modified yielding stress of structural steel
f_y	=	yield strength
f_k	=	characteristic strength
$f_{y,s}$	=	specified yield strength
$f_{y,s,d}$	=	design yielding stress of structural steel
$f_{y,s,k}$	=	characteristic yield strength of structural steel
$f_{y,s,v}$	=	design yielding shear resistance of structural steel
$f_{y,sr,d}$	=	design yielding stress of reinforcing steel
$f_{y,sr,k}$	=	characteristic yielding stress of reinforcing steel
$f_{y,p}$	=	specified yield strength of steel deck
$f_{y,sr}$	=	specified yield strength of steel reinforcement
$f_{y,sr}$	=	reduced specified yield strength of steel
f_u	=	specified tensile strength of steel
$f_{u,sc}$	=	ultimate tensile resistance of shear studs
h	=	height, thickness
h_{ac}	=	height of the outstanding leg of an angle connector
h_c	=	thickness of the solid concrete slab, thickness of the concrete above steel deck
h_p	=	overall depth of steel deck
h_n	=	distance between the line of plastic neutral axis and the line of centroid of cross-section
h_r	=	rib height
h_s	=	height of structural steel profiles of a composite beam
h_t	=	total thickness of composite slab
h^*	=	internal arm distance (distance between line of action of compression resultant and line of action of tension resultant)
k	=	factor, ordinate intercept of shear-bond regression line
k_c, k_s	=	coefficient for evaluation of shear resistance (for concrete and steel, respectively)
k_{rp}	=	reduction factor for resistance of stud in composite deck with rib parallel to the beam
k_{rt}	=	reduction factor for resistance of stud in composite deck with rib transverse to the beam
k_l	=	effective length of a column for buckling evaluation
i	=	ratio between the uncracked and cracked inertia of composite cross-section
l	=	length of a beam or column

l_0	= approximate distance between the points of zero moment
l_s	= shear span
$l_{s.f}$	= shear span at which full interaction is achieved in a composite slab
$l_{s.x}$	= distance from a cross-section and the closer support
m	= slope of shear-bond regression line, ratio between moments
n	= modular ratio: E_s/E_c
n_{ef}	= modular ratio for creep analysis $E_s/E_{c.ef}$
p	= vertical load per unit length
q	= force on a shear connector
q_u	= maximum resistance of shear connector
$q_{u.c}$	= shear resistance associated with concrete failure
$q_{u.s}$	= shear resistance associated with connector failure
$q_{u.tot}$	= total shear resistance
$q_{u.block}$	= shear resistance of the block
$q_{u.anchors}$	= shear resistance of the anchors
$q_{u.hoop}$	= shear resistance of the hoop
q_{Rd}	= design resistance of shear connector
r	= numerical factor for buckling evaluation, redistribution degree, ratio between moments
r_m	= radius of gyration of steel part of a composite column
s	= slip
t	= thickness
t_c	= thickness of the concrete slab
t_f	= flange thickness
t_w	= web thickness
v	= shear force per unit length
v_l	= longitudinal shear force per unit length
v_{sd}	= shear resistance of steel decking
w	= unit weight of concrete
x_e	= elastic neutral axis depth
x_{pl}	= plastic neutral axis depth
A	= area of the overall full composite section
A_0	= original cross-sectional area of steel specimen
A_c	= cross-sectional area of concrete
$A_{c.v}$	= area of concrete per unit length of a shear plane
$A_{ef.v}$	= effective area of transverse reinforcement per unit length
A_{f1}	= area of the front of the block connector
A_{f2}	= enlarged area of the front surface of the block connector
A_p	= cross-sectional area of steel deck for unit width
A_s	= cross-sectional area of structural steel
A_{sc}	= cross-sectional area of stud shear connector
A_{sd}	= area of steel decking
A_{sr}	= area of steel reinforcement
A_v	= vertical shear area of structural steel
A^*	= effective cross-section area
E_c	= modulus of elasticity of concrete
$E_{c.ef}$	= effective modulus of elasticity of concrete for creep analysis
E_d	= design load effect
E_m	= mean load effect

E_k	=	characteristic load effect
E_s	=	modulus of elasticity of steel
$(EI)_e$	=	global flexural stiffness of column cross-section for buckling evaluation
F	=	action, force, load
F_m	=	mean load
$F_{b.pr}$	=	preload force in bolt
F_c	=	compression force in the concrete slab
$F_{c.f}$	=	value of F_c associated with the plastic moment of the composite beam section
$F_{c.max}$	=	maximum possible stress resultant of concrete cross-sectional component
F_k	=	characteristic load value
F_s	=	tensile force in the steel profile
$F_{s.max}$	=	maximum possible stress resultant of structural steel cross-sectional component
F_{sr}	=	tensile force in reinforcing steel
F_t	=	tensile force in the concrete slab
$F_{t.f}$	=	tensile force in the concrete slab when bending moment is maximum
F_w	=	plastic axial load resistance of steel web
H_{sc}	=	overall height of a stud
I	=	inertia of the composite cross-section
I_c	=	inertia of the concrete cross-sectional component
I_s	=	inertia of the structural steel cross-sectional component
I_{sr}	=	inertia of the reinforcing steel cross-sectional component
I_1	=	inertia of the uncracked composite cross-section
I_2	=	inertia of the cracked composite cross-section
L	=	span, length
M	=	bending moment
M_{cr}	=	first cracking moment
M_e	=	bending moment before redistribution
M_{el}	=	elastic limit moment
M_{pl}	=	plastic moment
$M_{pl.d.c}$	=	design plastic moment of the composite cross-section
$M_{pl.c}$	=	plastic moment of the composite beam
$M_{pl.cs}$	=	plastic moment of the composite slab
$M_{pl.s}$	=	plastic moment of the steel section alone
$M_{pl.p}$	=	plastic moment of the steel deck alone
$M_{pl.pr}$	=	reduced plastic moment of the steel deck alone
M_r	=	bending moment after redistribution
M_s	=	bending moment resistant of the steel section alone
M_{sh}	=	bending moment induced by shrinkage
M_u	=	ultimate moment capacity of a partially composite beam
$M_{u.cs}$	=	ultimate moment capacity of a partially composite slab
M_{unf}	=	unfactored value of the moment capacity
N	=	axial load, number of connectors in shear span
N_{cr}	=	buckling load of a composite column
N_{el}	=	elastic axial resistance
N_f	=	minimum number of connectors required to transfer F_{cf}
N_r	=	number of studs in a rib of a composite slab
N_p	=	permanent part of the axial load
N_{pl}	=	plastic axial resistance of a section
$N_{pl.c}$	=	plastic axial resistance of concrete component
$N_{pl.p}$	=	plastic axial resistance of steel deck alone

$N_{pl.pc}$	= plastic axial resistance of steel deck in compression
N_{sh}	= axial load induced by shrinkage
$N_{pl.sr}$	= plastic tensile resistance of steel reinforcement
N_u	= ultimate axial load of a column
P	= applied load
Q_c	= resistance of the shear connection on a given beam length
Q_{cf}	= resistance of a full connection on a given beam length
R_d	= design value of the resistance
R_k	= characteristic value of the resistance
R_n	= nominal resistance
S	= first moment of area of the composite cross-section
T	= tensile force
V	= shear force
V_l	= longitudinal shear force
V_{ea}	= shear strength of an end anchorage
V_{pl}	= plastic vertical shear resistance
W_c	= plastic resistance modulus of concrete component
W_s	= plastic resistance modulus of steel component
W_{sr}	= plastic resistance modulus of reinforcing steel component
$W_{c.n}$	= plastic resistance modulus of concrete component in the range $\pm h_n$
$W_{s.n}$	= plastic resistance modulus of steel component in the range $\pm h_n$
$W_{sr.n}$	= plastic resistance modulus of reinforcing steel component in the range $\pm h_n$
α	= angle, shear reduction coefficient, imperfection factor
β	= angle, safety angle
δ	= beam deflection
δ_c	= structural steel contribution
δ_f	= beam deflection in case of full shear connection
δ_p	= beam deflection in case of partial shear connection
δ_s	= deflection of the steel section acting alone
δ_{sh}	= deflection due to shrinkage
δ_{ss}	= deflection of the simply supported beam
ε_c	= strain of concrete
ε_s	= strain of steel
$\varepsilon_{y.s}$	= strain of steel at welding
ε_{sh}	= shrinkage strain
ε_{sr}	= reinforcing steel strain
γ	= partial safety factor
γ_c	= partial safety factor for concrete
γ_F	= load factor
γ_m	= partial safety factor for material strength
γ_s	= partial safety factor for structural steel
γ_{sr}	= partial safety factor for steel reinforcement
γ_V	= partial safety factor for shear connectors
λ	= relative slenderness of a composite column
μ	= coefficient for the evaluation of ultimate moment, friction coefficient
σ_c	= concrete stress
σ_s	= structural steel stress
σ_{sr}	= reinforcing steel stress
σ_{cr}	= critical stress (F_{cr} following AISC symbols)

$\sigma_{c,\max(\min)}$	=	maximum (minimum) concrete compression stress
$\sigma_{s,\max(\min)}$	=	maximum (minimum) structural steel stress
$\sigma_{sr,\max(\min)}$	=	maximum (minimum) reinforcing steel stress
χ	=	stability curve factor
χ_n	=	effects of imperfection factor for buckling evaluation
η	=	degree of shear connection
μ	=	friction coefficient
τ_c	=	shear resistance of concrete
τ_u	=	mean ultimate shear stress in a composite slab
$\tau_{u,d}$	=	design value of τ_u
$\tau_{u,k}$	=	characteristic value of τ_u
ϕ	=	creep coefficient, resistance factor, non-dimensional term to define buckling curves, diameter of reinforcing bars
ϕ_c	=	resistance factor of column
ϕ_b	=	resistance factor of beam

References

- [1] Allern, D.N. de G. and Severn, R.T. 1961. Composite Action Between Beams and Slabs Under Transverse Load, *Struct. Eng.*, 39, 149-154.
- [2] Ansourian, P. 1975. An Application of the Method of Finite Elements to the Analysis of Composite Floor System, *Proc. Inst. Civil Eng.*, London, 59, 699-726.
- [3] Aribert, J.M. 1990. Design of Composite Beams with a Partial Shear Connection. *Proc. IABSE Symp. Mixed Structures Including New Materials*, 60, 215-220 (in French).
- [4] Aribert, J.M. and Abdel Aziz, K. 1990. Calcul de poutres mixtes jusqu'à l'état ultime avec un effet de soulèvement à l'interface acier-béton, *Construction Métallique*, 22(4), 3-36.
- [5] Bode, H. and Sauerborn, I. 1992. Modern Design Concept for Composite Slabs with Ductile Behavior, in *Composite Construction in Steel and Concrete*, 2nd ed. W.S. Easterling and W.M.K. Morris, ASCE, New York, 125-141.
- [6] Bradford, M.A. and Gao, Z. 1992. Distorsional Buckling Solutions for Continuous Composite Beams, *ASCE J. Struct. Eng.*, 118, (1), 73-89.
- [7] Brett, P.R., Nethercot, D.A., and Owens, G.W. 1997. Continuous Construction in Steel for Roofs and Composite Floors, *Struct. Eng.*, 65A, 355-363.
- [8] Buckner, C.D., Deville, D.J., and McKee, D.C. 1981. Shear Strength of Slab in Stub-Girders, *ASCE J. Struct. Div.*, February.
- [9] Carbone, V. and Nascè, V. 1985. On the Effective Width and Other Interaction Aspects in Composite Steel-Concrete Beams, in *Proc. of the 10th Italian Conf. Constructional Steel*, Montecatini, 121-135.
- [10] Climenhaga, J.J. and Johnson, R.P. 1972. Local Buckling in Continuous Composite Beams, *Struct. Eng.*, 50 (9), 367-374.
- [11] Cosenza, E., Mazzolani, S.M., and Pecce, M. 1992. Ultimate Limit State Checking of Continuous Composite Beams Designed to Eurocode Recommendations, *Costruzioni Metalliche*, 5, 273-287.
- [12] Cosenza, E. and Pecce, M. 1991. Deflections and Redistribution of Moments Due to the Cracking in Steel-Concrete Composite Continuous Beams Designed to Eurocode 4, in *Proc. ICSAS 91*, Elsevier Applied Science, 3, 52-61, Singapore, May.
- [13] Cosenza, E. and Pecce, M. 1993. Composite Steel-Concrete Structures and Eurocode 4; New Research Results: Cracked Analysis of Continuous Composite Beams, *Lecture notes, International Advanced School, Eurocode 3 and 4*, Budapest, Hungary, December.

- [14] Couchman, G. and Lebet, J-P. 1993. Design Rules for Continuous Composite Beams using Class 1 and 2 Steel Sections — Applicability of EC 4. *EPFL-ICOM Publication 290*, Lausanne, November.
- [15] Crisinel, M. 1990. Partial-Interaction Analysis of Composite Beams with Profiled Sheeting and Nonweld Shear Connectors, *J. Construct. Steel Res.*, Special Issue on Composite Construction, R. Zandonini, Ed., 15 (1&2), 65-98.
- [16] Dezi, L. and Tarantino, A. M. 1993. Creep in Composite Continuous Beams, I: Theoretical Treatment, *ASCE J. Struct. Eng.*, 7 (119), 2095-2111.
- [17] Dezi, L. and Tarantino, A. M. 1993. Creep in Composite Continuous Beams. I: Parametric Study. *ASCE J. Struct. Eng.*, 7 (119), 2112-2133.
- [18] Evans, H.R. and Wright, H.D. 1988. Steel-Concrete Composite Flooring Deck Structures, in *Steel-Concrete Composite Structures, Stability and Strength*, Narayanan, R., Ed., pp.21-52, Elsevier Applied Science, London.
- [19] Goble, G.G. 1968. Shear Strength of Thin Flange Composite Specimens, *AISC Eng. J.*, 5 (2).
- [20] Grant, J.A., Fisher, J.W., and Slutter, R.G. 1977. Composite Beams with Formed Steel Deck, *AISC Eng. J.*, 14 (1). 24-42.
- [21] Griffis, L.G. 1992. Composite Frame Construction, *Constructional Steel Design, An International Guide*, Dowling, P.J. et al., Eds., p. 523-553, Elsevier Applied Science, London.
- [22] Hancock, G.J. 1978. Local, Distorsional and Lateral Buckling on I-beams, *ASCE J. Struct. Div.*, 106 (ST7), 1557-1571.
- [23] Heins, C.P. and Fain, H.H. 1976. Effective Composite Beams Width at Ultimate Load, *ASCE J. Struct. Div.*, 102 (ST11), 2163-2179.
- [24] Lawson, R.M. 1992. Shear connection in Composite Beams, in *Composite Construction in Steel and Concrete*, 2nd ed. W.S. Easterling and W.M.K. Morris, ASCE, New York, pp. 81-97.
- [25] Luttrell, L.D. and Prassanan, S. 1986. Method for Predicting Strengths in Composite Slabs, in *Proc. 8th Intl. Speciality Conference on Cold Formed Structures*, pp. 419-431, University of Missouri-Rolla, St. Louis, Missouri.
- [26] Johnson, R.P. and Allison, R.W. 1981. Shrinkage and Tension Stiffening in Negative Moment Regions of Composite Beams, *Struct. Eng.*, 59b (1), 10-15.
- [27] Johnson, R.P. and Hope-Gill, M.C. 1976. Applicability of Simple Plastic Theory to Continuous Composite Beams, in *Proc. Inst. Civ. Eng.*, 61 (2), 127-143.
- [28] Johnson, R.P. and May, I.M. 1978. Tests on Restrained Composite Columns, *Struct. Eng.*, 56B, 21-8, June.
- [29] Johnson, R.P. and Molenstra, N. 1991. Partial Shear Connection in Composite Beams for Buildings, in *Proc. Inst. Civ. Eng.*, 91 (2), 679 - 704.
- [30] Johnson, R.P. and Anderson, D. 1993. Designer's Handbook to Eurocode 4: Part 1.1, Design of Steel and Composite Structures, British Standards Institution, London.
- [31] Kemp, A.R. and Dekker, N.W. 1991. Available Rotation Capacity in Steel and Composite Beams, *Struct. Eng.*, 69 (5), 88-97.
- [32] Mattock, A.H. and Hawkins, N.M. 1972. Shear Transfer in Reinforced Concrete — Recent Research, *J. Prestressed Concrete Inst.*, March/April, 55-75.
- [33] Mele, M. and Puhali, R. 1985. Experimental Analysis of Cold Formed Shear Connectors in Steel-Concrete Composite Beams, *Costruzioni Metalliche*, 36(5/6), 239-251, 291-302.
- [34] Moore, W.P. Jr. 1988. An Overview of Composite Construction in the United States, *Composite Construction in Steel and Concrete*, C.D. Buckner and I.M. Viest, Eds., ASCE, New York p.1-17.
- [35] Mottram, J.T. and Johnson, R.P. 1990. Push Tests on Studs Welded Through Profiled Steel Sheeting, *Struct. Eng.*, 68, 187-193.
- [36] Oehlers, D.J. 1989. Splitting Induced by Shear Connectors in Composite Beams, *ASCE J. Struct. Eng. Div.*, 115, 341-362.

- [37] Oehlers, D.J. and Bradford, M.A. 1995. *Composite Steel and Concrete Structural Members, Fundamental Behavior*, Pergamon Press.
- [38] Ollgaard, J.G., Slutter, R.G. and Fisher, J.W. 1971. Shear Strength of Stud Shear Connections in Lightweight and Normal Weight Concrete, *AISC Eng. J.*, 8 (2).
- [39] Porter, M.L. and Ekberg, C.E. 1976. Design Recommendations for Steel Deck Floor Slabs, *ASCE J. Struct. Div.*, 102 (ST11), 2121-2136.
- [40] Puhali, R., Smotlak, I. and Zandonini, R. 1990. Semi-Rigid Composite Action: Experimental Analysis and a Suitable Model, *J. Constructional Steel Res.*, Special Issue on Composite Construction, Zandonini R., Ed., 15 (1&2), 121-151.
- [41] Roik, K. and Bergmann, R. 1989. Report on Eurocode 4, Clause 4.8 and 4.9, Composite Columns, Harmonization of European Construction Codes, Report EC4/6/89, Minister fur Raumordnung, Bauwesen und Stadtebau der Bundesrepublik Deutschland, reference number RSII 1-6741028630, July.
- [42] Roik, K. and Bergmann, R. 1992. Composite Columns, in *Constructional Steel Design, An International Guide*, Dowling, P.J., Harding, J.E., and Bjorhovde, R. Eds., Elsevier Applied Science, p.443-470
- [43] Schuster, R. M. and Ekberg, C.E. 1970. Commentary on the Tentative Recommendations for the Design of Cold-Formed Steel Decking as Reinforcement for Concrete Floor Slabs, Research Report, Iowa State University, Ames, Iowa.
- [44] Slutter, R.G. and Driscoll, G.C. 1965. Flexural Strength of Steel-Concrete Composite Beams, *ASCE J. Struct. Div.*, 91 (ST2).
- [45] Stark, J.W.B. and Brekelmans, J.W.P.M. 1990. Plastic Design of Continuous Composite Slabs, *J. Constructional Steel Res.*, 15, 23-47.
- [46] Viest, I.M. 1992. Composite Construction: Recent Past, Present and Near Future, in *Composite Construction in Steel and Concrete*, 2nd ed., Easterling W.S. and Morris, W.M.K. Eds., ASCE, New York, p. 1-16.
- [47] Wakabayashi, M. and Minami, K. 1990. Application of High Strength Steel to Composite Structures, in *Proc. IABSE Symp. Mixed Struct. Including New Mater.*, 60, 59-64.
- [48] Trahair, N.S. 1993. *Flexural-Torsional Buckling of Structures*, Chapman and Hall, London, 1993.

Codes and Standards

American Concrete Institute. 1989. Building Code Requirements for Reinforced Concrete. ACI 318-89. Detroit, Michigan.

American Institute of Steel Construction. 1993. Load and Resistance Factor Design Specifications for Structural Steel Buildings, Chicago, Illinois.

American Iron and Steel Institute. 1986. Specifications for the Design of Cold-Formed Steel Structural Members, Washington, D.C.

American Society of Civil Engineers. 1991. Standard for the Structural Design of Composite Slabs, ANSI/ASCE 3-91, New York.

American Society of Civil Engineers. 1991. Standard Practice for Construction and Inspection of Composite Slabs, ANSI/ASCE 9-91, New York.

Architectural Institute of Japan. 1987. AIJ Standard for Steel Reinforced Concrete Structures.

European Committee for Standardisation (CEN). 1992. ENV 1992-1-1 Eurocode 2, Common Unified Rules for Reinforced Concrete Structures, Brussels, Belgium.

European Committee for Standardisation (CEN). 1992. ENV 1993-1-1 Eurocode 3,

Design of Steel Structures, Part 1.1, General Rules and Rules for Buildings, Brussels, Belgium.

European Committee for Standardisation (CEN). 1994. ENV 1993-1-3 Eurocode 3, Design of Steel Structures, Part 1.3 Cold Formed Thin Gauge Members and Sheeting, Brussels, Belgium.

European Committee for Standardisation (CEN). 1994. ENV 1994-1-1 Eurocode 4, Design of Composite Steel and Concrete Structures, Part 1.1 General Rules and Rules for Buildings, Brussels, Belgium.

European Convention for Constructional Steelwork. 1981. Composite Structures (Model Code for Eurocode 4: Part 1), The Construction Press, London.

European Convention for Constructional Steelwork. 1993. Composite Structures, Composite Beams and Columns to Eurocode 4, publication n. 72, TC 11.

Further Reading

- [1] Jonhson R.P. and Anderson, D. 1993. *Designer's Handbook to Eurocode 4 — Part 1.1: Design of Composite Steel and Concrete Structures*, Telford Press, pp. 182.
- [2] Jonhson, R.P. 1994. *Composite Structures of Steel and Concrete, Vol. 1 Beams, Slabs, Columns, and Frames for Buildings*, Blackwell, pp. 210.
- [3] Oehlers, D.J. and Bradford, M.A. 1995. *Composite Steel and Concrete Structural Members — Fundamental Behavior*, Pergamon Press, pp. 549.
- [4] Viest, I.M., Colaco, J.P., Furlong, R.W., Griffis, L.G., Leon, R.T., and Wyllies, L.A., Eds. 1996. *Composite Construction: Design for Buildings*, McGraw-Hill/ASCE, New York, pp. 416.